AN INVESTIGATION OF ACOUSTIC METHODS FOR MEASURING THE LENGTH AND GROUT QUALITY OF ROCK ANCHORS IN MINES

Gary David Agnew

A project report submitted to the Faculty of Engineering, University of the Witwatersrand, Johannesburg, in partial fulfilment of the requirements for the degree of Master of Science in Engineering

Johannesburg, 1990

DECLARATION

I declare that this project report is my own, unaided work. It is being submitted for the Degree of Master of Science in Engineering, in the University of the Witwatersrand, Johannesburg. It has not been submitted before for any degree or examination in any other university.

15th day of August 1990

ABSTRACT

A demand exists in the mining industry for an instrument capable of testing rock anchors quickly, reliably and non-destructively. This report describes laboratory tests in which the acoustic pulse interrogative technique is investigated for rock anchors up to 1,9m in length, using concrete cylinders to simulate rock. The results of the tests show that, under laboratory conditions, the length and grout coverage of a rock anchor up to this length can be deduced from its acoustic response. The tests were made using a magnetostrictive transducer to provide the acoustic stimulus and a piezoelectric transducer to detect the response of the rock anchors to the stimulus. A special case of the cepstrum method, the band limited envelope cepstrum, for processing acoustic signals from the rock anchors is introduced and the efficacy of the method in dealing with the very distorted rock anchor responses is demonstrated.

To my wife, Sue

ACKNOWLEDGEMENTS

The author wishes to thank the following persons and institutions for their assistance:

My supervisor, Professor Hanrahan, for his valuable advice, support and encouragement.

COMRO (the Chamber of Mines Research Organization), who made the project possible by initiating and financing it.

Alain Clavier of the non-destructive testing division of S A Electro-Medical, for the loan of a transducer and his advice and interest in the project.

Rod Green of the Bernard Price Institute of Geophysics (BPI) at the University, for the donation of piezoelectric transducers, the loan of books and his interest in the project.

Robert Cole of the BPI, for the donation of piezoelectric transducers, the loan of books and his valued encouragement.

The workshop staff of the Department of Electrical Engineering, for their patience and assistance during the time it took to develop the analog circuitry for the project.

Martin Turner of the Department of Electrical Engineering, for his advice and friendly assistance in supplying various instruments for the project.

Annie, without whose help and endless advice I would not have been able to cast the concrete cylinders.

My dear wife Sue for her understanding and support, especially during the more trying periods of the work.

CONTENTS PAGE

CONTENTS PAGE

CONTENTS PAGE

LIST OF FIGURES

FIGURE PAGE

FIGURE PAGE

1 INTRODUCTION

1.1 Background

The mining industry relies on rock anchors for the containment of rockbursts and support of surface layers of rock in mine tunnels. In performing this function, the integrity of rock anchor installations plays a vital role in mine safety. The failure of rock anchors in their stressful environment is not uncommon, and so to maintain the required level of safety underground, rock anchors must be tested in situ from time to time. The present (and only) method of testing rock anchors is the mechanical "pull test", in which the installation is stressed to the point of failure and, depending on the failure stress, it is decided whether or not the installation was acceptable. Because the test is destructive, it can be applied to rock anchors only on a sample basis. In addition to the fact that it is destructive, the pull test is unsatisfactory because it is slow and expensive: the hydraulic test equipment is cumbersome and takes time to set up. These disadvantages of the pull test have given rise to the need for a portable instrument which is capable of testing rock anchors quickly, reliably and non-destructively.

About 6 million rock anchors are installed in South African mines every year and the development of such an instrument would lead to improved safety underground and considerable savings to the mining industry. The research effort described in this report was commissioned by COMRO (the Chamber of Mines Research Organization) with the aim of ultimately producing a grouted rock anchor tester. Before detailing the nature of this research and how it relates to the problem of rock anchor testing, the reader is introduced to some rock anchor terminology and practice in section 1.2 below.

1.2 Overview of Rock Anchor Practice

Working mechanism of rock anchors

Rock anchors are steel rods inserted into holes drilled perpendicularly to the rock face in tunnel walls, and are fixed in position by filling the holes with a cementitious or resin grout. A small length of rock anchor is left protruding from the hole for the attachment of nuts, washers, cable and wire mesh. Stress in the surface layers of rock is transferred through the rod into deeper layers of rock, the bonding of the grout with the rock and the steel rod being instrumental in effecting this stress transfer. A large washer is sometimes fixed to the end of the rod to give additional stress distribution in the surface layer of rock. The function of the cable lacing and wire mesh is to contain fragments of rock which break away from the rock face. Where they are used, the mesh and lacing cover the entire rock face and are fixed

in position by the rock anchors, which are commonly installed one to two metres apart. Figures 1.1 and 1.2 illustrate some rock anchor installations in cross-sectional and plan view. The rock anchors shown in Fig. 1.1 have not been correctly (fully) grouted.

Rock anchor failure

Rust and ageing, poor initial installation, shearing or snapping of rods and the destruction of the grout-steel bond are common reasons for the failure of rock anchors. Earth movement is the cause of grout bond destruction, shearing and longitudinal snapping, hence the need for an instrument which is capable of measuring the length of the rod. Since the mechanical strength of the rock anchor installation depends on the area of intact grout bond at its surface, the proposed instrument must also be capable of determining this area. A coarse measure of this area, and a convenient means of expressing the area for a particular rock anchor type, is the equivalent length over which the rock anchor is assumed to be fully grouted.

It has been found that above a certain area (or length) of rod-grout bond the rod snaps under excessive longitudinal stress, and below this length the grout-steel bond is destroyed. The length of bond at the transition between these failure mechanisms is referred to as the "critical bond length". The critical bond length of the commonly used rock anchor and grout types is between a half and one metre.

Poor initial installation usually amounts to the installation of rods which are shorter than they should be, or the use of too little grout in the drillhole. Testing of rock anchor installations is therefore warranted both at installation time, as a quality control check, and at appropriate periods thereafter, to detect damage caused by earth movement.

Rock anchor size and types

Rock anchors are generally between one and three metres in length and between 15 and 25mm in diameter, depending on the requirements of the mine. Of the large variety of rock anchors used in mining operations, most can be placed into the categories "smooth bar" or "rebar" and "straight bar" or "shepherds crook".

Rebars have ribbed surfaces to improve the overall strength of their grout bond, the height of the surface ribs being typically 1 to 2mm. Smooth bars are circular in cross section and have no surface features apart from threads which are cut at the ends of the rod for the attachment of nuts and washers.

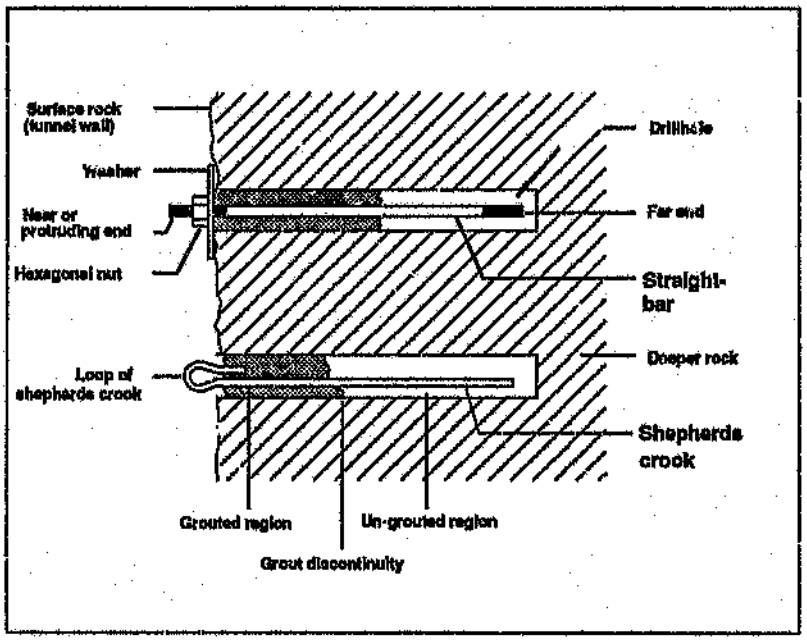

Figure 1.1 Rock anchor terminology: a straight-bar and a shepherds crook (not to scale)

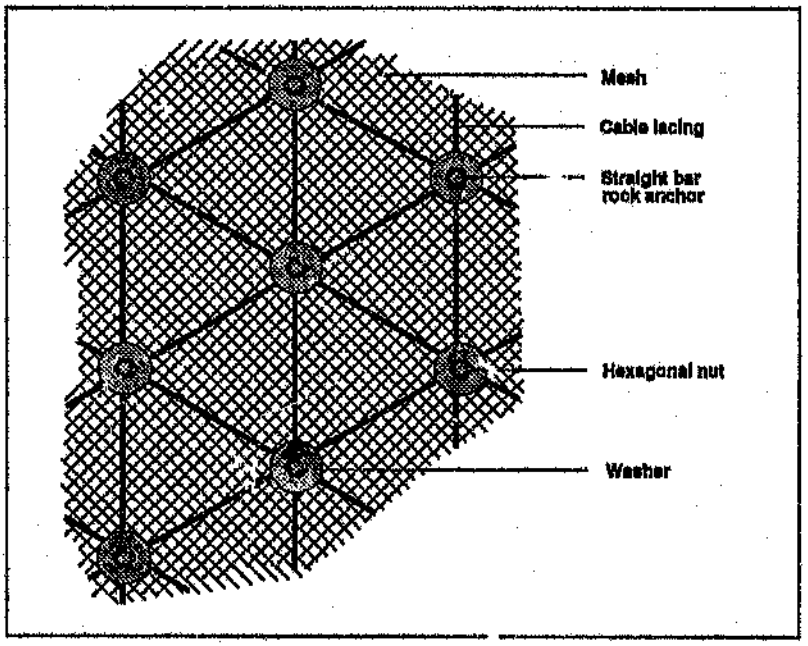

Figure 1.2 Mesh and cable lacing held in place by straight-bar rock anchors (not to scale)

As its name implies, the straight bar is a simple rod. The shepherds crook terminates in a loop, for convenience in attaching cables and mesh. This loop is closed by burying both ends of the rod in the drillhole at installation time.

Grout quality or coverage: is the proportion of rod area which is bonded with the grout. Grout coverage is sometimes expressed as a percentage and sometimes as a length, where the area of the rod for that length is assumed to be fully bonded.

Grout discontinuities: are points on the rod where a transition from a grouted to an ungrouted area occurs.

Grout distribution: is the geometry, or pattern in which grout bonding occurs on the rod, defined by the location of grout discontinuities on the rod.

Near and far end: The near end of a rock anchor is the portion of rod protruding into the tunnel after installation, and is accessible for the purpose of testing. The far end of the rod is buried in the deeper layers of rock and is inaccessible.

1.3 Instrument Specifications and Conditions in Mines

The objective of the research described in this report is not to produce a complete rock anchor testing instrument. Rather, it is concerned only with the signal processing aspects of a future instrument, whose specifications are given below. The discussion below should therefore be seen as background information which puts the research into perspective. The scope of this research will be discussed in section 1.6.

The requirements of the rock anchor test instrument, as laid down by the mining industry, can be summed up as follows:

The instrument should be:-

* Capable of measuring the length and grout quality of rock anchors in situ with a precision of 20cm.

* Capable of testing rock anchors quickly (in about 4 minutes maximum), and should therefore not rely on special preparation of the rod, for example filing and polishing of the rod surface.

* Non-invasive. That is, the rock anchor installation may not be tampered with or changed, even temporarily.

* Robust, portable and self-contained (not need an external power supply).

* Easy to use, even by semi-skilled people.

* In compliance with mine safety regulations.

Since the efficacy of the rock anchor installation depends primarily on its grout coverage, measurement of grout coverage is considered the more important feature of the instrument. The proposed instrument must perform to specification for a variety of rock anchor types under mine conditions, which are less than ideal. Some of these conditions are;

* The near end of the rock anchor may be covered in rust, debris and moisture and does not necessarily have a flat face: it is sometimes wedge-shaped because of the process used to manufacture it.

* Rock anchors are not installed with much consistency: the protruding length of the near end varies and one or more nuts may be present on it. Sometimes nuts are positioned at the very end of the protruding rod. Washers, mesh and cable lacing may or may not be attached to the near end of the rod. The rods are sometimes bent, and are not always installed perpendicularly to the rock face.

* A variety of rock types and conditions may exist in the mine: the rock may be wet or dry, cracked, and the face of the tunnel wall may be rough and craggy, and may or may not be covered in mesh and cable lacing.

* The diameter of the drillhole is not necessarily fixed, and different grout types are used. The cementitious grout type is, however, normally used in gold mines.

* Rock anchors installed in a tunnel roof are not easily accessible.

* Rock anchors may be under any stress from zero to the point of failure.

1.4 The Acoustic Method as a Solution

The following discussion does not attempt to justify the use of the acoustic pulse method fully and should be seen as the background to, and broad argument for, the use of the method. The goal of the research was to evaluate the acoustic method under laboratory conditions. More detail on the nature of this evaluation will be given in section 1.6.

Of all the conditions found in rock anchor installations listed above, the measurement principle of "the ideal instrument" should produce information which depends on two only: the length and grout coverage of the rock anchor. If the physical principle exploited for the purpose of measurement shows a dependence on other quantities which are known and can be corrected for (such as rod, grout and rock type), the instrument may be more difficult to calibrate and use, but may nevertheless be practicable. If, on the other hand, the principle has an unacceptably strong dependence on unknowns which cannot be determined (such as rock moisture content or crack geometry), it is useless.

Because the grout coverage is the more important quantity to be measured, the primary concern in finding a principle on which to base the instrument should be with grout coverage. If the length information cannot be found using the same principle, a second principle which gives length information may be employed by the instrument.

A microwave radar unit (for imaging the inside of the rock) and the "antenna method" have, for example, been used to find rock anchor lengths. The principle of the latter is to treat the rock anchor as an antenna, and to find the impedance minimum which occurs at the resonant frequency of the antenna - this resonant frequency is directly related to the length of the rod. (A problem with the antenna technique is that the resonant frequency also depends strongly on the rock's permittivity and moisture content). Naturally, these principles cannot give information on the area over which the steel of the rod is bonded with the grout. In the opinion of the author, the only principles which offer a solution to the problem of finding grout coverage are the thermal and acoustic ones. The principle of the thermal method is that the thermal resistance between the rock anchor and the surrounding rock (measurable with a thermal stimulus) is directly related to the grout coverage of the rod. Because the thermal method will be very slow and consume a large amount of energy, it is likely that it will be more costly and cumbersome than the pull test. By elimination, it appears that the acoustic method is the only principle on which to base the instrument.

The foundation of the acoustic method is that acoustic energy induced into the rod is confined to the rod if its grout coverage is small, but leaves the rod rapidly by "leaking" through the grout-steel bond if grout coverage is good. By recording the acoustic response of the rod after the introduction of the energy, this rate of leakage can be gauged and from it the grout coverage of the rod can be inferred. If the stimulating acoustic signal is chosen to be a pulse, a rather simple means of finding both the grout coverage and the length of the rod suggests itself: if the pulse induced into the rod traverses the length of the rod, is reflected at the far

end and returns to the source of excitation as an echo, then the amplitude of the (attenuated) echo should relate to grout coverage and the time taken for the echo to arrive should relate to rod length.

Naturally, there is a variety of other stimulus types which can be used, for example white noise or continuous sine excitation, but with the correct signal processing manipulations they can be considered equivalents. The choice of excitation type must therefore depend chiefly on the practicability and limitations of the transducers used.

The method selected for the laboratory investigation, then, was the acoustic pulse echo method. Further reasons for the choice of pulse excitation will be seen later. Naturally, the premise that pulse attenuation depends only on grout coverage and time of arrival depends only on rod length cannot be strictly true. Deviations from these ideals will be dictated by the "real" acoustical laws of the system, applied to every element of its complex geometry and material. The philosophy behind the use of the simple pulse attenuation and time of arrival model, then, is highly empirical: starting with the model, corrections are made for every material and geometrical variation which:

* Affects the measured pulse attenuation and time of arrival significantly (that is, by an amount in excess of that allowed by the tolerances in the specification).

* Occurs in real rock anchor installations.

* Can be determined (that is, is a known quantity) for rock anchors under test in situ.

This is easily done in the case of parameters such as rock anchor, grout and rock type by collecting calibration data for every combination of the three. Quantities which cannot be determined by inspection of the rock anchor installation and the possible effects of which are more subtle pose a problem, however. Examples of these are the effects of grout distribution and end effects (where the far end of the rod is buried in grout) on the measured pulse attenuation and time of arrival. The treatment of this problem is discussed later in the report.

1.5 Previous Work on Rock Anchor Testers

To the best of the author's knowledge, no treatment of this problem, or one close to it, is available in the literature. The United States Bureau of Mines (USBM) has produced private documents [1], [2] describing the development of a instrument based on the acoustic

method. Their documents do not discuss the characteristics of the acoustic medium or the signal processing used to deal with it, in any detail. The development of this instrument (which the USBM calls "the rock bolt bond tester" or RBBT) has been abandoned because, according to a recent report from the USBM, the repeatability of their results was not good and sufficient acoustic energy could not be induced into rock anchors.

A Swedish organization, "Geodynamik AB", has produced an instrument (the "Boltometer") which uses the acoustic pulse technique. Documentation on the instrument's development and working principles has not been made available by them to date. Both the RBBT and the Boltometer use a piezoelectric transducer and pressure contact with rock anchors for the induction of acoustic energy into the rods, and consequently require that the near end of rods have a flat face.

1.6 Scope and Structure of the Work

In this report, the description of the work done is limited to:

* A study of cep -based signal processing for use on the acoustic responses of simulated rock anchors (clad with concrete cylinders).

* Experiments on simulated rock anchor installations and the application of the band-limited envelope cepstrum to the acoustic response of these installations.

The following paragraphs attempt to put this work into perspective and show how it relates to the problem of producing a rock anchor testing instrument. A description of the report layout is given at the end of this section. A more specific statement of the work done on the signal processing study and experiments is given in the description of the layout.

For the acoustic method, the different aspects of the research and design necessary to produce a final, working instrument can be enumerated as follows:

* Investigation of the behaviour and properties of the acoustic medium, developing models where necessary.

* Development of signal processing techniques for treating the acoustic responses of rock anchors and extracting their grout coverage and rod length information.

* Investigation and optimization of acoustic interfaces coupling signals into and out of the rod, with the emphasis on speed and ease of use, and minimizing rock anchor preparation needed.

* Assessment of effects of, and design to take into account, variable mine conditions such as rust, nuts, washers, cable lacing and mesh and shepherds crooks.

* Collection and treatment of calibration data for various rock anchor, grout and rock types.

* Design of the instrument's hardware and software. Consideration of mine safety regulations, portability and ergonomics.

* Production engineering.

Clearly the problem is a multi-faceted one, but the heart of the matter, and that upon which all else rests, is establishing the measurement principle of the instrument. That is, the excitation and signal processing needed which, after tailoring to suit the observed properties of the medium, produce the quantities required to be measured to specification. The purpose of the laboratory study using the acoustic pulse method, therefore, was to:

* Investigate the properties of the acoustic medium, using concrete cylinders to simulate rock.

* Develop the signal processing techniques needed to deal with the acoustic responses of rock anchors.

* Treat the laboratory study as a feasibility study and a pointer to further research necessary to produce a real instrument.

The object of this report is to convey to the reader the outcome of these investigations, and the discussion of issues which are peripheral to the above points will thus be kept to a minimum. The layout of the remainder of the report is as follows:

Chapter 2 describes the purpose and details of construction of the concrete cylinders used to simulate rock. The simulation was performed on two sample rock anchors. The physical equipment used in the study is introduced, and its interconnection is described. Part of this equipment are the magnetostrictive and piezoelectric transducers and their associated circuitry. The magnetostrictive transducer was used to create acoustic pulses in the rock

anchors and the piezoelectric element was used to detect the acoustic response of the rock anchors. These are discussed briefly, and problems associated with the particular combination of transducers used are reported. An attempt is made at describing the transducers and problems only insofar as they affect the integrity of the signals of interest, and insofar as an understanding of the experimental setup is necessary.

Chapter 3 discusses the signal processing needed in the analysis of the rock anchor responses. Because the signal processing can be viewed as the key to understanding and dealing with the properties of the acoustic medium, it is explored in some detail. The cepstrum is introduced and synthesized data is used to illustrate the use of the method. Variations of the cepstrum are described and lead to the introduction of the band-limited envelo cepstrum, which was used in the final analysis of the rock anchor responses. An exampl ck anchor response is used to illustrate the use of the band-limited envelope cepstrum, and the method of using the cepstrum to remove unwanted signal components is demonstrated. The signal processing methods described in this chapter were implemented in the Turbo Pascal programming language, on an IBM AT-compatible PC (personal computer).

Chapter 4 describes the two sample rock anchors used in the laboratory tests and the method of application of the concrete cylinders to the rock anchors. The instrument settings and data recording are discussed briefly. The acoustic responses (the "raw data", or "time records") of the rock anchors, obtained using the hardware described in Chapter 2, are presented and discussed. The log magnitude spectra and band-limited envelope cepstra of these time records are presented and discussed. An acoustical interpretation of the rock anchor responses is given, and pulse attenuation and arrival time curves for the rock anchors are derived from the time recordings, using the band limited envelope cepstrum.

Chapter 5 summarises the principle of the instrument and the signal processing method used. The shortcomings of the laboratory study are identified and recommendations for further research necessary to complete the feasibility study are given.

Appendix D gives the results of further tests, done on real rock anchor installations. This appendix is self-contained, and reviews the outcome of the laboratory study and recommends future work which should be done on the project.

2 EXPERIMENTAL SETUP AND APPARATUS

2.1 Use of Concrete Cylinders to Simulate Rock

The point of using concrete cylinders to simulate rock is for convenience in laboratory tests; with correct placement of concrete cylinders, various grout distributions and coverages can be simulated. The idea originated with the USBM, who verified the relationship between pulse attenuation and the strength (coverage) of the steel-grout bond by applying the pull test to concrete clad rock anchors to the point of destruction. The use of the method assumes that:

* The acoustic behaviour of concrete is not too different from that of rock.

* Acoustic energy entering the concrete is dissipated and does not return to the steel of the rock anchor.

The validity of these assumptions is commented on later in the report. In developing their instrument, the USBM [1] found that concrete cylinders of diameter 25cm could be used to simulate rock adequately.

Details of the concrete cylinders which were used in this study are:

* Dimensions of 40cm length and 110mm diameter for the cylinders were decided upon. The length of 40cm allows six tests to be performed on a two metre rock anchor (from zero to full grout coverage) - this was considered sufficient for a laboratory study of this nature. The diameter of 110mm, which gives the concrete a cross-sectional area 25 times that of the rock anchors tested, was considered adequate for the dissipation of acoustic energy entering the cylinder.

* The cylinders were cast as half-cylinders, to be grouted together on application to the rock anchor. A half-cylindrical recess of diameter 35mm was cast into the inside of each half-cylinder, for accommodation of rock anchors up to this diameter.

* Ordinary building cement and river screed were mixed in the ratio 2:3 by volume, in producing the half-cylinders. In the building industry it is generally agreed that this is the ratio for which concrete has its maximum strength. Each half-cylinder was allowed to set under water for 7 days and was dried slowly for three days after that.

Conbextra medium-set grout capsules (manufactured by Fosroc) were used to grout concrete half-cylinders together, and onto test rock anchors. The full strength curing time of this grout, and hence the minimum time allowed between acoustic tests and application of concrete cylinders, was three days. It was assumed that each concrete cylinder was fully bonded with the rock anchor under test, and no pull tests were applied to the rock anchors to verify this assumption.

2.2 Coupling the Acoustic Stimulus into the Rock Anchor

To avoid the difficulties associated with using a piezoelectric transducer for stimulating the rock anchor (that is, filing and polishing to produce a good acoustic interface), a magnetostrictive transducer and associated circuitry were produced: magnetostriction is the phenomenon in which a magnetic material subjected to a magnetic field experiences a mechanical contraction or expansion [3]. A coil placed around the near end of a rock anchor and excited with a high current of short duration thus amounts to a magnetostrictive transducer, the steel of the rock anchor itself being the magnetic material which is acoustically excited. Clear advantages of using a magnetostrictive transducer are:

* The method is non-contacting, and thus requires no acoustic interface preparation: acoustic pulses are induced directly into the rod.

* A fixed, known amount of acoustic energy can be imparted to the rod for a given rod type and coil geometry.

* The transducer produces a longitudinal acoustic wave in the rod.

Disadvantages of using the magnetostrictive transducer are:

* A lack of control over the waveform of the acoustic signal induced into the rod, because this waveform depends in a complex way on:
  - the magnetostrictive characteristics of the rod material
  - rod and coil geometry and placement
  - the current flowing in the coil.

* The magnetostrictive transducer is non-linear, mainly because the mechanical deformation of the material is independent of the polarity of the current flowing in the coil. This is not a problem in pulse excitation where the exact shape of the pulse is not important. Where the transducer is to be used for continuous sine excitation, however, the current drive to the coil has to be designed for operation in the linear region of the material's magnetostriction characteristic.

* Application of the magnetostrictive transducer assumes that some free end of the rock anchor is available for coil placement. Use of the transducer in a real instrument would require the design of a range of coils for testing rock anchors: for example, a hexagonal coil would be called for where a nut has been placed at the tip of a rock anchor's near end.

The coil used to excite the rock anchors investigated in the laboratory study was evenly wound with 100 turns of 24SWG enamelled copper wire, onto a former 20mm in diameter and 25mm long. The circuit diagram of the circuit used to excite the magnetostrictive transducer is shown in Fig. 2.1.

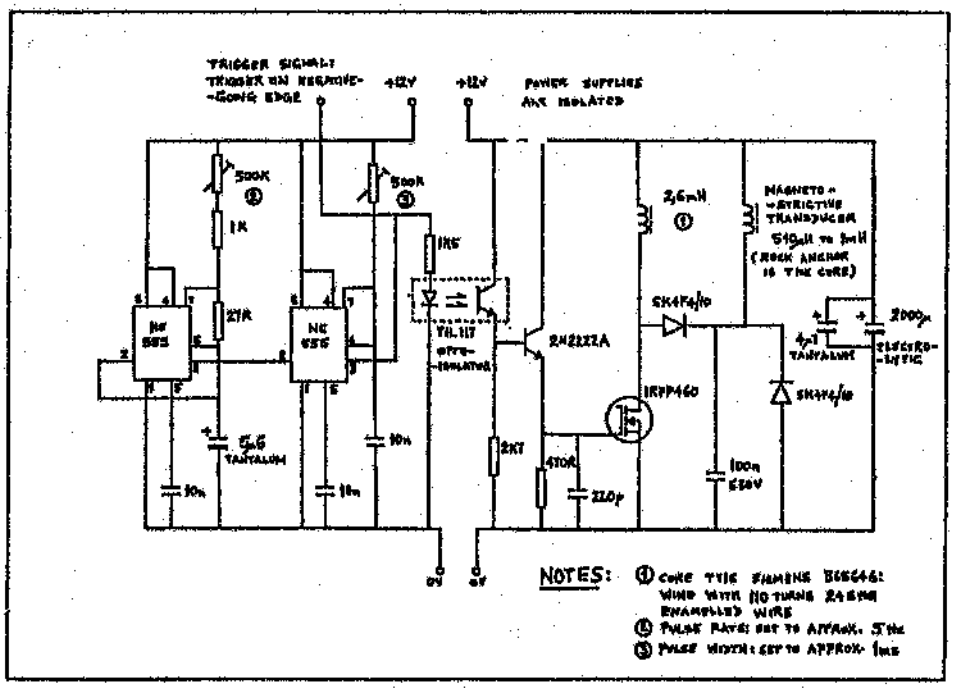

Figure 2.1 Circuitry used to excite the magnetostrictive transducer

This magnetostrictive drive circuit is capable of producing a current pulse of up to 10A of duration approximately 20μs in the transducer. The acoustic "clicks" thus produced in the rod are clearly audible up to a metre away from the rod. Because the magnetic material of rock anchors (solid mild steel) was not designed with its magnetostrictive properties in mind, the transducer is inefficient. This inefficiency can be compensated for by increasing the current drive to the coil, but does result in a problem (a stimulus artefact) which will be discussed in section 2.4.

2.3 Coupling the Acoustic Signal out of the Rock Anchor

A PZT (lead zirconate titanate) piezoelectric disc of diameter 16mm and thickness 3mm was used to detect the acoustic response of rods in the laboratory investigation. The PZT disc (part no. 4322 020 02300, manufactured by Philips) was chosen for its convenient physical dimensions and the fact that it has a smooth frequency response (that is, no resonant peaks) over the signal bandwidth of interest. The importance of using transducers with a smooth frequency response will be seen in Chapter 3.

The acoustic interface for the piezoelectric transducer (piezo) was formed by filing, but not polishing, a flat face onto the rods and pressing the piezo onto this face with the well-known commercially available product "Prestik" (otherwise known as "Blue-tac"). Although lossy, Prestik was found to have good acoustic properties, comparable to that of beeswax, and performs satisfactorily when used in thin layers. This interface is not practical in a real instrument, but it was used because of its good properties, and to maintain a division between the issues of acoustic interface design and the investigation of the acoustic medium.

The circuit diagram of the circuit used to amplify and filter the signal from the piezo is shown in Fig. 2.2. The amplifiers have a gain of about 54dB, to bring the signal up to a level which suits the analog to digital converter (A/D) used to sample and record the rock anchor responses. The function of the high-pass filter which cuts in at 4kHz is to remove strong low frequency noise (for example, 50Hz mains and mechanical vibrations) which might otherwise unnecessarily limit the dynamic range over which signal components are quantised by the A/D. The high frequency cutoff of the amplifiers (100kHz) is set naturally by the characteristics of the operational amplifiers used in the circuit. The bandwidth 4kHz to 100kHz was considered sufficient to convey all the pulse information needed in the analysis of rock anchor responses.

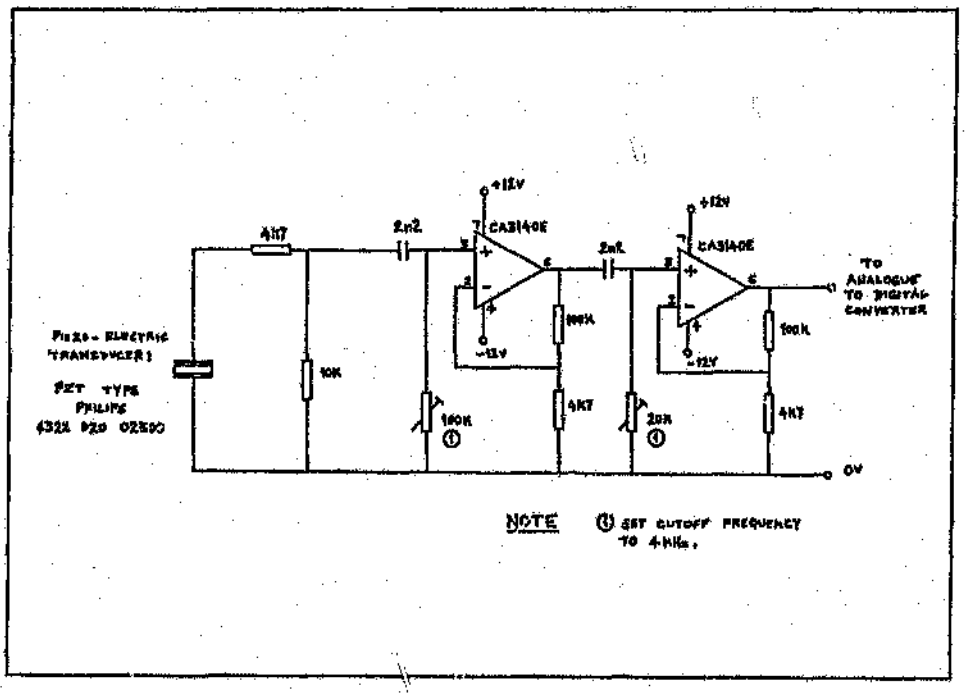

Figure 2.2 Amplifier for piezoelectric transducer

2.4 The Combination of Transducers and the Stimulus Artefact

Of the many combinations of acoustic transmitter and receiver considered for the investigation, the magnetostrictive transmitter and piezo receiver described above were selected, both for their convenience in the laboratory tests and as a prospective combination for use in a real instrument. Use of the ma tostrictive transmitter means that the piezoelectric receiver measures both the direct and reflected pulse, in correct proportion. This proportion is an important part of the signal processing and is needed to gauge the attenuation of the pulse which has travelled the length of the rod. The use of a single piezo for transmitting and receiving acoustic energy would make a comparison of the direct and reflected pulses more difficult.

This particular combination of transmitter and receiver does, however, give rise to a problem which might be called a "stimulus artefact". Because of the unavoidable proximity of the piezo and magnetostrictive transducers at the end of the rod, and the high voltage and current associated with the magnetostrictive transducer, a pulse is electromagnetically introduced at the electrical connections to the piezo. This artefact obscures the direct pulse measured by the piezo at the time the magnetostrictive transducer is stimulated and, although its shape

is similar to that of the direct pulse, it must be considered destructive because it isn't a "real" part of the acoustic response of the rod. An attempt to remove the stimulus artefact in the laboratory by subtracting two recordings in which the piezo had been acoustically connected and then disconnected from the rod, was unsuccessful. It was therefore concluded that the artefact does not simply add to the measured signal, and that some other way of dealing with it must be found.

Two immediately obvious ways of controlling the stimulus artefact are the careful design and screening of transducer leads, and maximizing the signal level delivered by the piezo. The latter can be achieved by using the entire area of the piezo's disc in the acoustic interface with the rod, and by minimizing the thickness of interface material (Prestik) between the piezo and the rod. In this way, the stimulus artefact in the laboratory was kept to a relatively low level. The stimulus artefact must nevertheless have affected the results obtained to some not insignificant degree, and perhaps the most important means of dealing with the problem in both an investigation and in a real instrument is to keep the magnitude of the artefact at a constant level.

The requirement of filing to produce a large, flat contact surface is in conflict with the specifications for a real instrument, and other ways of connecting the piezo to the rod were briefly investigated in the laboratory. One of these was a brass conical adaptor which has its base mounted on the piezo face, and a sharp apex which is simply pressed into the surface of the rock anchor. This arrangement performed satisfactorily, except for the unacceptably large stimulus artefact caused by the relatively small amount of acoustic energy admitted to the piezo through the point contact. If a more effective means of dealing with the stimulus artefact can be found, the point contact receiver should be useful, and will satisfy the requirement that no rock anchor preparation be necessary in a real instrument. Ideally, though, the method of detecting the acoustic response of rock anchors should be non-contacting, use of an optical or capacitive transducer, for example. A real instrument with a non-contacting transmitter and receiver would be elegant, completely non-intrusive and insensitive to the surface condition of the rock anchor being tested.

The transducers used in the laboratory study will certainly have to be adapted if they are to be used in a mining environment, and should therefore be viewed merely as pointers on the way to developing the transducers for a real instrument.

2.5 Overall Setup of Instruments

The interconnection of experimental apparatus for the tests was as shown in Fig. 2.3. The circuit diagrams of Fig. 2.1 and 2.2 are shown as blocks in the interconnection diagram. The function of the other devices in the diagram are:

* A/D converter (Thurlby DSA524): sampling and quantising the rock anchor responses delivered by the amplifier set. The A/D quantises samples with a precision of 8 bits and records and memorises up to 1024 samples. It is able to perform averaging on up to 255 consecutive records, and has an adjustable sensitivity and sampling rate.

* The AT-compatible PC has an RS-232 communications connection with the A/D and downloads records from the A/D which it then stores as disk files. Except for signal averaging, all processing of the rock anchor signals was performed on the PC.

* The oscilloscope displays the rock anchor responses as a check that the apparatus is functioning correctly, and to allow the correct sensitivity setting to be selected on the A/D.

The magnetostrictive drive circuit is free-running, and produces about 5 pulses per second in the rock anchor under test. The "trigger signal" shown in the interconnection diagram synchronises "single-sweep" record captures in the A/D with the direct pulse in the rod. When given a data capture command by the PC, the A/D makes a 1024 sample recording on the next trigger signal which appears at its trigger input.

More detail on the placement of the concrete cylinders and the use of 8 bit quantisation will be given in section 4.1, "Experimental Procedure".

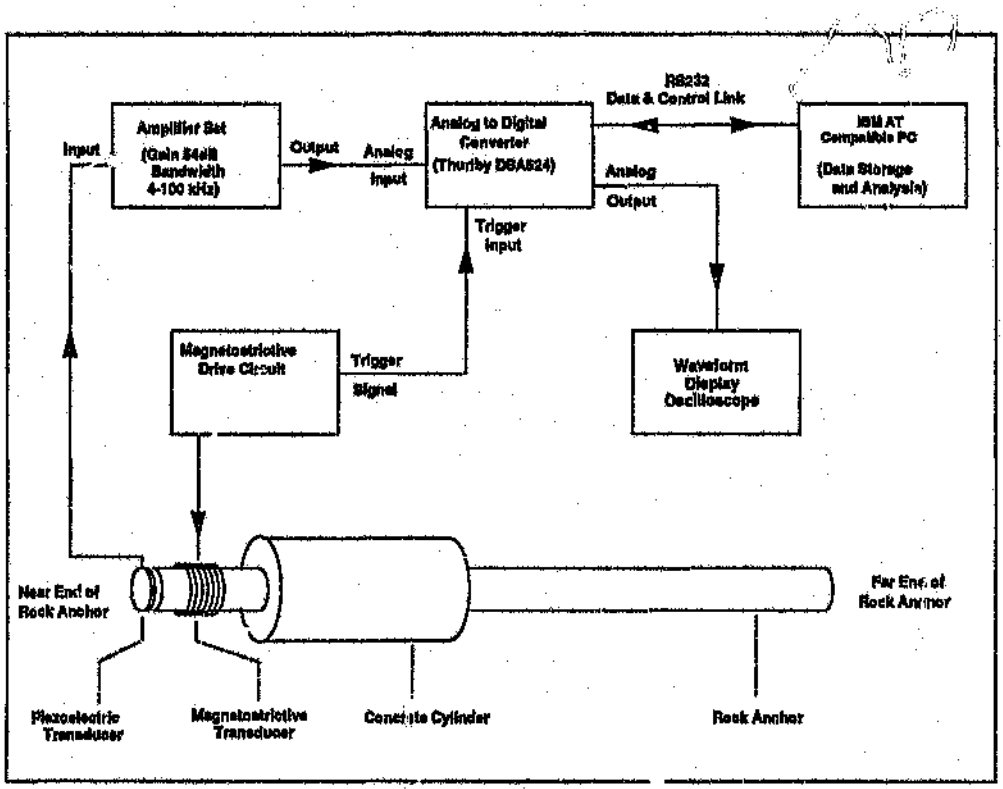

Figure 2.3 Overall setup of experimental apparatus

3 SIGNAL PROCESSING METHODS

The object of the signal processing used to deal with the rock anchor responses is to quantify the echo attenuation and arrival time, the parameters which are used in applying the principle of the instrument. As in any signal processing application, the tactics employed depend on the nature of the signal being dealt with. Therefore, to initiate this discussion on signal processing and justify the use of the cepstrum in the problem, one of the rock anchor responses obtained in the laboratory tests is shown in Fig. 3.1. This example response, from a 1,9m smooth bar rock anchor clad with one concrete cylinder, will be used throughout this chapter to guide the discussion on the cepstrum method and the special [illegible] made on it by the rock anchor responses. A full discussion of results is given [illegible] the example response given here should be seen only as an aid in establish[illegible]ignal[illegible]ssing needs of the problem.

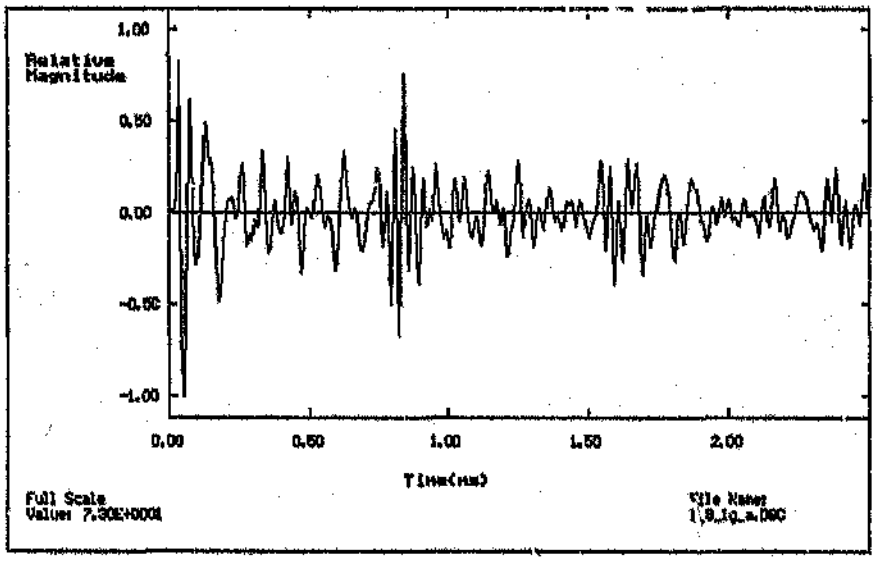

Figure 3.1 Acoustic response of 1,9m smooth bar clad with one concrete cylinder

The time waveform of Fig. 3.1 shows the stimulating pulse (applied by the magnetostrictive transducer) at the time origin of the graph and a reflection from the far end of the rod at about 0,8ms. Points of note in the graph are:

* The shape of the direct and echo pulses in the graph are not simple.

* The echo is not a replica of the direct pulse, but is distorted.

* There are signal components other than the direct and echo pulses in the graph. These components will be called "the background signal" until later, when an explanation for the phenomenon is offered. The background signal is not a reflection from the far end of the rod and therefore does not assist in implementing the principle of the instrument.

* Noise from quantisation of the signal and other sources must be present in the signal.

Where the echo pulse is simple and undistorted, and no signal components appear between the direct and echo pulses, simple peak detection can be used to quantify the echo pulse amplitude and time of arrival satisfactorily. In the rock anchor responses, however, the echo pulse shape changes due to distortion and where rods are well grouted (as will be seen later), the echo is hidden in the signal component which appears throughout the time record. Clearly, a more sophisticated scheme for detecting the echo pulse, which is sensitive to the shape of the pulse, is required.

Choice of the cepstrum method for detecting echoes

In choosing a means of quantifying pulse amplitude and arrival time, the needs of an instrument which will ultimately be based on the method have to be considered. The instrument will have to be able to "examine" the acquired data, using a software algorithm, and put a figure on the echo pulse amplitude and time of arrival. The figures thus obtained would be used to give a readout of rock anchor length and grout coverage. To the human eye, the echo in Fig. 3.1 is easily identified because of the natural ability of the brain to recognize patterns. The task is not so easily accomplished by a machine, especially in well-grouted rods, where the echo is smaller than the background signal component.

A short discussion of possible methods for detecting the echo follows, and leads to the cepstrum method. An introduction to the topics below can be found in [4].

Peak detection

The peak detection method is effected by finding an absolute maximum in the part of the signal following the direct pulse. The position of this maximum is assumed to be the pulse arrival time, and its value is assumed to be the echo pulse amplitude. Because the echo pulse is a tone burst, it comprises a number of peaks. The use of peak detection on the signal of Fig. 3.1 would therefore lead to a significant error in quantifying the pulse time of arrival. Further, because the echo pulse is distorted, the relative amplitude of the peaks changes considerably with only small changes in grout coverage of the rod. This leads to a substantial error in the pulse amplitude delivered by the peak detection method. Where the pulse echo is smaller than the background signal, any of the peaks in Fig. 3.1 may be misinterpreted as the echo pulse.

Autocorrelation

The use of the autocorrelation function gives a small improvement over peak detection: the autocorrelation is sensitive to the shape of the pulse and reaches a peak value at the correct pulse time of arrival, where the best "match" between the direct and echo pulses is found. Due to the nature of the autocorrelation function, however, the pulse arrival point is surrounded with other peaks: the autocorrelation produces an "echo pulse" which is a more complex version of the original pulse. This, together with the fact that the autocorrelation is not able to reject the background signal, means that it is not the best method for dealing with the rock anchor signals. Use of the autocorrelation could quite easily cause one of the surrounding peaks to be misinterpreted as the echo arrival, due to the presence and effects of the background signal. This was found to occur often in the rock anchor responses obtained in the laboratory. The autocorrelation of the signal shown in Fig. 3.1 looks very similar to that signal, except that the peaks in the background signal are very nearly the same size as the echo pulse.

Cepstrum

The cepstrum, like the autocorrelation, is sensitive to the shape of the echo pulse and reaches a peak at the pulse time of arrival. The cepstrum, however, offers a significant advantage over the autocorrelation function: the cepstrum identifies a delayed replica of the direct pulse as a *delta function* in the data record produced by the processing, irrespective of the pulse shape. This property of the cepstrum puts it into the class of pattern recognition techniques - a simple peak detection operation performed on the cepstrum of the signal will correctly yield the pulse arrival time and amplitude. Also (as will be seen), the use of the cepstrum allows for rejection of the unwanted (background) signal component. Where noise and

distortion are present in the signal, the delta function marking the echo pulse arrival becomes spread out, but is nevertheless a well-defined, single peak. The cepstrum satisfies all the requirements discussed above, and was thus selected for dealing with the rock anchor responses. A discussion of the cepstrum applied to real (that is, not ideal or synthesized) signals is given in section 3.2. A comparison of the autocorrelation and cepstrum methods applied to signals with noise and distortion can be found in [5].

The remainder of this chapter is devoted to the development of the cepstrum method and enhancements which improve its performance in its application to rock anchor responses. Because it is a specialised topic, a development of the cepstrum method from first principles is given in section 3.1, with a bias towards echo detection (it does have other uses). The concepts introduced in this section are illustrated with a synthesized waveform containing a direct pulse and echoes. In section 3.2 practical issues in the use of the cepstrum are introduced and illustrated with the example rock anchor response. The example is used in the development of the "band-limited envelope cepstrum", the method applied in the final analysis of the results to quantify pulse attenuation and arrival time. Section 3.3 describes a technique for finding the magnitude and group delay response of the acoustic medium. This procedure was not used in the final treatment of the results for reasons given in that section, but is presented here as it may prove valuable in future research on real rock anchor installations.

The two examples used in this chapter will be referred to as "the synthesized waveform" and "the example rock anchor response".

3.1 Cepstrum Theory

3.1.1 The complex cepstrum

Consider a signal y(t), composed of a stimulus x(t) applied to an acoustic system, and the system's response to the stimulus. The response in the problem at hand will take the form of some kind of echo, with amplitude a_0, after a delay t_0. Where the system (which will also be called "the medium" and "the channel") is distortionless and the echo is a delayed and diminished replica of the stimulus, the signal y(t) can be described as follows:

$$y(t) = x(t) + a_0 x(t - t_0) \tag{3.1}$$

Let x(t) be called the "direct" or "source" signal and let y(t) be called the "observed signal". Where the channel introduces some modest distortion into the transmitted pulse, the observed signal can be expressed as:

$$y(t) = x(t) + x(t)*g(t-t_0) \tag{3.2}$$

Here * denotes convolution and g(t) models the frequency-dependent attenuation and dispersion of the channel, but not the gross delay time of the echo which is taken into account by the term ($t-t_0$).

In general, these equations can be written as:

$$y(t) = x(t) + x(t)*h(t) \tag{3.3}$$

where the impulse response of the system h(t) accounts for both the frequency-dependent properties of the medium and the gross time delay t_0.

In what follows, reference will be made to all of these models, and the symbols used will be consistent with their definitions above. Fourier transforming (3.3) above gives:

$$Y(j\omega) = X(j\omega)[1 + H(j\omega)] \tag{3.4}$$

Let $[1 + H(j\omega)]$, which is independent of the source signal, be called "the echo effect". Taking the natural logarithm of this equation makes the source and echo effects additive in the frequency domain:

$$\log[Y(j\omega)] = \log[X(j\omega)] + \log[1 + H(j\omega)] \tag{3.5}$$

If $|H| < 1$, which is usually the case for passive reflectors, the log expansion

$$\log(1+\varepsilon) = \varepsilon - \frac{\varepsilon^2}{2} + \frac{\varepsilon^3}{3} - \frac{\varepsilon^4}{4} + \ldots \tag{3.6}$$

can be used in (3.5) to give:

$$\hat{Y}(j\omega) = \hat{X}(j\omega) + H(j\omega) - \frac{1}{2}H(j\omega)^2 + \frac{1}{3}H(j\omega)^3 - \ldots \tag{3.7}$$

The carets in the above equation denote the logarithmic operation. For the distortionless model of the medium (3.1), $h(t) = a_0\delta(t - t_0)$, so that (3.7) above becomes

$$\hat{Y}(j\omega) = \hat{X}(j\omega) + a_0 e^{-j\omega t_0} - \frac{a_0^2}{2} e^{-j2\omega t_0} + \frac{a_0^3}{3} e^{-j3\omega t_0} - \ldots \tag{3.8}$$

Upon inverse Fourier transforming the above equation, a time signal results in which the additive property introduced by taking logs, is maintained:

$$\hat{y}(\tau) = \hat{x}(\tau) + a_0\delta(\tau - t_0) - \frac{a_0^2}{2}\delta(\tau - 2t_0) + \frac{a_0^3}{3}\delta(\tau - 3t_0) - \ldots \tag{3.9}$$

Although the units of the independent variable τ in the above equation are time, $\hat{y}(\tau)$ has a special meaning and should not be interpreted as an ordinary time signal. To emphasise this special meaning (which will be discussed in the following paragraphs), the symbol τ is used, and the name given to the units of τ is "quefrency" [6]. $\hat{y}(\tau)$ is called the "complex cepstrum" of y(t) and $\hat{x}(\tau)$ is the complex cepstrum of x(t). The process for finding the complex cepstrum of y(t) is summed up in the following equation:

$$\hat{y}(\tau) = \mathcal{F}^{-1}\{\log \mathcal{F}\{y(t)\}\} \tag{3.10}$$

where $\mathcal{F}\{\cdot\}$ denotes the operation of Fourier transformation. Some noteworthy features of the cepstrum example given above are:

* The convolutional relationship between the source and impulse response in (3.3) has been transformed to an additive one in (3.9).

* The source and echo effects are separated and clearly distinguishable in the cepstrum, the source effect appearing as $\hat{x}(\tau)$ and the echo effect appearing as the series of delta functions in (3.9). This will be demonstrated graphically in the synthesized waveform which is given below. Separation of these components in the cepstrum is often possible, even if the direct and echo signals overlap in time, but there are of course limits to this separability. Some prerequisites for separability are mentioned after the example below.

* Delta functions occur at multiples of the echo delay time t_0 and the size of the first delta function, at the time of arrival of the echo, is directly proportional to the size of the echo $a_0x(t-t_0)$.

* The distortion of the spectrum introduced by the log function in (3.5) gives rise to the infinite series of delta functions in (3.9), even though only one echo is present in the observed signal.

* A second echo in the observed signal, at twice the delay time t_0, gives rise to another infinite series of delta functions in quefrency, beginning at $2t_0$ in (3.9). This second series of delta functions interferes with the second and higher order delta functions (also called

"rahmonics") of the first reflection, making it difficult to identify the second reflection and ascertain its size. The first (fundamental) rahmonic due to the first reflection remains inviolate, however, and is therefore a direct indicator of the amplitude of the first reflection.

* In spite of its name, the complex cepstrum is real-valued because inverse Fourier transformation of the conjugate-even function $\hat{Y}(j\omega)$ produces a real-valued function. Its name is derived from the fact that complex algebra is used in every step of the calculation of $\hat{y}(\tau)$ and all the information in y(t) is present in $\hat{y}(\tau)$; y(t) is fully recovered in following the reverse of all the operations used to find $\hat{y}(\tau)$.

The process of recovering y(t) from its cepstral form is summarised in the following equation:

$$y(t) = \mathcal{F}^{-1}\{\exp \mathcal{F}\{\hat{y}(\tau)\}\} \tag{3.11}$$

Because of the two transform operations in (3.10), the way in which the cepstral domain relates to the frequency domain has much in common with the way in which the frequency domain relates to the time domain.

In keeping with this analogy between the two relationships, the terms in the table below have been proposed [6] (and are now generally accepted) in the cepstrum literature:

Original Term	Derived Term
Spectrum	Cepstrum
Frequency	Quefrency
Phase	Saphe
Period	Repiod
Harmonic	Rahmonic
Magnitude	Gamnitude
Filter	Lifter

Table 3.1 Some accepted terms from the cepstrum literature

Where the terms in the right-hand column arise in the text, Table 3.1 above should be consulted - the meaning of a derived term in the cepstrum can be inferred from the meaning of the original term in the spectrum.

Example using a synthesized waveform

The synthesized waveform and its cepstrum are given here to illustrate some of the concepts discussed above. Fig. 3.2 is the graph of a signal containing a stimulus (a decaying sine wave) and two distortionless echoes, not well separated in time [7:18]. Figures 3.3 and 3.4 show the log magnitude $\log Y_m(\omega)$ and phase $\phi_y(\omega)$ which need to be found in the evaluation of (3.5), and Fig. 3.5 shows the cepstrum as derived in equation (3.9). The source effect $\mathcal{E}(\tau)$ is clearly limited to regions near the time origin $\tau = 0$ and the echo effect appears at $\tau = t_0$ (0,30ms in the figure), along with its rahmonics.

Finding the complex log of the spectrum

The usual method for calculation of the complex log of Y(jω) is to convert Y(jω) to its polar representation:

$$Y(j\omega) = Y_m(j\omega)e^{j\phi_y(\omega)} \tag{3.12}$$

The complex log of Y(jω) is then

$$\log[Y(j\omega)] = \log\left[Y_m(\omega)e^{j\phi_y(\omega)}\right] = \log Y_m(\omega) + j\phi_y(\omega) \tag{3.13}$$

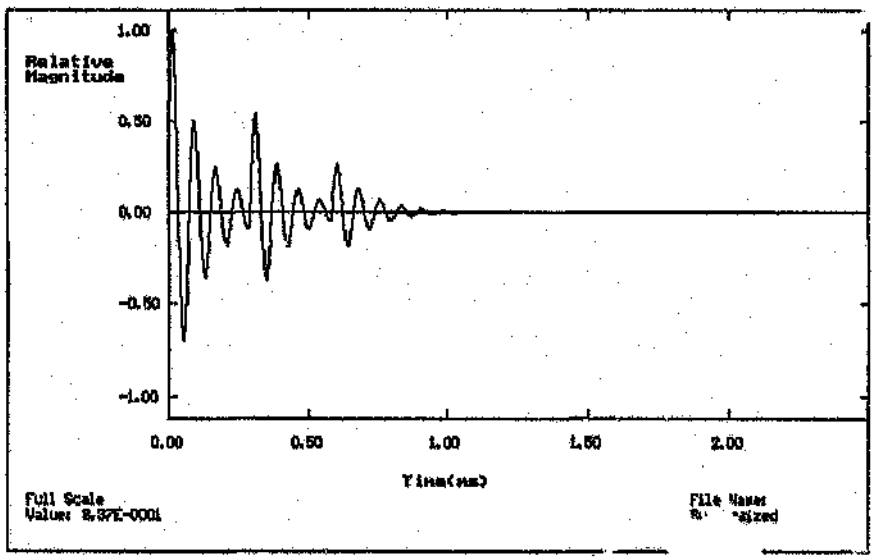

Figure 3.2 Synthesized waveform comprising a stimulus and two distortionless echoes

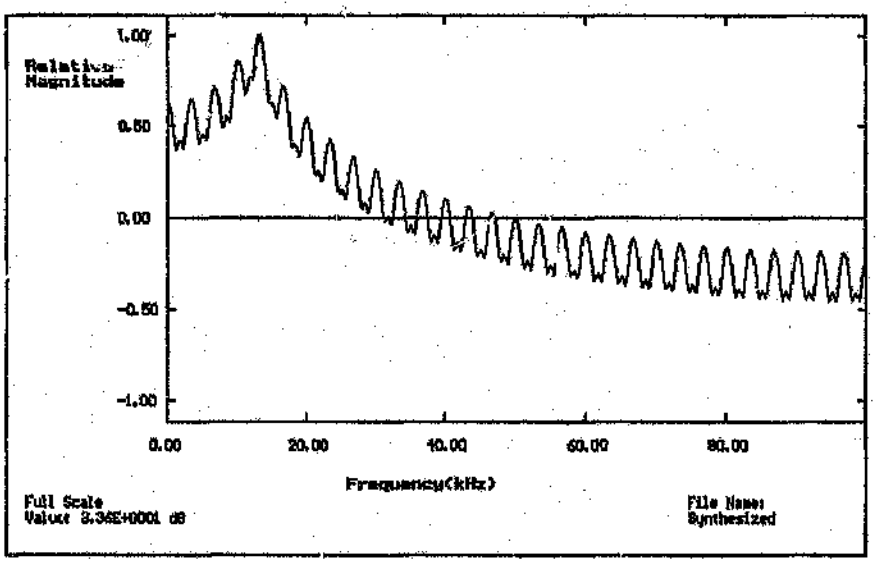

Figure 3.3 Log magnitude spectrum of synthesized waveform

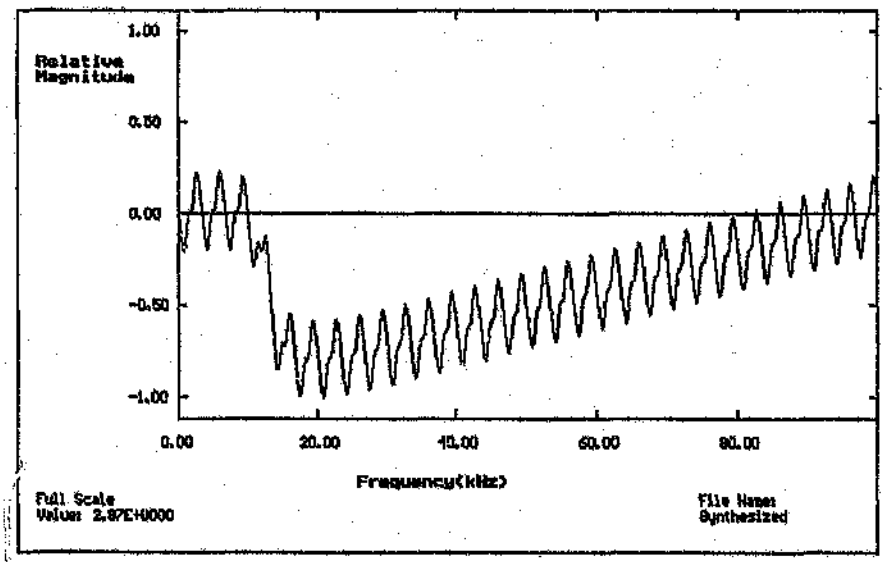

Figure 3.4 Phase spectrum of synthesized waveform

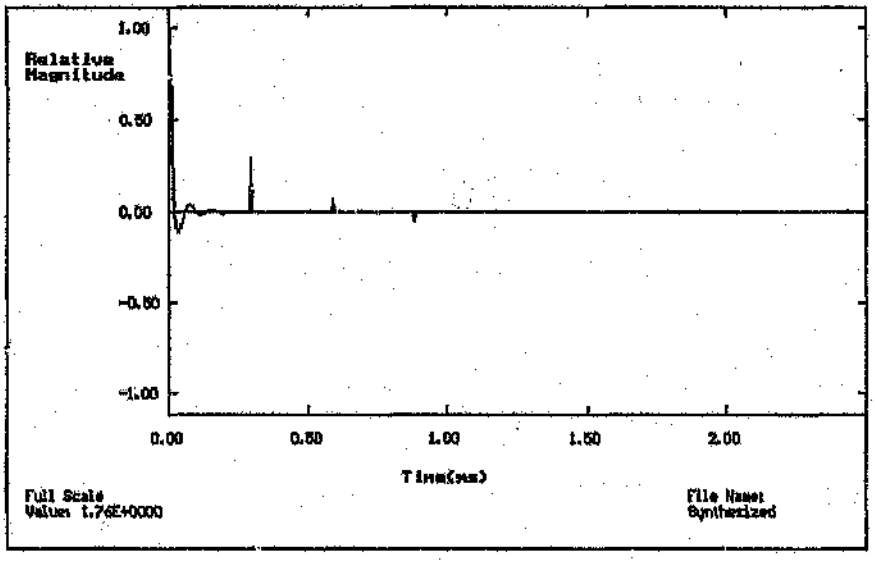

Figure 3.5 Complex cepstrum of synthesized waveform

Phase calculation

If $\phi_y(\omega)$ is calculated using the arctangent routine, its value modulo 2π will be found. Because of the need for $\phi_y(\omega)$ to be analytic on the unit circle [4], it has to be unwrapped (converted to a continuous function) before the inverse Fourier transform of $\hat{Y}(j\omega)$ can be taken, to find $\hat{y}(\tau)$. The simplest way of unwrapping $\phi_y(\omega)$ is to search for discontinuities of more than π and to subtract or add 2π to the cumulative phase at these points, whichever is appropriate. This method is suitable for functions which change slowly with ω, but for functions which are not so "well-behaved", a more sophisticated method is called for [4], [8], [9].

A strong linear phase component in $\phi_y(\omega)$ aggravates the problem of phase unwrapping - a standard procedure for reducing the number of discontinuities it has is to remove the bulk of its linear component by re-positioning the time origin of y(t) before finding the forward Fourier transform of y(t) [7:34], [10:1434]. Any remaining component can then be removed, if so desired, in the frequency domain. $\phi_y(\omega)$ has to be calculated in radians so that the units of (3.13) are compatible.

Log magnitude calculation

Calculation of $\log Y_m(\omega)$ presents a problem when nulls in $Y_m(\omega)$ occur. This can happen where synthesized data is used, but $\log Y_m(\omega)$ is usually limited to finite values by the noise content of $Y_m(\omega)$ when "real" data is used. It is standard procedure to remove the average value of $\log Y_m(\omega)$ before inverse transforming $\hat{Y}(j\omega)$ [7:34]: this average value amounts to a scaling factor in y(t), and can be re-inserted when performing the reverse operations to recover y(t). Similarly, the linear phase component removed from $\phi_y(\omega)$ can be re-inserted if y(t) needs to be fully recovered (positioned correctly in its time record).

Waveform editing

Source signal recovery and echo removal

Because the complex cepstrum is reversible, the source signal x(t) can be recovered from the observed signal if the source and echo effects are sufficiently well separated in quefrency. This is done by removing (or "liftering") the echo effect, including all its rahmonics, from the cepstrum to obtain only the source information $\hat{x}(\tau)$. When the inverse cepstrum (3.11) of $\hat{x}(\tau)$ is calculated, the source signal x(t) is recovered. Fig. 3.6 shows the source signal of the synthesized waveform, recovered by notch liftering the cepstrum shown in Fig. 3.5. This method of source signal recovery ("homomorphic deconvolution") has been used extensively by seismologists to recover the source signal or "wavelet", as they call it, from seismic events [8], [10], [11], [12].

Impulse and frequency response extraction

The cepstrum of the model of systems with modest distortion (3.2) can be shown to be:

$$\hat{y}(\tau) = \hat{x}(\tau) + g(\tau - t_0) - \frac{1}{2} g(\tau - 2t_0) * g(\tau - 2t_0) + \frac{1}{3} g(\tau - 3t_0) * g(\tau - 3t_0) * g(\tau - 3t_0) - \ldots \qquad (3.14)$$

by using $H(j\omega) = G(j\omega)e^{-j\omega t_0}$ in (3.7). In the above equation, it is seen that the impulse response g(t) of the system appears in place of the delta functions of equation (3.9). The fundamental rahmonic of (3.14) is the in.. .se response of the system, and the higher rahmonics are convolutions of the impulse response with itself. This useful feature of the cepstrum makes it possible to find the frequency response of the system directly: isolating the impulse response in (3.14) and forward Fourier transforming it gives $G(j\omega)$. This application of the cepstrum has been demonstrated in the measurement of transfer functions and acoustical reflection coefficients [13].

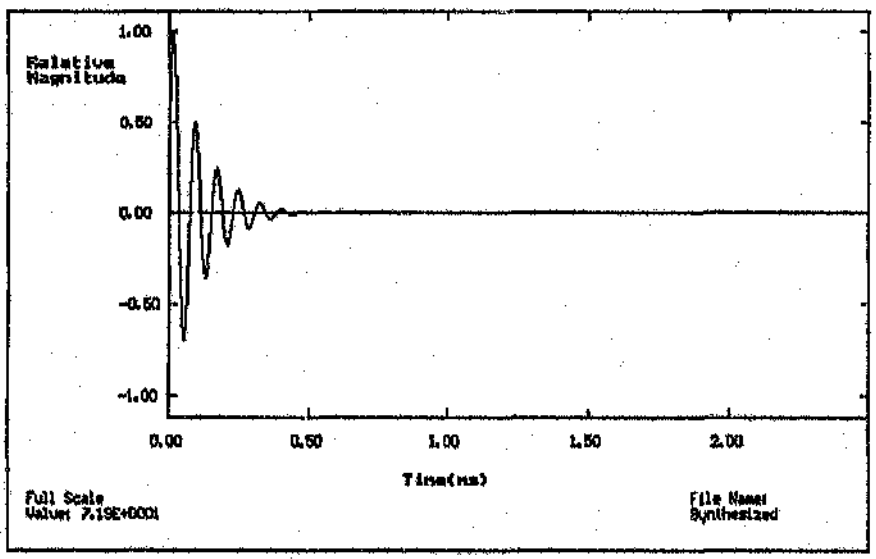

Figure 3.6 Source signal recovered from synthesized waveform

An alternative means of finding the impulse response is to lifter the source component $\hat{x}(\tau)$ from the cepstrum and perform an inverse cepstrum operation on the remaining echo effect and its rahmonics. This could possibly be more effective where reflections are large and the cepstral separation of source and echo effects is not very good.

The success with which the source signal or impulse response can be found using the above methods depends on how well the source signal and impulse response are separated in quefrency. This separability is, in turn, highly dependent on the signals being analyzed [10], [12]. If the source signal $\hat{X}(j\omega)$ has a broadband characteristic which varies slowly with frequency (that is, contains only low quefrency components) and if the echo effect $[\log(1+H(j\omega))]$ varies rapidly with frequency and has no slowly-varying components (that

is, contains only high quefrency components), then the source and echo effects will be well separated in quefrency: $\hat{x}(\tau)$ will be confined to the region near $\tau = 0$ and the echo effect $a_0 g(\tau - t_0)$ will be confined to the region around $\tau = t_0$. More will be said about the question of separability in the discussion of the power cepstrum.

3.1.2 The power cepstrum

The purpose of analyzing the power cepstrum in this section, apart from being a treatment of the power cepstrum in its own right, is to provide a basis for the discussion of the envelope cepstrum in section 3.1.3. The detail in which the power cepstrum is treated here should therefore be noted as being a step in dealing with the envelope cepstrum.

The original definition of the cepstrum [6] was what is now called the power cepstrum:

$$\hat{y}_p(\tau) = |\mathcal{F}^{-1}\{\log|\mathcal{F}\{y(t)\}|^2\}|^2 \tag{3.15}$$

The power cepstrum of a function can be described as the power spectrum of the logarithm of the power spectrum of that function. Alternative definitions exist, and the one used here is after [10]. Three effects of using the power cepstrum instead of the complex cepstrum which are immediately evident from (3.15) above, are:

(i) The use of inverse or forward Fourier transforms in (3.15) is immaterial because each power spectrum produced is real and even. As a consequence of this, the power cepstrum is real and even. The inverse Fourier transform is indicated in (3.15) for consistency with the earlier definition (3.1C) of the complex cepstrum.

(ii) A consequence of discarding phase information by using the squared magnitude of the transforms in (3.15) is that y(t) cannot be recovered from $\hat{y}_p(\tau)$ (because information is lost). Waveform editing (for echo removal, for example) is therefore not possible with the power cepstrum.

(iii) The use of power spectra obviates the need for phase unwrapping, because phase information is discarded in (3.15).

Although waveform editing cannot be performed using the power cepstrum, it is generally agreed [14:745], [10:1434] that it is the superior method where amplitude and time of arrival of an echo need to be determined. According to [10], the reason for this superiority is that the phase term $\phi_y(\omega)$ in (3.13) masks the echo in the cepstrum when real data is used. Because of points (i) and (iii) above, practical use of the power cepstrum is easier than that of the

complex cepstrum. Use of the power cepstrum is therefore recommended when only arrival time and amplitude of echoes have to be found; the complex cepstrum is used only when waveform editing or preservation of phase information in the frequency domain is necessary.

How the power cepstrum relates to the complex cepstrum

The power spectrum of the signal described in model (3.2) is:

$$|Y(j\omega)|^2 = |X(j\omega)|^2 \left|1 + G(j\omega)e^{-j\omega t_0}\right|^2 \tag{3.16}$$

The logarithm of the above equation can be expressed as:

$$\log|Y(j\omega)|^2 = \log[X(j\omega)X(j\omega)^*] + \log\left[\left(1 + G(j\omega)e^{-j\omega t_0}\right)\left(1 + G(j\omega)^* e^{j\omega t_0}\right)\right] \tag{3.17}$$

where the superscript * denotes complex conjugation. Expanding the log terms,

$$\begin{aligned}\log|Y(j\omega)|^2 = {} & \log X(j\omega) + \log X(j\omega)^* \\ & + G(j\omega)e^{-j\omega t_0} - \frac{1}{2}G(j\omega)^2 e^{-j2\omega t_0} + \frac{1}{3}G(j\omega)^3 e^{-j3\omega t_0} + \dots \\ & + G(j\omega)^* e^{j\omega t_0} - \frac{1}{2}G(j\omega)^{*2} e^{j2\omega t_0} + \frac{1}{3}G(j\omega)^{*3} e^{j3\omega t_0} + \dots\end{aligned} \tag{3.18}$$

The squared magnitude of the inverse Fourier transform of the above equation is:

$$\begin{aligned}\hat{y}_p(\tau) = {} & [\hat{x}(\tau) + \hat{x}(-\tau) \\ & + g(\tau - t_0) - \frac{1}{2}g(\tau - 2t_0) * g(\tau - 2t_0) + \frac{1}{3}g(\tau - 3t_0) * g(\tau - 3t_0) * g(\tau - 3t_0) - \dots \\ & + g(-\tau - t_0) - \frac{1}{2}g(-\tau - 2t_0) * g(-\tau - 2t_0) + \frac{1}{3}g(-\tau - 3t_0) * g(-\tau - 3t_0) * g(-\tau - 3t_0) - \dots]^2\end{aligned} \tag{3.19}$$

Equation (3.19) shows how the power cepstrum relates to the complex cepstrum (3.14), and is clearly an even function of τ. The echo information and its rahmonics appear at the same quefrencies as for the complex cepstrum, as well as in the negative quefrencies. Also, the cepstrum is squared; taking the square root of this cepstrum leads to what could be called an "amplitude cepstrum" :

$$\hat{y}_a(\tau) = \left|\mathcal{F}^{-1}\{\log|\mathcal{F}\{y(t)\}|^2\}\right| \tag{3.20}$$

The amplitude cepstrum gives echo information which is more consistent with that of the complex cepstrum, because in taking the square root of the power cepstrum the proportionality between the echo amplitude and echo effect in the cepstrum is restored. This definition of the amplitude cepstrum concurs with that of [7].

Note that taking the inverse Fourier transform of (3.16) above gives the autocorrelation function of y(t) - it is the action of finding the logarithm of the spectrum which gives the cepstrum its distinctive features.

Fig. 3.7 shows the amplitude cepstrum of the synthesized signal. Note its similarity to the complex cepstrum of Fig. 3.5.

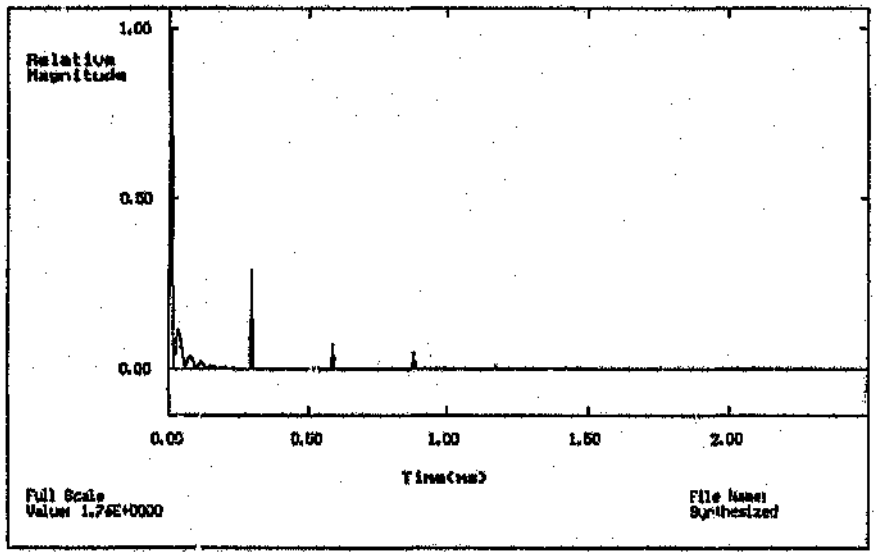

Figure 3.7 Amplitude cepstrum of synthesized waveform

Periodicity in the log spectrum as the bearer of reflection information

The contribution to the log spectrum of the echo effect in (3.16) above is:

$$\hat{Z}(j\omega) = \log\left|1 + G(j\omega)e^{-j\omega t_0}\right|^2 \qquad (3.21)$$

Using the polar representation of G,

$$G(j\omega) = G_m(\omega)e^{j\phi_g(\omega)} \tag{3.22}$$

the echo effect can be written as:

$$\hat{Z}(j\omega) = \log\left|1 + G_m(\omega)e^{-j(\omega t_0 - \phi_g(\omega))}\right|^2 \tag{3.23}$$

Expanding this expression using de Moivre's relation gives:

$$\hat{Z}(j\omega) = \log|1 + G_m(\omega)\mathrm{Cos}[\omega t_0 - \phi_g(\omega)] - jG_m(\omega)\mathrm{Sin}[\omega t_0 - \phi_g(\omega)]|^2 \tag{3.24}$$

Evaluating the squared-magnitude term and using the log expansion series (3.6) leads to:

$$\hat{Z}(j\omega) = 2G_m(\omega)\mathrm{Cos}[\omega t_0 - \phi_g(\omega)] - G_m(\omega)^2\mathrm{Cos}\,2[\omega t_0 - \phi_g(\omega)] + \ldots \tag{3.25}$$

When $G(j\omega)$ has a small magnitude and shows little dependence on frequency (as in the distortionless model of the system), the cosine terms in (3.25) above form an even rahmonic series in the log spectrum. It is this cosinusoidal ripple in the log spectrum which gives rise to the delta functions in the cepstrum when (3.25) above is inverse Fourier transformed. The magnitude ($2G_m(\omega)$) and repiod ($\frac{2\pi}{t_0}$) of the first rahmonic in (3.25) contain all the reflection information required, the amplitude of the ripple relating to the magnitude of the echo and the repiod giving the time of arrival of the echo.

Fig. 3.3 clearly shows the cosinusoidal ripple in the log magnitude spectrum which contains the reflection information: the Fourier transform of the source signal alone has the same broad shape as Fig. 3.3, but lacks the fine cosinusoidal ripple seen in the figure. When the edium is not distortionless, the exact rahmonic structure of (3.25) is disturbed and the delta functions in the cepstrum become spread out over a range of quefrencies. If the distortion caused by the medium is not too severe, the cosinusoidal ripple in (3.25) is clearly discernible but is "amplitude modulated" by $G_m(\omega)$ and "phase modulated" by $\phi_g(\omega)$ in (3.25) above - hence the term "spectral modulation" [10:1430] which is used to describe these effects. As will be seen later, identifying and making use of this periodic component in the log spectrum is of fundamental importance when dealing with band the limited reflections which occur in rock anchor responses.

Another accepted definition of the power cepstrum [7] is:

$$\hat{y}_p(\tau) = \mathcal{F}^{-1}\{\log|\mathcal{F}\{y(t)\}|^2\} \tag{3.26}$$

This definition is different to the previous one only in that the inverse transform is not followed by a magnitude-squared operation. The mathematical analysis and properties of the previous definition (3.15) of the power cepstrum apply equally to this definition, save for some minor differences introduced by the squaring operation (see equations (3.15) and (3.19)). As will be seen shortly, the above definition is useful in relating the envelope cepstrum to the power cepstrum.

3.1.3 The envelope cepstrum

This version of the cepstrum is defined as:

$$\hat{y}_e(\tau) = |\mathcal{F}^{-1}\{\log|\mathcal{F}_1\{y(t)\}|^2\}| \tag{3.27}$$

where $|\mathcal{F}_1\{\cdot\}|^2$ denotes the single-sided (that is, negative frequency components set to zero) power spectrum of the operand.

Because the single-sided power spectrum is used in its definition (3.27), a mathematical analysis of the envelope cepstrum is substantially more involved than that of the power cepstrum. The expression of the envelope cepstrum in terms of the impulse response g(t) is more complex than the equivalent expression (3.19) for the power cepstrum, and is not particularly illuminating. The envelope cepstrum can be better understood by relating it to its close counterpart, the power cepstrum. Therefore, instead of treating the envelope cepstrum in the same mathematical detail as was done for the power cepstrum, the approach taken here will be to express the envelope cepstrum in terms of the power cepstrum. This allows conclusions about the properties of the envelope cepstrum to be drawn from the analysis of the power cepstrum in section 3.1.2.

The power spectrum of the original time wave is even, and so in zeroing the negative portion of the spectrum in creating the envelope cepstrum, no information is lost: the difference between the power and envelope cepstrum is a "mathematical" one. The features (i) to (iii) of the power cepstrum in section 3.1.2 apply also to the envelope cepstrum, and the spectral ripple remains the bearer of reflection information, as discussed in that section. The relationship between the envelope and power cepstrum, and its implications, are discussed in the following paragraphs.

How the envelope and power cepstrum are related

In relating the envelope cepstrum to the power cepstrum, the definition (3.26) of the power cepstrum will be used. The product of inverse transforming a real, single-sided sequence is a complex sequence in which the imaginary part (which is odd) is the inverse Hilbert transform of the real part (which is even). Further, the real part of this inverse transform is half of the "true" power cepstrum - the cepstrum obtained by inverse transforming the double-sided log power spectrum. The above relations arise as a result of the fact that any real sequence can be decomposed into an odd and an even part which are related by the sign function [7:7]. The envelope cepstrum is then formed by finding the magnitude of the sequence produced by the inverse transform, as indicated in (3.27). The way in which the envelope and power cepstrum are related can thus be worded as follows: The envelope cepstrum is half the square root of the sum of the square of the power cepstrum and the square of the Hilbert transform of the power cepstrum:

$$\hat{y}_e(\tau) = \frac{1}{2}\sqrt{\hat{y}_p(\tau)^2 + \mathcal{H}\{\hat{y}_p(\tau)\}^2} \tag{3.28}$$

where $\mathcal{H}\{\cdot\}$ denotes the operation of Hilbert transformation.

Advantage of using the envelope cepstrum

The envelope and power cepstrum are equally effective in giving amplitude and time of arrival information about echoes, except where a power spectrum has been band-limited and has its frequency origin incorrectly positioned (this situation could arise, for example, when using a spectrum analyzer which performs a frequency sweep over a limited band). In this case (or any case where the saphe of the cosinusoidal ripples of equation (3.25) has been shifted), the power cepstrum does not give the amplitude of the echo correctly. Strictly speaking, the fault here lies not with the power cepstrum itself, but with attempting to form a double-sided spectrum from incorrectly positioned information. The envelope cepstrum, on the other hand, will always give the correct echo amplitude because of its insensitivity to the saphe of the spectral ripple. Fig. 3.8 shows the envelope cepstrum of the synthesized waveform.

Although the power and envelope cepstra have different appearances the echo amplitude values they give at the time of arrival of the echo are the same, save for the factor of two in (3.28). This is because the Hilbert transform of $\hat{y}_p(\tau)$ zeroes at the arrival time of the echo [7:10]. Thus, the envelope cepstrum is deemed to be the easiest and most reliable cepstrum to use, where the amplitude and arrival time of echoes need to be found. Note that the Hilbert

transform is not actually used to calculate the envelope cepstrum: its appearance is merely a consequence of using the single-sided power spectrum, and is needed to describe the relationship between the envelope and the power cepstrum mathematically.

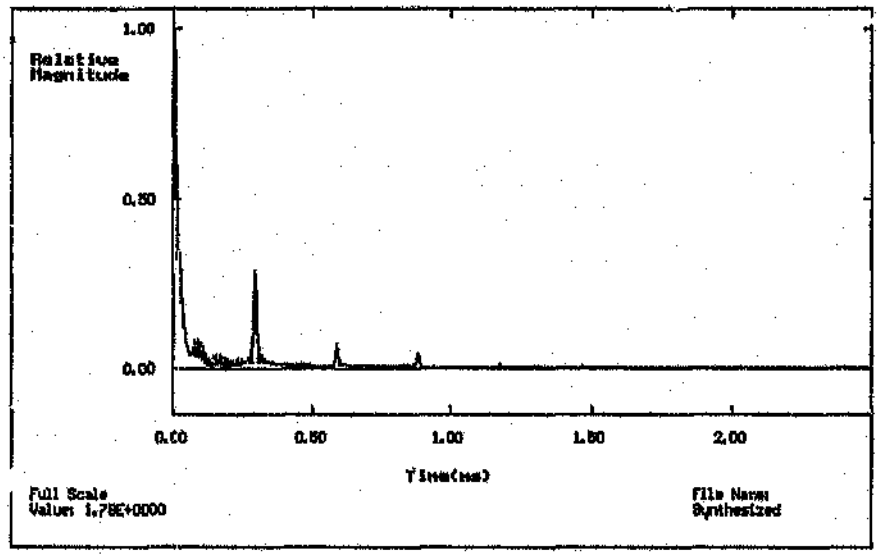

Figure 3.8 Envelope cepstrum of synthesized waveform

The leakage seen in the cepstrum of Fig. 3.8 is due to the truncation of the log spectrum to make it single-sided. A tapered window in the frequency domain can be used to reduce this leakage if it is undesirable. Naturally, the choice of this window would have to be made judiciously to avoid discarding echo information which is important. More will be said about windowing frequency domain data in the discussion of the cepstrum and real data, below.

3.2 Use of the Cepstrum on Real Data

When dealing with real data, the Fourier transform operators of section 3.1 must necessarily be replaced with the discrete Fourier transform (DFT) because of the use of finite length sampled data sequences. This leads to the usual problems of leakage and aliasing associated with the truncation and sampling of a continuous signal. By adjusting the record length (number of samples) and sampling rate and with sufficient attention to the design of analogue circuitry, these phenomena can be kept at an acceptable level - whatever the "acceptable level" for the particular application happens to be. If the record length is made to be a power of two, the fast Fourier transform (FFT), which is a special and efficient case of the DFT, can be used to operate on the data.

In addition to the considerations above, some difficulties peculiar to the cepstrum arise when cepstral techniques are employed. Each of these is introduced below, along with a means of alleviating the problem.

It has been observed that the problems associated with the cepstrum are highly data dependent [10:1428], [12:259], and the application in this case is no exception: the methods described here were developed with a bias towards the rock anchor problem and the emphasis on, and relevance of, these methods may shift in another application.

3.2.1 Problems peculiar to the cepstrum

Out of band noise - band-limited signals

If the FFT of the composite signal y(t) does not occupy the entire discrete spectrum, noise will dominate the spectrum in the "out of band" regions. Where the energy content of this noise is usually insignificant in normal spectra, it may be comparable to, or even greater than, the signal level in the log spectrum. This out of band noise in the log spectrum produces a "noisy" cepstrum and tends to mask the echo information and its rahmonics in the cepstrum.

If y(t) has a low-pass characteristic (due to a low-pass anti-aliasing filter, for example) then careful choice of the sampling rate or low-pass cutoff point will give a signal which just fills the discrete spectrum. If the signal y(t) has a band-pass characteristic (this could be caused by a transducer response or the characteristics of the excitation signal, for example), some other means of dealing with the noise problem is required. Tribolet [8] has suggested a method which maps the band-pass signal to a full-band signal. The more commonly used and less computationally intensive technique, however, is simply the application of a window to the frequency domain data [15].

In band noise

The effect of in band noise has been researched by Hassab and Boucher [5] who have found that in addition to producing a noisy cepstrum, the in band noise has the effect of reducing the amplitude of the echo indicated by the cepstrum. This amplitude reduction is troublesome only at relatively low signal to noise ratios (SNRs) and is therefore not a point of concern in the rock anchor problem, where the in band SNR was typically 40dB. Where possible, time and cepstral averaging alleviate the problem. Cepstral averaging is computationally intensive, however, and [15:27] has reported subtle difficulties caused by averaging the cepstrum.

Cepstral aliasing

Finding the logarithm of the magnitude spectrum introduces a rahmonic series into the spectrum. If the "sampling rate" in the spectrum is too low, these higher rahmonics alias in the cepstrum. Cepstral aliasing worstens as the echo delay increases and as the echo becomes stronger: for large echo delays, the spacing of rahmonics in the cepstrum is large. For strong echoes the log expansion series (3.6) converges slowly, giving a large number of echo rahmonics with significant amplitude, which extend over a broad range of quefrencies. Commonly used means of combating cepstral aliasing are:

* Extending the time record with zeroes [15:27]. This effectively increases the "sampling rate" in the frequency domain.

* Weighting the time record with an exponentially decaying sequence [10:1437].

Spectral notching

Spectral nulls appear as deep notches in the log magnitude spectrum. These deep notches cause slowly decaying oscillations in the cepstrum [15:25] and in so doing, degrade the cepstral separation of source and echo effects. Spectral notching can be caused by filter, transducer or excitation signal characteristics and can be avoided by ensuring that all of these have a broad, smooth behaviour in the frequency domain. In general, any fine structure (or "spectral roughness") in the source signal's spectrum manifests itself as high-quefrency components in the cepstrum [...:221] and should be done away with if good cepstral separation of source and echo effects is to be obtained.

3.2.2 The envelope cepstrum applied to the example rock anchor response

A full description of the envelope cepstrum technique applied to the example rock anchor response of Fig 3.1 is given here. This technique was the one used in the final analysis of the rock anchor responses and includes enhancements which take advantage of characteristics specific to the rock anchor responses. To provide a background for the discussion of these enhancements, a brief introduction to the characteristics of the log magnitude spectrum of the example follows.

Observations on the example rock anchor response

Fig. 3.9 shows the log magnitude spectrum of the time record of the example. The source signal component of this spectrum, $\hat{X}(j\omega)$, which combines additively with the echo information, is shown in Fig. 3.10.

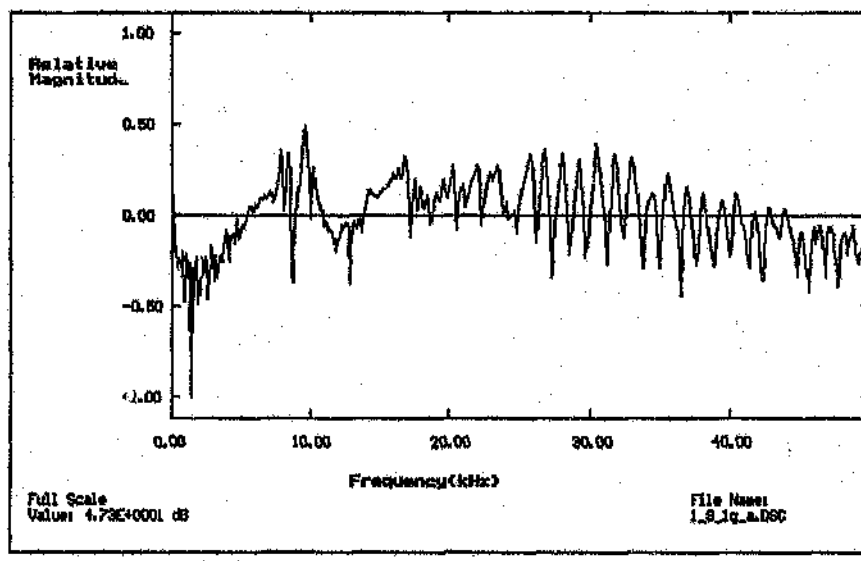

Figure 3.9 Log magnitude spectrum of example rock anchor response .

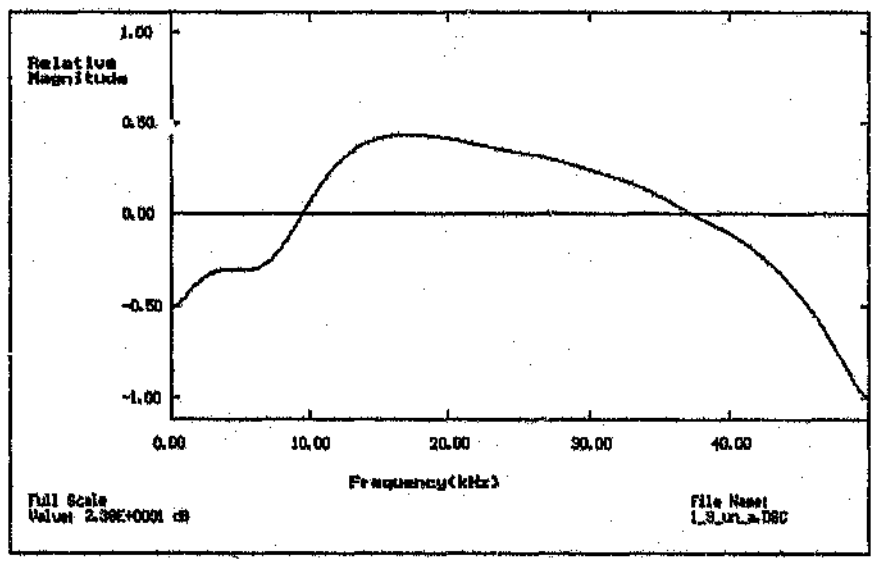

Figure 3.10 Log magnitude spectrum of source signal used to stimulate rock anchor

This source component was found by isolating a single pulse in the time response of the free rock anchor (that is, the same rock anchor with no concrete cladding) and calculating its log magnitude spectrum. Note that $\hat{X}(j\omega)$ has the smooth, broad and slowly varying properties required of a good source signal. Bearing in mind the characteristics of the source signal, the following observations about the combined log magnitude spectrum can be made:

* The echo information (spectral ripple) is strongly band-limited to the band above 25kHz, even though the source signal's energy spectral density peaks at about 17kHz.

* The region 5kHz to 25kHz contains peaks which are not echo information, but appear to be connected with some other characteristic of the medium. Note that this is an "in band" region - source signal components exist in this band, but have not returned to the point of excitation as a coherent reflection.

* A small area around 0kHz is dominated by noise, due to a low SNR at those frequencies.

The envelope cepstrum technique with enhancements

An explanation of some of the steps in the procedure below will be given in the "discussion" which follows point (iv).

(i) The FFT of the composite signal y(t) is found, giving $Y(j\omega)$. The magnitude of $Y(j\omega)$ is calculated and phase information is discarded.

(ii) The logarithm of $Y_m(\omega)$, the magnitude spectrum, is found and its average component is removed, giving $\hat{Y}_m(\omega)$. Note that the average value, in this context, means the average of the spectrum and not the average value of the time record. All negative frequency components (that is, the upper half of the spectrum produced by the FFT) are zeroed, in accordance with the definition of the envelope cepstrum (3.27). Performing a magnitude inverse FFT operation on the frequency domain data record at this point would give the "full band" envelope cepstrum shown in Fig. 3.11.

(iii) The log magnitude spectrum is high-pass liftered with an FIR (finite impulse response) lifter, to remove source components $\hat{X}(\omega)$ from the spectrum. The FIR lifter is a conventional FIR filter, applied to frequency domain data. After liftering, the band of frequencies identified as carrying the reflection information is selected with a rectangular window (all other frequency components being set to zero). The choice of lifter and window used at this point will be discussed in the paragraphs which follow point (iv).

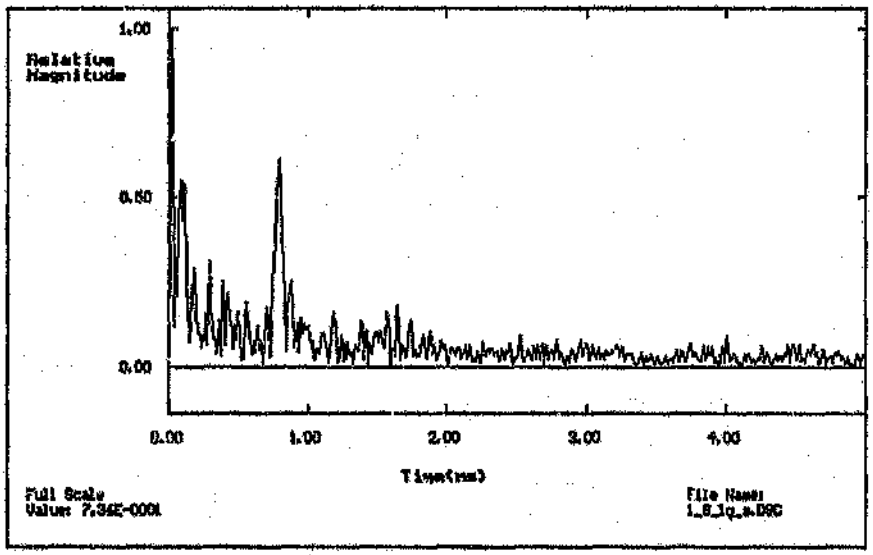

Figure 3.11 Full band envelope cepstrum of example rock anchor response

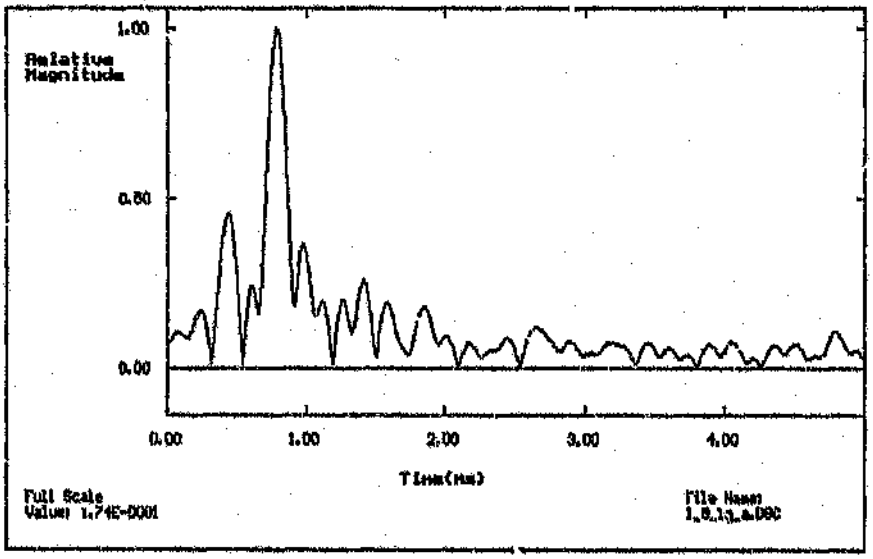

Figure 3.12 Band-limited envelope cepstrum of example rock anchor response

(iv) The magnitude of the inverse FFT of the data remaining in the frequency domain data record is found. This gives what could be called "a band-limited envelope cepstrum", and is shown in Fig. 3.12 for the example rock anchor response. The time of arrival of the pulse indicated by the cepstrum (0,78ms) agrees with the position of the echo seen in the time record, Fig. 3.1.

Discussion

The actions taken above, especially in step (iii), demand some explanation. The primary purpose of step (iii) is to take advantage of the fact that the echo information is band-limited, by selecting only that information with a window. The cepstrum is improved by rejecting both the noise and the "in band" regions which do not contain echo information: the band 5kHz to 25kHz seen in the log magnitude spectrum of Fig. 3.9 contains high quefrency components which, rather than contributing to the echo information, have a destructive effect on the cepstrum. The severity of this "destructive effect" increases with smaller echoes, as will be seen in the presentation of the results. With the relatively strong echo of this example the advantage of the band-limited cepstrum (Fig. 3.12) over the conventional cepstrum (Fig. 3.11) is not immediately obvious.

The motive for liftering is to remove source components from the spectrum: since liftering in the frequency domain is equivalent to windowing in the quefrency domain, a high-pass lifter will remove source components (low quefrencies) from the cepstrum. Because the envelope cepstrum is insensitive to the saphe of the spectral ripple, the saphe shift caused by the FIR lifter does not affect the cepstrum obtained. The design details of the lifter will, of course, depend on the application. In this example the lifter was a 45th order high-pass filter with a cutoff replod of 4,88kHz, corresponding to a cutoff quefrency of 0,21ms. The cutoff quefrency of the lifter will place a limit on the earliest echo detectable in the cepstrum; in this case it is 0,21ms. The use of a reasonably low cutoff quefrency lifter does not handicap the method because very low quefrency components can be considered to be part of the source signal, which for practical purposes are indistinguishable from the source signal.

Although a rectangular window was used to select the echo information, any window which suits the application can be used to further reduce leakage in the cepstrum. In the case of rock anchor responses it was found empirically that using a tapered window tends to discard useful information which exists near the band edges, because the responses are strongly band-limited. Van Veen [15:26], in his analysis of snow, found it useful to apply a cosine

taper at the edges of his window, where the quality of the spectral ripple decays gradually towards the edges of his window. The band 32kHz to 39kHz was used to produce the cepstrum shown in Fig. 3.12.

An alternative to liftering to remove the source component is simply to subtract it from the spectrum, if it is known. The advantage of liftering, however, is that the source signal need not be known *a priori* and that the memory needed for storage of the source signal is saved in a real instrument. This is subject, of course, to the proviso that the source signal is smooth (contains only low quefrency components).

The method described in this section for finding band-limited envelope cepstra is summarised in Fig. 3.13.

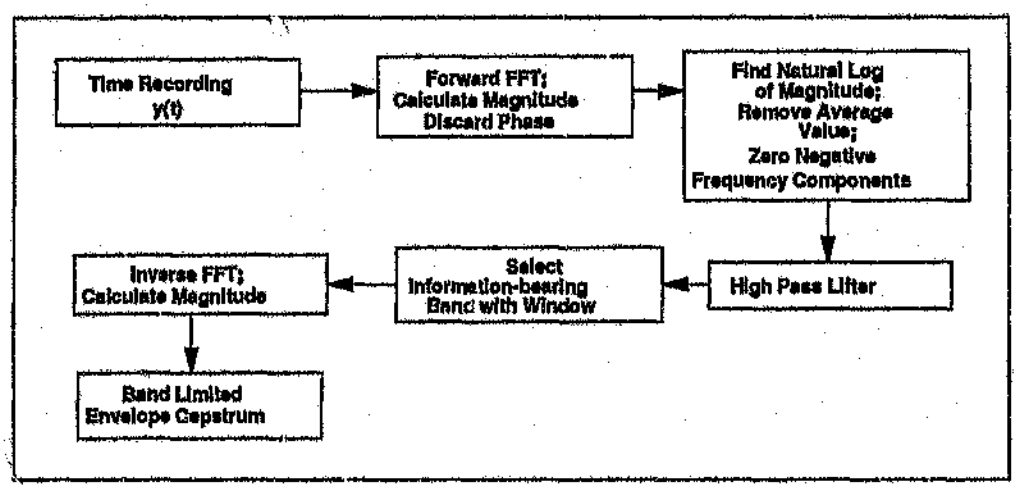

Figure 3.13 The envelope cepstrum with enhancements

3.3 Extraction of System Frequency Response over a Limited Band

In this section, a technique for the extraction of the system frequency response $H(j\omega)$ over a limited band of frequencies will be described. The reason for treating the signal over a limited frequency band is, of course, because of the natural band-limiting of echo information seen in the rock anchor responses.

The technique was developed because it was thought that the "dispersiveness" of the medium could possibly relate better to grout coverage than does the pulse attenuation. Although it must be true that the dispersion of the pulse increases with increasing grout coverage, it was

found that the group delay response does not change uniformly and predictably with increasing grout coverage. Thus, putting a single figure on the dispersion in order to relate it to grout coverage is not easy and it was decided that the pulse attenuation remains the better indicator of grout coverage. The description of this technique is included here as it may be of value where the medium is less dispersive, as may prove to be the case for real rock anchor installations, or for rods buried in a softer material like coal or sandstone.

The method is demonstrated first on the synthesized waveform, in section 3.3.1, and then on the example rock anchor response, in section 3.3.2.

3.3.1 Synthesized data

The system frequency response extracted from the synthesized waveform will take the form of magnitude and group delay response. Note that the "system frequency response" in this context has the meaning of $H(j\omega)$ as discussed in section 3.1.1 - it is not merely the Fourier transform of the time waveform (which comprises both direct and echo pulses), but is independent of the excitation signal characteristics and the direct pulse. Thus, $H(j\omega)$ characterises the acoustic medium and can be used to find the acoustic response of the system to any stimulus which falls within the frequency band of interest. Because the echo in this example is distortionless, the extracted magnitude and group delay response are expected to be constants. Any deviation from this ideal response will thus be helpful in identifying artefacts produced by the signal processing technique, and point the way to improvements which can be made to the method. The primary objective of this section, however, is to expound the technique.

(i) The FFT of the signal y(t) is taken and its complex logarithm is found. This gives a data set with log magnitude as the real part and unwrapped phase as the imaginary part.

(ii) By examining the magnitude or phase component of the log FFT, the band of frequencies bearing reflection information is identified. For the synthesized signal it is known that all parts of the band carry reflection information, so the band 20kHz to 60kHz was selected for the purposes of illustration. (Refer to Figs. 3.3 and 3.4). All other frequency components are zeroed in both the log magnitude and phase records. The linear component, including any average (or "DC") offset, is removed from both the log magnitude and phase record over the selected band by subtraction, after finding the straight line which best fits the data in the mean error sense. If the selected band is reasonably wide (that is, its width is significantly larger than the repiod of the echo information ripples), the linear component

in the log magnitude record will be due largely to source effects. Since isolation of the impulse response $h(\tau)$ in the cepstrum is a step in finding the frequency response $H(j\omega)$, removal of source components in the frequency domain is acceptable.

(iii) The real and imaginary parts of the data record are windowed with a Hamming window over the selected frequency band to further reduce leakage in the cepstrum. Although the windowing operation distorts the magnitude response part of $H(j\omega)$, this distortion can be corrected for, as will be seen.

(iv) The frequency domain record is made conjugate symmetrical and inverse Fourier transformed, so that the cepstrum produced is real. This band-limited cepstrum is shown in Fig. 3.14. Fig. 3.15 shows the same cepstrum for frequency domain data which has not been windowed with a Hamming window. Comparison of the figures clearly shows the leakage caused by using a rectangular window.

(v) The band-limited impulse response $h(\tau)$ (at approximately 0,3ms in Fig. 3.14) is selected with a rectangular window, discarding its higher rahmonics and any remaining source information which appears at $\tau = 0$. At this point, it would be possible to shift $h(\tau)$ to the cepstrum origin, and in doing so, remove the delay t_0 from the record's information [13:228]. This would yield $g(\tau)$ (see section 3.1.1). Leaving $h(\tau)$ in its original position is preferred, however, as this gives a basis for comparing the group delay response part of $G(j\omega)$ with the gross delay time t_0, thus providing a means of judging the severity of the pulse dispersion for the distance the pulse has travelled.

(vi) The cepstrum containing only the band-limited impulse response $h(\tau)$ is forward transformed, to give the frequency response $H(j\omega)$ in rectangular co-ordinates. An inverse Hamming window is applied to the real and imaginary parts of the data record, to correct for the distortion introduced by the Hamming window used in step (iii).

(vii) A (second) rectangular to polar conversion and phase unwrapping operation are performed on the frequency domain data record, to give a magnitude and phase representation of $H(j\omega)$. Finally, differentiating the phase part of $H(j\omega)$ numerically gives its group delay response $\Gamma_h(\omega)$.

A graphical summary of the above steps for finding the response $H_m(\omega), \Gamma_h(\omega)$, is given in Figure 3.16.

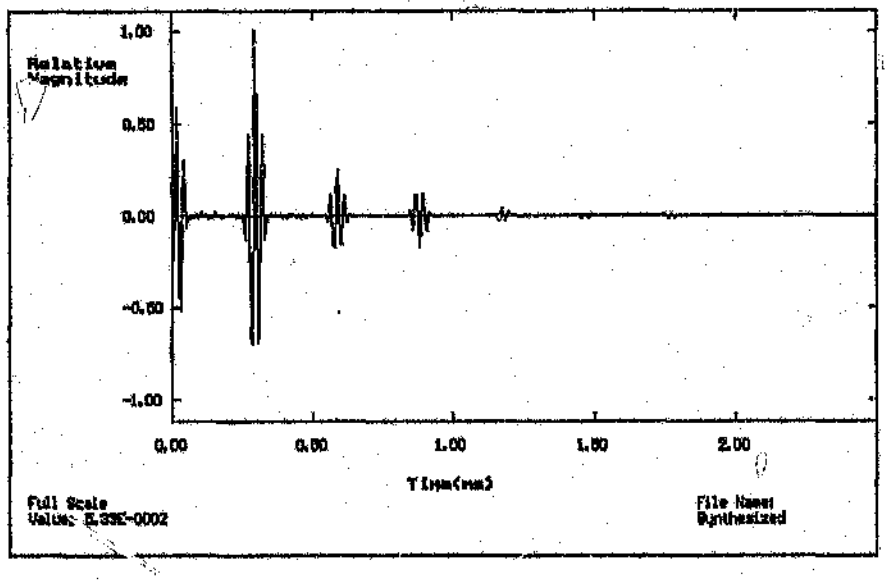

Figure 3.14 Band-limited complex cepstrum for synthesized waveform, produced using a Hamming window in the frequency domain

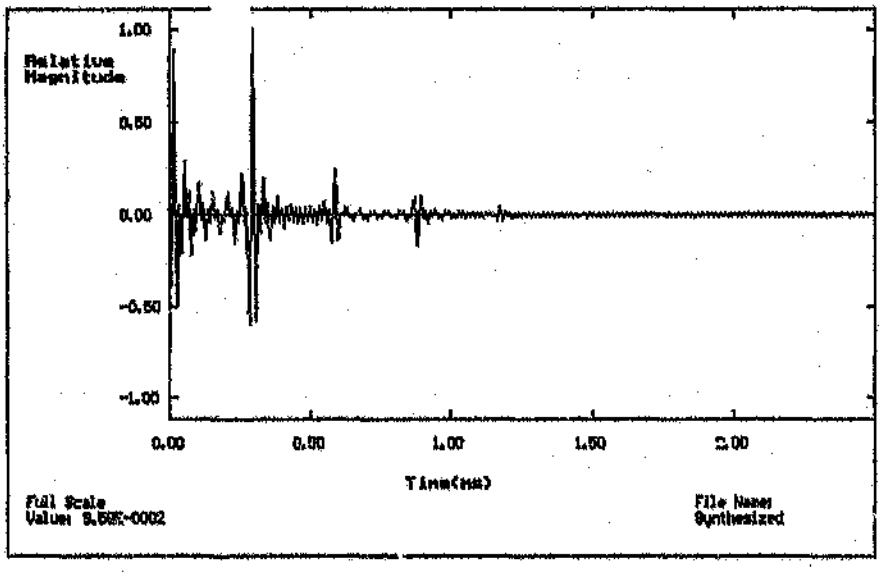

Figure 3.15 Band-limited complex cepstrum for synthesized waveform, produced using a rectangular window in the frequency domain

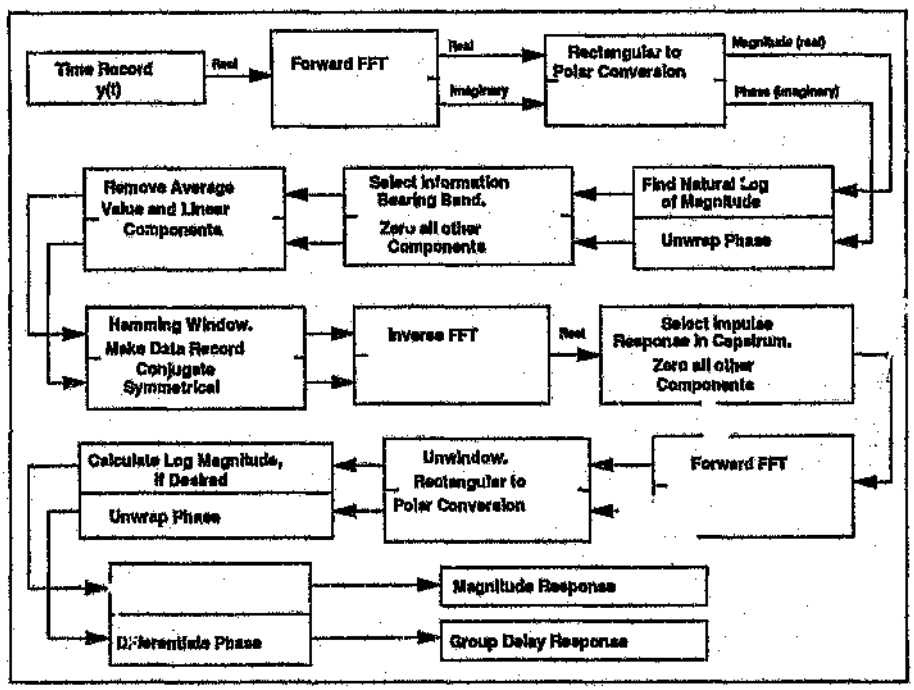

Figure 3.16 Use of the band-limited complex cepstrum to extract the magnitude and group delay characteristics of the mc

Discussion

The operations performed in step (ii) will be justified in this discussion. As pointed out earlier, the average value removed from the log magnitude record is simply a scale factor in the time record. The linear component removed from the phase record is connected with the positioning of the origin of the time record, also mentioned earlier. Any additive phase offset removed affects the proportions in which the time signal is represented in the real and imaginary parts of its time record

The reason fo. removing source components, especially any average offset, at this stage of the processing is to control leakage in the cepstrum produced by truncating the frequency record to the selected band. Liftering the data to remove source components could be considered, as was done for calculation of the amplitude cepstrum (section 3.2.2). This would, however, shift the saphe of the frequency domain echo information and (unless this shift is corrected for) lead to incorrect response $H(j\omega)$. If for some reason liftering has to be performed in the frequency domain, the zero phase method of Bolton and Gold [13:224] could be employed.

It is interesting to digress on the interpretation of the real and imaginary parts of the frequency domain data record at point (ii) in the signal processing: because a rectangular to polar conversion was performed in finding the complex logarithm of the frequency record, the real part can be thought of as the log magnitude and the imaginary part as the phase of the FFT of the signal y(t). From the "point of view" of the frequency response $H(j\omega)$, however, the real and imaginary components of this data record are still in rectangular from, as evidenced by equations (3.18) and (3.22). Hence the further rectangular to polar conversion and phase unwrapping operation in step (vii), needed to find $H(j\omega)$ in its polar form.

Figures 3.17 and 3.18 show the magnitude and group delay response for the distortionless example. As can be seen from Fig. 3.17, the magnitude response is relatively flat, with a value of 0,5 over most of the band of interest. This result concurs with the amplitude of the first reflection seen in the original time waveform, Fig. 3.2. The deviation from this ideal response at the band edges is an artefact introduced by truncating, removing linear components from, and windowing the frequency domain record. The group delay response in Fig. 3.18 is flat over the same proportion of the band, with some distortion at the band edges. The time of arrival of the first reflected pulse shown by the group delay response (0,3ms) agrees with the time of arrival seen in the time record, Fig. 3.2. Note that the vertical lines in the magnitude and group delay graphs are delimiters of the band edges, produced by the graphing software.

Figs. 3.19 and 3.20 demonstrate the effects of not using the Hamming window in the frequency domain. Here, significantly more distortion is seen in the magnitude and group delay responses over the band of interest. The rectangular window used in the cepstrum of Fig. 3.15 to obtain this result was centred at 0,3ms and extended over 44 data points.

3.3.2 Real data

In this section results for the above procedure repeated on the example rock anchor response are given. The band carrying the reflection information, and thus the band selected for processing, is 26kHz to 40kHz, evident in the log magnitude record of Fig. 3.9. The extracted magnitude and group delay responses are shown in figures 3.21 and 3.22 respectively.

The selected frequency band in this example was windowed with a Hamming window. Thirty points to the left and right of the reflection peak at 0.78ms in the cepstrum (shown in Fig. 3.23) were selected as being representative of the pulse echo, and were used to produce the magnitude and group delay responses above. Because of the pulse spreading in the cepstrum (and in the time record), the magnitude and group delay responses show the wide fluctuations needed to account for the dispersion of the pulse.

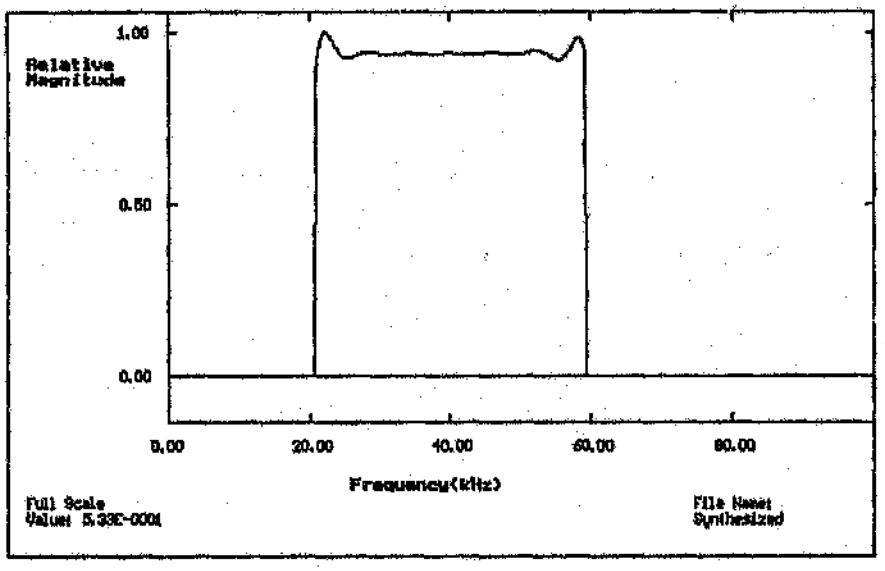

Figure 3.17 Magnitude response for synthesized waveform, extracted over a limited band

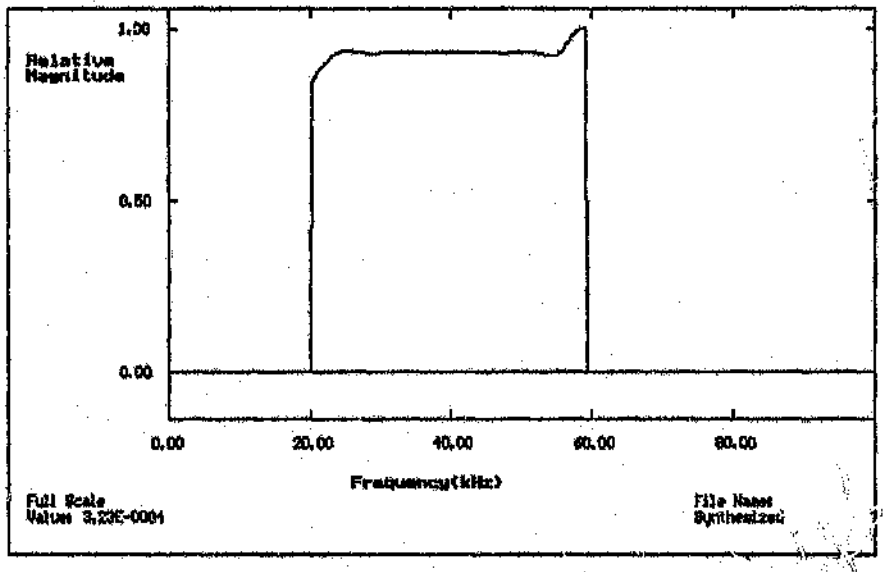

Figure 3.18 Group delay response for synthesized waveform, extracted over a limited band

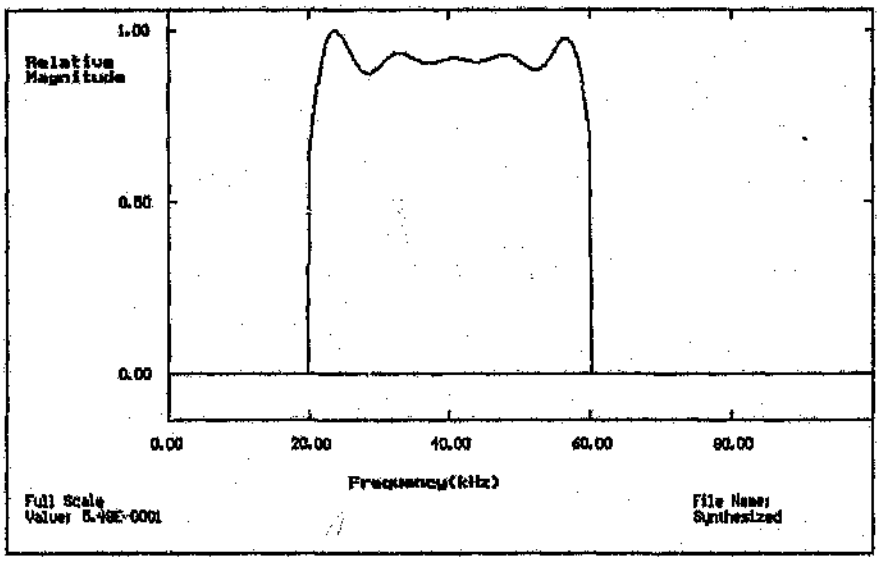

Figure 3.19 Extracted magnitude response of synthesized waveform, produced using a rectangular window in the frequency domain

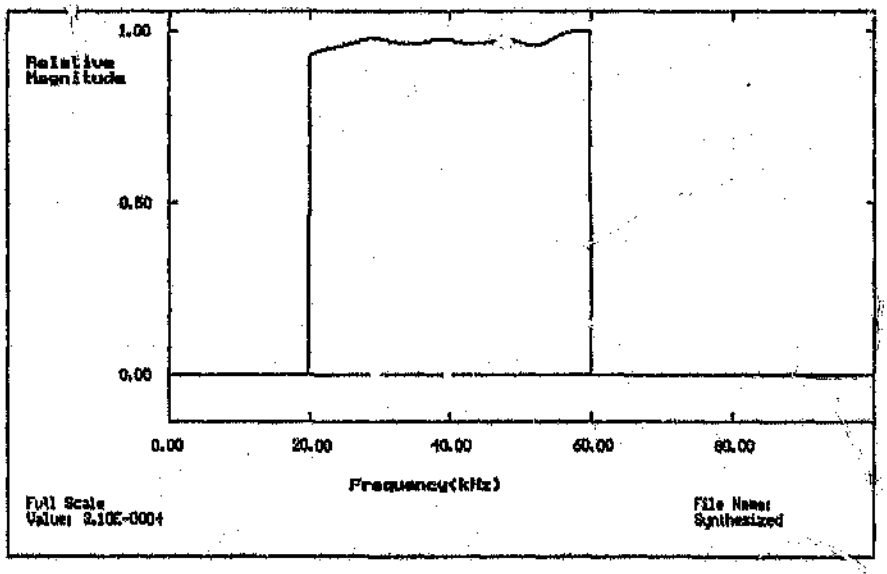

Figure 3.20 Extracted group delay response of synthesized waveform, produced using a rectangular window in the frequency domain

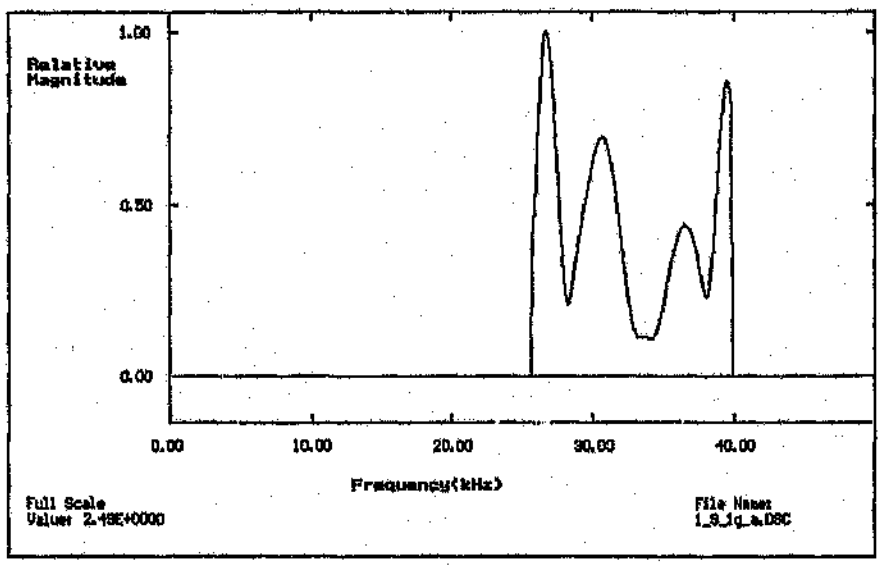

Figure 3.21 Band-limited magnitude response of example rock anchor response

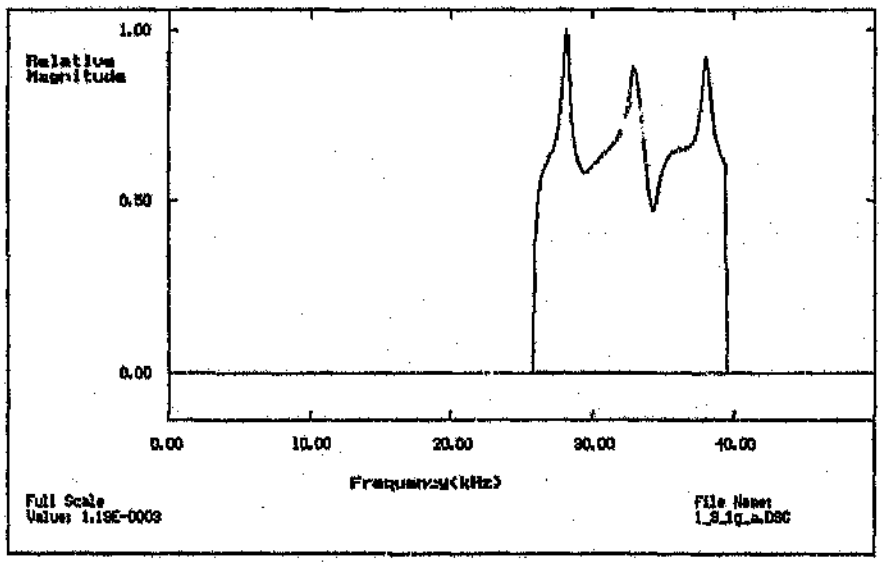

Figure 3.22 Band-limited group delay response of example rock anchor response

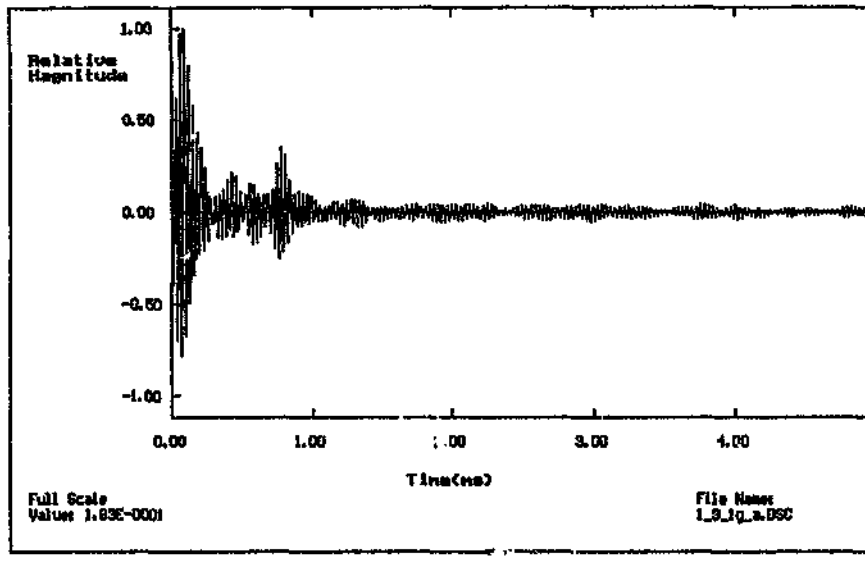

Figure 3.23 **Band-limited cepstrum of example rock anchor response**

4 RESULTS

4.1 Experimental Procedure

4.1.1 Choice of sample rock anchors

Two sample rock anchors thought to be representative of the kind of rock anchors used by the mining industry were chosen for investigation in this study. They were a straight, smooth bar of length 1,90m and diameter 20mm (hereafter referred to as "the smooth bar"), and a straight 1,80m rebar of diameter 16mm (which will be referred to as "the rebar"). The smooth bar used in the study was unthreaded, and the rebar was threaded over the last 15cm of its far end. Both rock anchors were made of mild steel. Although shepherds crooks are the most widely used type of rock anchor (50 to 70% of installations being of this type), a shepherds crook was not investigated in the study for the following three reasons:

* The shepherds crook is a more complex case (acoustically) of the straight bar problem, and it was thought prudent to restrict a preliminary study to the simpler case.

* The method of using concrete cylinders to simulate rock is not suited to testing shepherds crooks - these are best tested in situ.

* Application of both the piezoelectric and magnetostrictive transducers to the shepherds crook requires further investigation and special design considerations.

4.1.2 Testing strategy

Starting 10cm from the near end of the smooth bar, 40cm concrete cylinders were grouted onto the rod until its entire length (except for the 10cm exposed end) was concrete-clad. Each cylinder was grouted onto the previous one, so that the last (fifth) one covered only 20cm of rod at the far end. After allowing three days curing time for each cylinder, the acoustic response of the rod was recorded and another cylinder was grouted onto the rod, giving a total of six recordings for the smooth bar. The first recording for the smooth bar was taken in its free (ungrouted) state.

The rebar was treated in the same way: six time records for zero to fully grouted were obtained, and the last concrete section covered 10cm of rod at the far end. Choice of the distance 10cm for the exposed part of the near end was made to allow for investigation of different magnetostrictive transducers and their positioning on the grouted rods, were the need to arise. Also, this distance is not too different from the one found in real rock anchor installations. To make the simulation as realistic as possible, no special surface preparation was given the rods. In applying each concrete cylinder and grout, care was taken to ensure that grout coverage was as homogeneous as possible, with no large air bubbles.

The testing procedure described above is geared primarily to examining the affect of grout coverage on pulse attenuation, with no attention to grout discontinuities and possible reflections from grout discontinuities. As will be demonstrated in a discussion of the responses of the rock anchors, there is no direct evidence of reflections from grout discontinuities and certainly no reflection with coherence comparable to that of a reflection from the far end of the rock anchor. It was therefore decided that an investigation of reflections from grout discontinuities best be left as a later, more detailed study.

In mines, an under-grouted rock anchor which has insufficient grout at the near end is easily identified by inspection of the installation: the empty portion of the drillhole at the near end should be visible in cases where washers have not been used in the installation. Also, according to miners who have experience in rock anchor grouting, an incompletely grouted rock anchor tends to have its grout concentrated at the near end. Hence the decision to grout the test samples from the near end backwards.

4.1.3 Transducer setup and data capture

Transducer setup

The Phillips piezoelectric receiver and Prestik interface, as described in section 2.3, were used for all recordings. The near end of each rod was filed flat and the face of the piezo pressed concentrically onto the end face of the rock anchor with Prestik. Pressure was applied to the piezo until the thickness of Prestik between the piezo and rock anchor was typically 0,5mm. The effect of small variations in this thickness of Prestik was only to scale the magnitude of the signal delivered by the piezo. The piezo placement and interface formed in this way had a repeatable, broadband and smooth (non-peaked) frequency response suitable for investigating the response of the medium.

The magnetostrictive transducer described in section 2.2 was placed 25mm from the near end of the rod for all recordings.

Sampling rate and record length

The sampling rate of the A/D was set to 200kHz and the record length to 1024 samples for all recordings. Samples were recorded with a precision of 8 bits (which is fixed for the A/D used), giving a signal to quantising noise ratio of about 48dB. This precision was considered adequate for the responses obtained in the laboratory study. As will be seen in the presentation of results, the reflections are fairly strong in most recordings. The dispersion of the pulse and its obfuscation by other signal components was assumed to be the dominant limitation in detecting the echo. Some justification for this assumption will be seen in the presentation of the log magnitude spectra of the time recordings: due to the partial ability of the spectrum to separate the echo from other signal components (which will be discussed shortly), echoes which are not visible in the time records are visible as a periodic component in the log spectrum. Only when the size of the echo approaches the limit of resolution of the A/D (1 part in 256, roughly speaking) will the resolution of 8 bits become a serious limitation. Below this level, the echo will be lost in the quantising process. Because a periodic ripple consistent with a reflection from the far end of the rod was seen in all the log spectra, it was assumed that this limit wasn't reached.

Signal averaging

In the case of the smooth bar, the noise level at the output of the analog amplifiers was below that of the quantising noise of the A/D and no signal averaging was used. In the case of the rebar, the analog noise was typically 15dB above the quantising noise and the signal averaging capability of the A/D (set to 64 averages) was employed to reduce the analog noise to a level slightly below that of the quantising noise. The inefficiency of the magnetostrictive transducer was largely the cause of the relatively low SNR for the rebar, which has a diameter of only 16mm.

4.2 Time Waveforms for the Two Samples

Appendix A shows the six time recordings for each rod. Figs. A1 to A6 are the recordings for the smooth bar, from zero to fully clad, and Figs. A7 to A12 are for the rebar from zero to fully clad. The following observations on the time responses of the rods can be made:

4.2.1 Smooth bar

* Fig. A1, the response of the free smooth bar, shows three successive reflections in the rod produced by the injection of a single pulse from the magnetostrictive transmitter. The stimulating pulse is situated at the left hand extremity of the graph. The pulses are well-defined and show little energy loss or distortion.

* The response of the rod clad with one concrete cylinder, Fig. A2, shows a distorted reflection at about 0,78ms. This reflection is distorted to the extent that it does not resemble a delayed replica of the stimulating pulse, as was the case in the free rod. A large, relatively low frequency wave follows the stimulating pulse directly and continues throughout the time record, decaying slowly. This characteristic is visible in all the recordings where the rod was concrete-clad. A second pulse reflection is discernible at about 1,6ms, twice the delay time of the first reflected pulse.

* The first reflected pulse is not discernible by eye in the time records where the rod is clad with two or more concrete cylinders (Fig. A3 onwards).

4.2.2 Rebar

The comments above on the time responses of the smooth bar apply equally to the rebar, except for the following differences:

* Large, decaying oscillations are visible in the response of the free bar, immediately after each pulse. These oscillations are the result of the use of an amplifier with a high-pass characteristic, having a sharp cut in frequency of 10kHz. This amplifier was used for recording the response of the free rebar only, and for no other reason than that the analogue electronics for the experimental setup was still under development at the time. In spite of the effects of the 10kHz filter, it can be seen from the response of the free rebar that each reflection is more distorted than its predecessor. This dispersion of the travelling pulse is a result of the more complex geometry (surface features) of the rebar.

* The first reflected pulse is not discernible by eye where the fourth and fifth concrete sections have been added.

4.2.3 Stimulus artefact

The magnitude of the stimulus artefact for all measurements on the smooth bar was approximately 3% of the magnitude of the stimulating pulse. For the rebar, the figure was

approximately 10%. The size of the stimulus artefact in each case was found by disconnecting the piezo acoustically from the rod and observing the resulting waveform on the display oscilloscope.

4.3 Log Magnitude Spectra of the Recordings

Figures B1 to B6 in Appendix B show the log magnitude spectra of the time responses (Figs. A1 to A6) of the smooth bar. Figures B7 to B12 show the same for the rebar. Because the time records for both bars were oversampled to aid inspection of the time waveforms, all the time records seen in Appendix A were compressed by a factor of two before forward transforming them to find their spectra. This compression gave a new time record comprising 512 data points, the remaining 512 points being padded with zeroes. The following observations regarding the log magnitude spectra for the rebar can be made:

* The periodic ripple structure containing the reflection information can be seen throughout the spectrum for the free rebar (Fig. B7), except over the first 10kHz where the information has been removed by the 10kHz filter used for that recording.

* The spectrum for the rebar with one concrete cylinder shows reflection information which is limited to the band approximately 20kHz to 40kHz. Sharp spectral peaks occur at about 7,5kHz and 18kHz.

* For two and more cylinders, the band containing reflection information narrows progressively until it occupies a small region around and just below 30kHz. The spectral peaks at 7,5kHz and 18kHz maintain their position for increasing concrete coverage.

Observations on the spectra of the smooth bar are much the same, with the following differences:

* Reflection information is visible across the entire spectrum (Fig. B1) for the free rod.

* A spectral peak at 7,5kHz occurs in all spectra where the rod is concrete-clad.

* A band of reflection information which is consistent with a reflection from the far end of the rod appears to converge around 35kHz in the spectrum.

The observations of this section lead to a signal processing strategy for quantifying pulse attenuation and time of arrival, which is detailed in the following section.

4.4 Band-limited Envelope Cepstra of the Time Records

To optimise cepstral information about the reflection from the far end of the rod, a narrow band in the spectra for each rod was chosen for calculation of band-limited envelope cepstra, as described in section 3.2.2. The band for the smooth bar was 32kHz to 39kHz, and for the rebar 25kHz to 35kHz. The band chosen for each rod has to be fixed and used in the calculation of all cepstra for that rod, so that the amplitude information in the cepstra can be meaningfully compared. The basis for the choice of these bands was thus rather subjective: they appear to represent the bands upon which the band-limited reflection information converges as the concrete coverage of each rod increases. The choice of band for a particular rod is complicated by the fact that as the concrete coverage of the rod increases the spectral ripples become less regular, and the validity of the assumption that the chosen band contains information about an echo from the far end of the rod becomes questionable. A point in support of this assumption will be made in section 4.5.

Figures C1 to C6 in Appendix C show the cepstra for the smooth bar and Figs. C7 to C12 show the cepstra for the rebar. Naturally, better cepstra can be obtained by using a broader band in cases where less concrete has been applied to the rod: see the band 25kHz to 50kHz in Fig. B2, for example. Use of such a broad band on spectra for the same rod with more concrete cladding (see Fig. B6, for example) would, however, include information which is not related to the echo from the far end of the rod. It is therefore necessary to use the "worst-case" band - the one seen to bear the echo information when the rod is fully clad.

To illustrate the advantage of the band-limited cepstrum over the full-band cepstrum when the information bearing spectral band has been correctly identified and used, the full-band cepstrum for the smooth bar clad with five concrete sections is shown in Fig. 4.1. Here, the peak so clearly visible in Fig. C6 cannot be unambiguously identified as the pulse echo. The spectrum used to produce the full-band cepstrum was high-pass liftered to remove the low quefrency components which would otherwise dominate the cepstrum of Fig. 4.1.

4.5 Attenuation and Arrival Time Curves from the Cepstra

From the cepstra shown in Appendix C it is possible to plot curves of pulse attenuation and time of arrival against grout coverage. The "pulse attenuation" is simply the peak value of the first rahmonic in the cepstrum and the time of arrival is the quefrency value at which the first rahmonic occurs. Figs. 4.2 and 4.3 show these curves for the smooth bar and Figs. 4.4 and 4.5 show the curves for the rebar.

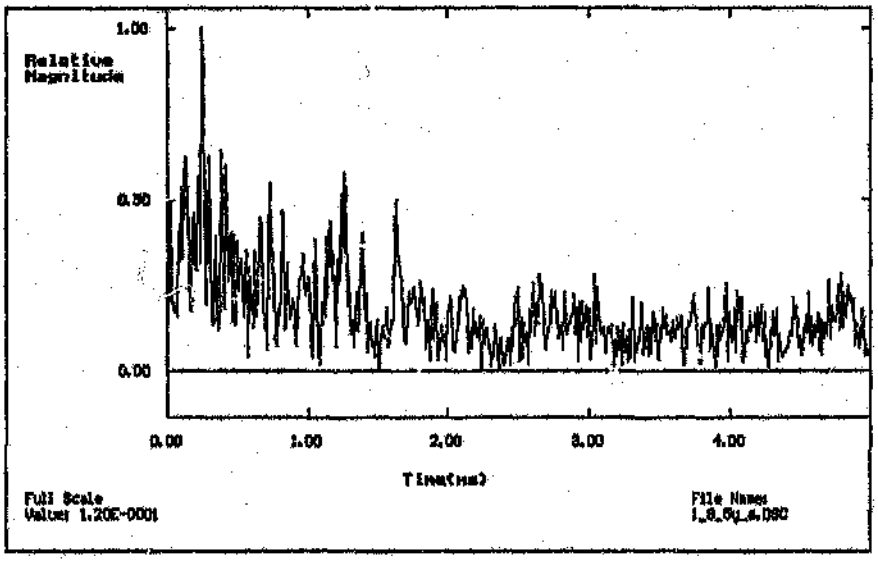

Figure 4.1 Full band envelope cepstrum for smooth bar with five concrete sections

These curves are central to the operating principle of a real instrument for finding rod length and grout coverage: the grout coverage of the rod under test can be deduced from the measured pulse attenuation, using a "calibration curve" such as the one shown in Fig. 4.2, and the rod length is determined from the pulse time of arrival.

The following observations with regard to the curves for the smooth bar can be made:

* Except for the first point on the attenuation curve, the pulse attenuation shows a monotonic decrease with concrete coverage.

* The pulse time of arrival shows a gentle dependence on concrete coverage, increasing monotonically with coverage, except for the last point. This dependence, which has a range of 30% over zero to fully clad, is sufficient to necessitate making a correction to the length of the rod calculated from the pulse time of arrival in order to find the rod length to within 20cm of the correct value - once the grout coverage has been found from the attenuation curve, the rod length can be determined correctly from a "calibration curve" such as the one in Fig. 4.3.

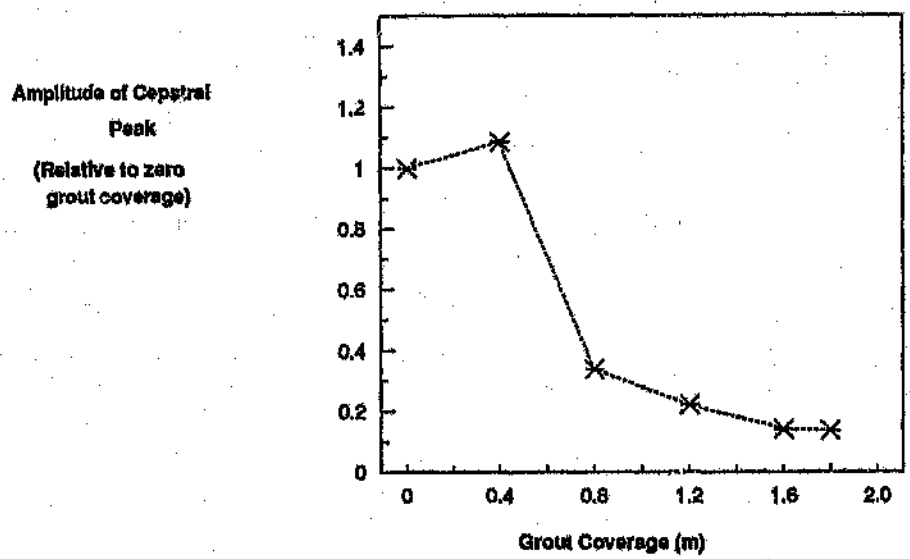

Figure 4.2 Attenuation curve for smooth bar

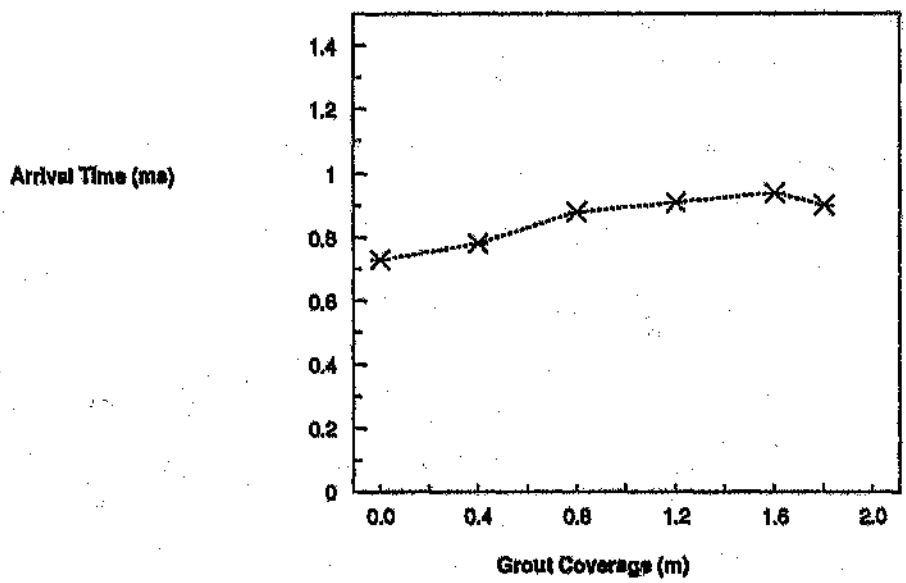

Figure 4.3 Pulse time of arrival curve for smooth bar

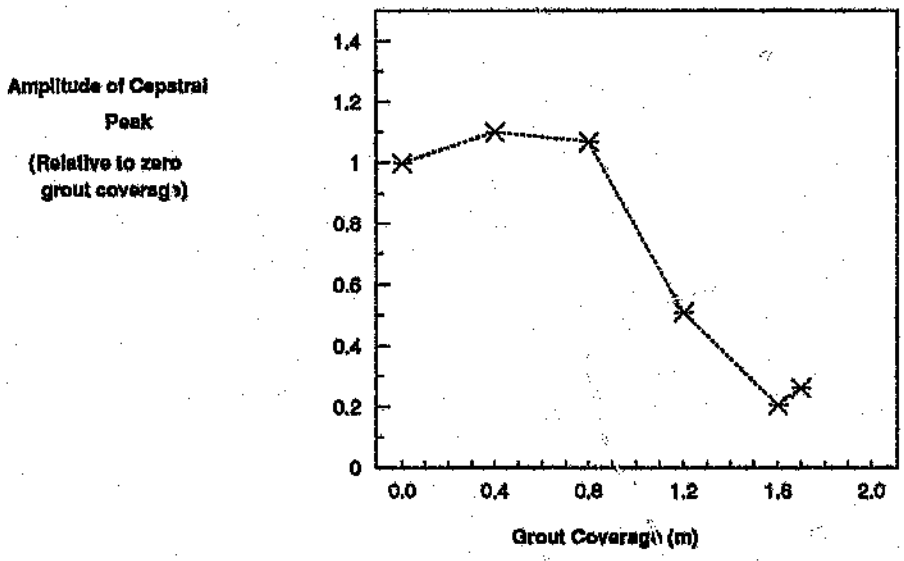

Figure 4.4 Attenuation curve for rebar

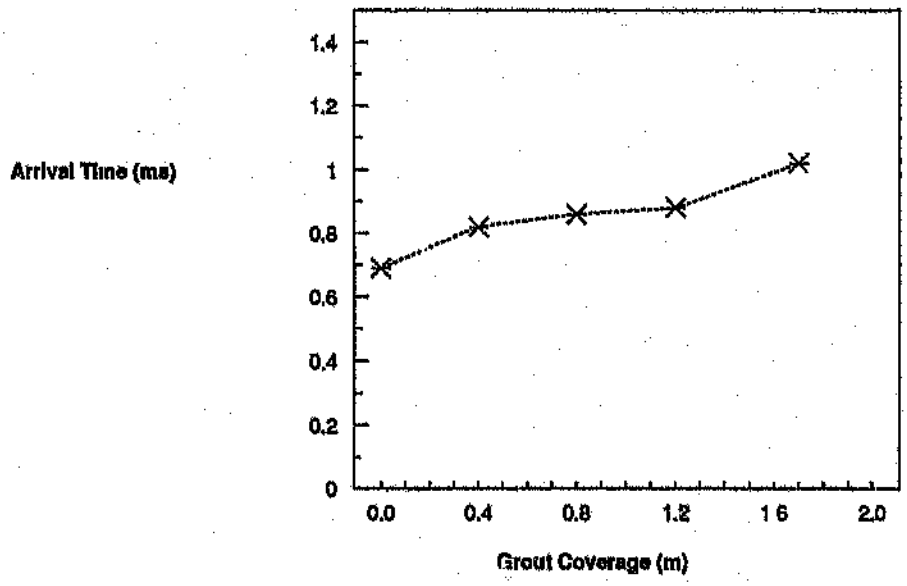

Figure 4.5 Pulse time of arrival curve for rebar

* The attenuation curve of Fig. 4.2 is not a true reflection of the energy loss of the pulse with grout coverage: in finding the cepstrum of the time record, a narrow band of frequencies representing the least attenuated components of the pulse was selected. The true energy loss of the pulse must therefore be substantially greater than that indicated by the curve.

* The behaviour of the attenuation curve does not follow the simple exponential decay model for plane waves in a lossy medium: the logarithm of the pulse attenuation deviates significantly from what "should" be a linear dependence on grout coverage. The attenuation curve of Fig. 4.2 can therefore not be replaced with a single attenuation figure (in Nepers per metre) for the purpose of inferring the grout coverage of a rod.

Apart from some minor differences, the comments on the curves for the smooth bar apply equally to those of the rebar. One particular point in the rebar's attenuation curve appears to be out of place with respect to its neighbours, however (please see the point for 1,6m grout coverage in Fig. 4.4). This data point was generated by the cepstrum of Fig. C11. As can be seen from the cepstrum, a peak does not appear at a position consistent with the peaks from the other cepstra for the rod. To make the data set for the attenuation curve as complete as possible, a value for the curve was selected from a minor peak at 0,90ms in the cepstrum, where the correct peak "should have been". A possible explanation for the failure of the cepstrum here is the occurrence of a large spectral notch at 34kHz (see Fig. B11) in the spectral band 25kHz to 35kHz used to create the cepstrum. Of the twelve cepstra for the smooth bar and the rebar, this appears to be the only one which failed.

Aliasing in the cepstrum for the free rod

The first point (for zero grout coverage) on the attenuation curve for both rods is below the second point, as a result of cepstral aliasing: the strong multiple reflections of almost equal amplitude in the free rod violate the requirements for successfully forming the cepstrum of the signal (see section 3.2.1). The aliasing can be alleviated by windowing the time record with an exponentially decaying sequence, but in the context of the rock anchor problem this aliased point is of no consequence: real rock anchor installations will always be grouted to some extent, and even if the reflection is very strong an alternative (possibly time domain) technique can be used to deal with this special case.

Choice of band limits for cepstrum

In section 4.4 the choice of the "worst-case" spectral band was justified on the behaviour of the information-bearing band with increasing grout coverage. Some signal processing experiments were carried out to determine the effect of deliberately selecting the "wrong"

band for creation of the cepstra - when the band was widened or shifted it was found that the attenuation and arrival time curves became irregular, and no longer seemed to be representative of reflections from the end of the rod. The consistency of the data points in the curves of Figs. 4.2 to 4.5 therefore appears to support the basis on which the information-bearing bands were chosen.

4.6 Discussion

In this section an acoustical interpretation of various phenomena observed in the rock anchor responses is offered. Since these phenomena will ultimately have an influence on the performance of a rock anchor testing instrument, the contribution below to the understanding of the acoustic medium should be of value in future research undertaken, and in the development of the "real instrument".

4.6.1 Spectral peaks and nulls

The log spectra of all the recordings for both rods, except the free rod case, have spectral peaks which are fairly consistently located at 7,5kHz. The fact that the peaks have a fixed location suggests that they are caused by a resonance in the free 10cm portion of the near end of the rod. Further evidence to support this explanation is found in the frequency of the resonance: if the mode of resonance is assumed to be the quarter-wavelength transverse mode, then the frequency of resonance calculated from the wavelength and the transverse wave speed in mild steel (3235m/s, from [16]) is 7,6kHz.

The origin of the transverse wave component could be in the geometry and acoustics of the rod and grout bond where the acoustic wave encounters the grouted section of the rod, or in the geometry of the magnetostrictive transducer and the rod: if the placement of the transducer coil with respect to the rod is eccentric, a transverse (shear) wave component may be introduced into the rod. Support for the latter explanation appears in the fact that the peaks for the rebar are more pronounced than the peaks for the smooth bar: in all recordings for the rebar, the magnetostrictive transducer of diameter 20mm was allowed to lie (horizontally) on the rebar of diameter 16mm.

The spectral nulls (also more pronounced in the spectra for the rebar) may be related to the resonance in the free near end of the rod. If this is the case, then both the peaks and the nulls will spread out to higher frequencies for real rock anchor installations, where the free near end length of rod is generally less than 10cm. Because of the nuts and washers attached to the exposed end of real rock anchor installations, it is also likely that these peaks will be less pronounced due to the more complex geometry.

An alternative explanation for the spectral notching is the phenomenon of multipath: if two similar pulses follow different paths in the medium (for example, one at the grout bond with the rod and the other at the outer surface of the concrete cylinder) and arrive at slightly different times at the receiver, then the spectrum will show notches whose spacing is related to the delay time between the pulses. With decreasing delay time between the pulses, the spacing of the spectral notches increases. This explanation for the spectral notching is less feasible for the following reasons, however. Firstly, the notching is severe in the rebar and almost indiscernible in the smooth bar. Secondly, one would expect the delay time between two signal paths to increase with increasing concrete coverage; the spacing of the notches should therefore decrease with increasing concrete coverage. This trend is not evident in the spectra for the rebar. If the spectral notching and multipath is due to the finite dimensions of the concrete cylinders, the problem will not be encountered in real rock anchor installations.

4.6.2 Speed of sound in the medium

The speed of sound in the free smooth bar can be found from the echo delay time (0,73ms), seen in Fig. A1, and the total distance the pulse has travelled in that time (3,6m). The value, 5200m/s, agrees with the speed of longitudinal sound waves in thin, mild steel rods published in [16]. In a separate experiment, the speed of longitudinal sound waves in a slab of the same concrete used to cast the concrete cylinders was found to be 3600m/s. The relatively lower speed of sound in concrete explains the steadily increasing pulse arrival time with concrete coverage seen in Figs. 4.3 and 4.5. Due to some complex acoustic interaction between the concrete and the steel rod, the speed of the pulse is reduced to a value between that of steel and concrete; using the pulse arrival time for the fully clad smooth bar, this "effective speed" is calculated to be 4200m/s.

4.6.3 Reflections at grout discontinuities

Coherent reflections, as one may expect to find where there is a step change in the acoustic impedance of a medium, are not visible in the time records or cepstra of the recordings. The grout discontinuity at 50cm from the near end of the smooth bar with one concrete cylinde. for example, does not show a reflection at the expected position of 230μs in its time record - see Fig. A2. (The pulse return time of 230μs is derived from the pulse travel time in the free 10cm section of rod and the clad 40cm section of the rod, using the pulse speeds of 5200m/s and 4200m/s respectively). It may be possible to model the grout discontinuities

for compressional waves in the rod as a change in acoustic impedance, and obtain the reflection coefficients for these discontinuities; the observations above imply that the reflection coefficients are likely to be very small.

The transverse resonance in the free portion of the rod's near end, on the other hand, can be viewed as being sustained by a large impedance discontinuity where the rod enters the concrete, and so it is evident that reflections at grout discontinuities should be modelled with caution. Modelling impedance discontinuities could aid in interpreting the response of the medium and provide a more sophisticated means of dealing with responses.

4.6.4 Band-limiting of the echo

As yet, no explanation for the band-limiting of the echo has been found. Should an explanation be forthcoming, it may provide a better criterion for making the band selection used to find the cepstrum.

4.6.5 Point of failure of the method

As the length of grouted rod is increased, there will be a point at which the cepstral peak marking the returned pulse is of lower amplitude than the surrounding cepstral "disturbances". At this point, the returned pulse can no longer be unambiguously identified in the cepstrum (without prior knowledge of the rod length and grout coverage) and the method must be considered to have failed for that rod, grout and rock combination. It is true that leakage caused by windowing must make some contribution to the "cepstral disturbances", but it is more likely that the limitation in the length of rod which can be tested lies in the dispersion of the signal by the medium. As evidenced by the time recordings and their cepstra, some components of the pulse are spread out to the extent that they cannot be considered representative of reflections from the end of the rod, for the purposes of the measurement. When these components, which cannot be distinguished from the "true" reflection with the band-limited cepstrum technique, are of the same amplitude as the true reflection, the limit of the method has been reached.

If some new way of identifying reflections from the end of the rod can be found, it may be possible to extend this limit. Judging from the cepstra of the two rods tested, the author is of the opinion that the length limit for both rods in the experimental setup is around 2m.

5 CONCLUSION

This laboratory study has demonstrated the principles of instrumentation required in an instrument for measuring rock anchor length and grout coverage acoustically, and has laid some foundations for the instrument's signal processing and transducer requirements.

The cepstrum method is not central to the principle of the instrument, but should be seen as an aid in quantifying echo pulse attenuation and arrival time in recorded rock anchor responses - were the rock anchor responses to contain only a direct pulse of simple shape and an echo which is a delayed replica of the direct pulse, a peak detection would satisfy the instrument's signal processing requirements. Some important advantages of using the band-limited envelope cepstrum are its ability to:

* "recognize" echo pulses

* reject out of band noise in the signal

* identify and use the limited band in which the echo appears

* reject sharply peaked natural resonances in the transducer and rock anchor

* produce a convenient data record, in which a simple peak detection operation identifies the echo, its amplitude and its time of arrival.

The working principle of the proposed instrument is to determine the pulse attenuation and arrival time for a rock anchor and to infer its length and grout coverage from attenuation and arrival time curves like the ones shown in Chapter 4.

Because these curves were found once only for each rock anchor type investigated, and concrete cylinders were used to simulate rock, the following questions arise regarding the value of the results obtained:

* Do the concrete cylinders simulate rock adequately - that is, are the results of the simulation representative of the results which will be seen in real rock anchor installations ?

* For a given rod length and grout coverage, are the results repeatable for a variety of rock, grout, rock anchor types and grout distribution ?

These questions are dealt with in the following assessment of the laboratory simulation, and recommendations for further research.

5.1 Adequacy of Concrete Cylinders in Simulating Rock

The discussion and interpretation of results in Chapter 4 centred around an acoustic medium comprising rock anchors clad with concrete cylinders. The applicability to real rock anchor responses of the observations made and signal processing tactics employed in that chapter is therefore questionable.

It is likely that the severe pulse dispersion seen in the laboratory results is due to multipath conditions in the concrete cylinders. That is, pulse components entering the cylinders are not dissipated (due to the finite size of the cylinders), but return to the near end of the rod after being reflected at the boundaries of the cylinders. Therefore it seems reasonable to conclude that echo pulses in real rock anchor installations will be significantly smaller, but more coherent. The slowly decaying oscillations due to resonance in the exposed near end of the rod should appear in real installations, also. Because the band-limiting of echoes does not appear to be connected with the inadequacy of the concrete cylinders, it seems likely that echoes in real installations will be band-limited.

If the above speculations on the acoustic response of real rock anchor installations prove to be correct, the signal processing methods used to deal with the responses obtained in the laboratory simulation will retain their usefulness in dealing with real responses. Naturally, though, the differences which will be seen in real rock anchor responses will demand changes in the finer details of the signal processing used. The extent of the deviation of real responses from the simulated ones can be ascertained only by examining the responses of real rock anchor installations.

5.2 Recommendations for Further Work

Although the principle of the proposed instrument has been demonstrated in the laboratory simulation, it has yet to be validated for real rock anchor installations: the feasibility (in the fundamental sense) of producing a real instrument has not yet been established, and depends on the outcome of tests on real rock anchor installations. Collection of calibration information for the instrument is of secondary importance, and should only be done after the principle of the instrument has been validated. The nature of further work on the problem is thus two-fold:

* Completing the feasibility study by determining the repeatability of results with parameters which cannot be corrected for.

* Collecting calibration data for various rock anchor, grout, rock and drillhole types, and in so doing, ascertaining the types of rock anchor installation for which the principle of the instrument is workable.

Near the end of the laboratory study the author had the opportunity of testing some real rock anchor installations at the Boart Experimental Mine. Unfortunately, due to a time constraint on the project, it was not possible to perform the comprehensive tests described above, but the few tests which were made (these are described in detail in Appendix D) brought to light the following:

* The echoes in real rock anchor responses are, in fact, smaller and more coherent than the ones seen in the simulation using concrete cylinders.

* An A/D with better precision (16 bits) will therefore be required in further investigations.

* Echoes are band-limited and a resonance in the near end of the rock anchor appears in the time record. The band-limited envelope cepstrum therefore retains its usefulness in dealing with the rock anchor responses.

With the improved A/D recommended above, the laboratory method will therefore be applicable to future research done in the field.

Repeatability

The effects on pulse attenuation and arrival time of quantities which are unknown at a rock anchor test site pose a problem to the principle of the instrument, because they cannot be corrected for. Such quantities must therefore be regarded as affecting the repeatability of the instrument. Examples of such quantities are grout distribution and possibly grout density and air bubble content, and cracks in the rock near the rod.

In the opinion of the author, the effect of variable grout distribution presents the greatest threat in the validation of the instrument's principle: the fact that the attenuation curves in Chapter 4 do not show an exponential decay with grout coverage lends support to this speculation. (Further investigations may reveal that some other "unknown" affects measurements more severely, however). Finding the "worst-case" effect of grout distribution on pulse attenuation and arrival time for a fixed grout coverage should therefore assume priority in further work done.

This can be done by analyzing the response of appropriately installed test rock anchors, or possibly with the correct treatment of an analytic or numerical model. An analytic treatment of a realistic model is not recommended, however. This task would be arduous (if at all possible), and the same objective can be achieved numerically with finite element modelling (FEM) or measurements made on a testbed of real rock anchors.

If it is found that the attenuation and pulse arrival time curves show an unacceptably strong dependence on grout distribution, it may be possible to establish a simple rule which relates pulse attenuation and arrival to grout distribution. A real instrument could then use this rule in conjunction with the calibration data to deduce the correct grout coverage and length of a rod under test. Unfortunately, though, an instrument which makes use of this rule would have to be capable of deducing the grout distribution of a rod from its acoustic response. As seen in the results, longitudinal reflections from grout discontinuities must be very small (undetectable in the laboratory data) and it does not seem likely that this will be possible. If a dependence on grout distribution cannot be corrected for in this way, the instrument's performance will be limited by the uncertainty in grout coverage due to the dependence. It should, however, be possible to temper this limit with a statistical knowledge of the grout distribution in under-grouted rock anchors.

Calibration

The effects of rock anchor type on the attenuation and arrival time curves can be seen by comparing the laboratory results for the smooth bar and the rebar; undoubtedly, these curves will show a dependence on rock and grout type, and drillhole diameter as well. All of these "known" quantities (and any others which are found to affect the curves significantly) can be taken into account by generating curves from test installations for every combination of the above, which occur in mines. The data thus obtained could be stored as a set of "calibration curves" in a real instrument, the appropriate curve being recalled and used to test a rock anchor of unknown length and grout coverage.

The success of an instrument which finds rock anchor length acoustically depends on both the practical issue of dealing with mine conditions and the validity of the principle on which the instrument is based. The more pressing issue in further research is that of validating the instrument's principle. If further research shows that rock anchor length and grout coverage can be inferred from the rod's acoustic response unambiguously, and with a precision of 20cm, the principle of the instrument is sound. If not, the principle of the instrument must be considered invalid and the acoustic method should be abandoned. For the types of rock anchor installation for which the principle proves workable, the limit of performance of a real instrument will be set by the worst-case mine conditions which the instrument's transducers and signal processing is capable of dealing with.

APPENDIX A

Pulse responses for the two sample rock anchors

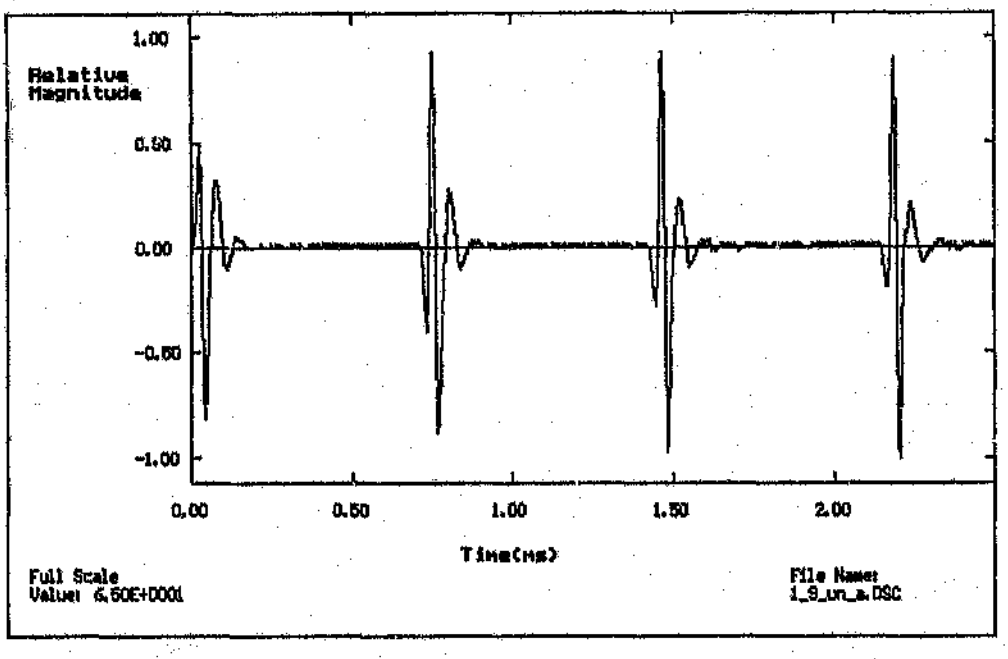

Figure A1 Pulse response of free 1,9m smooth bar

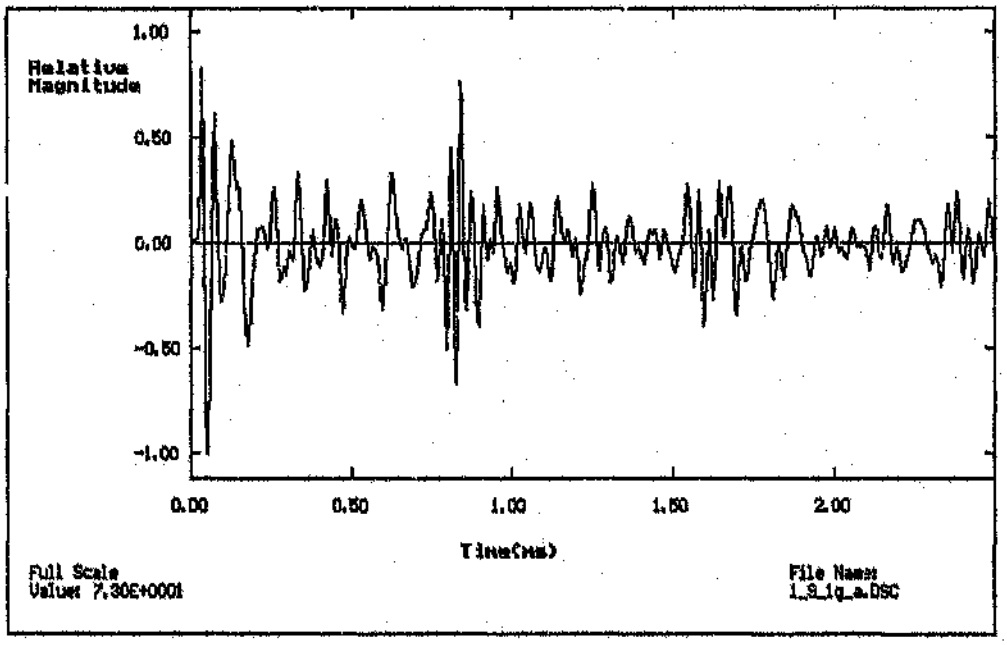

Figure A2 Pulse response of smooth bar: one concrete cylinder

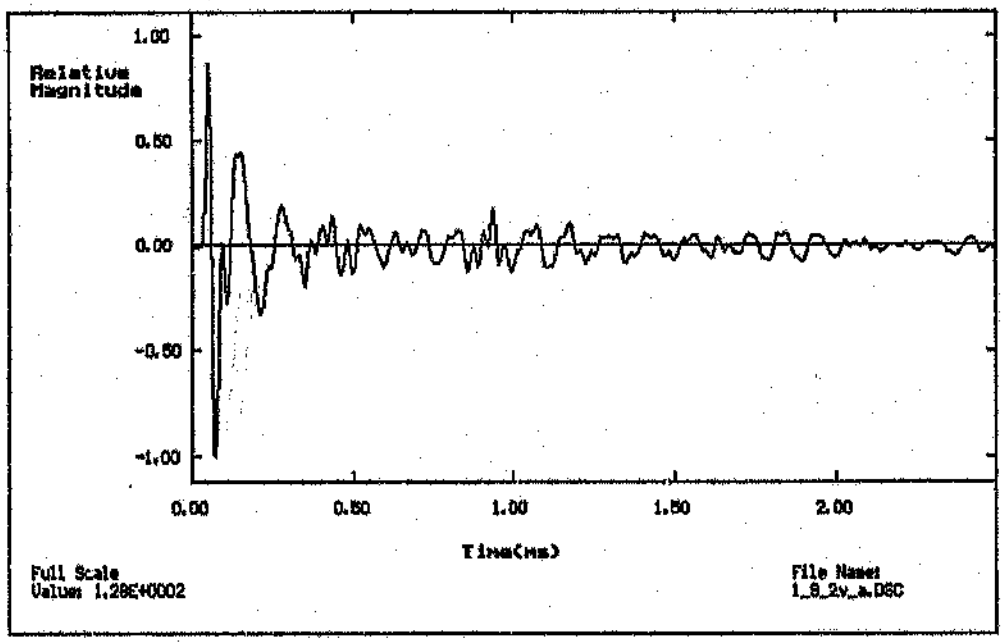

Figure A3 Pulse response of smooth bar: two concrete cylinders

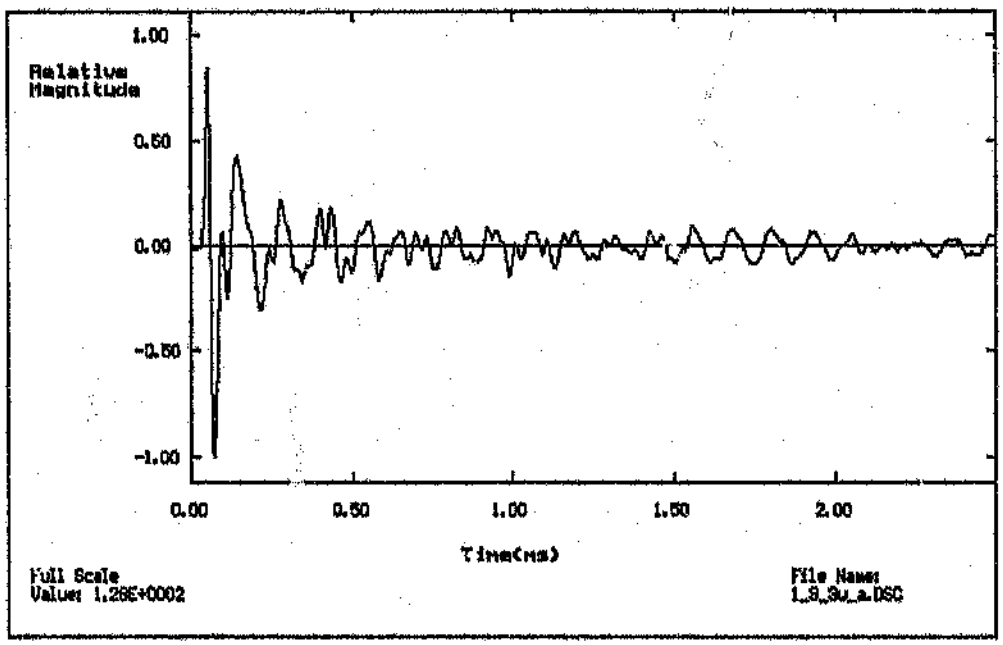

Figure A4 Pulse response of smooth bar: three concrete cylinders

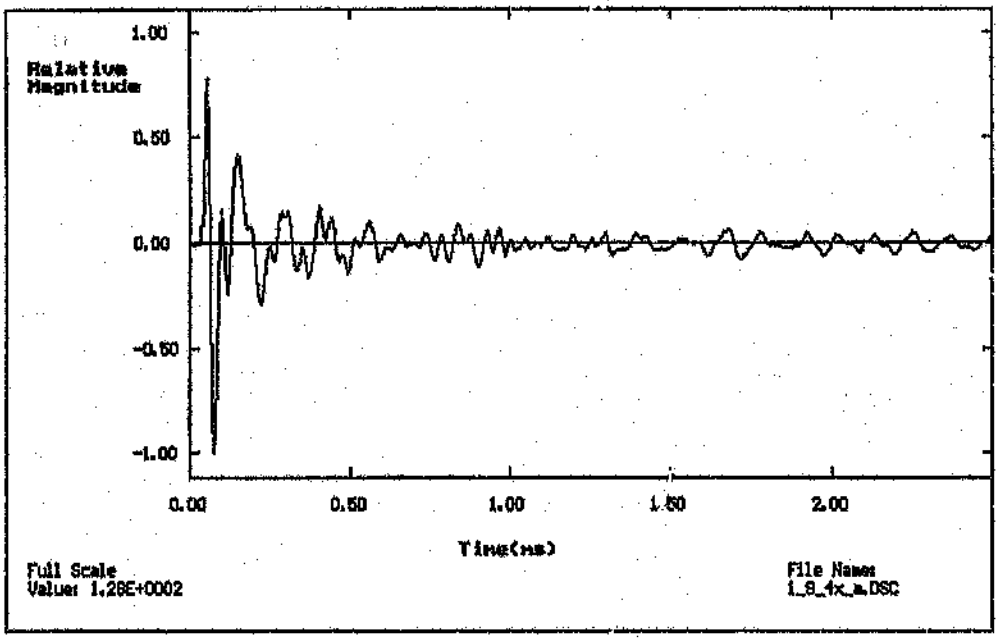

Figure A5 Pulse response of smooth bar: four concrete cylinders

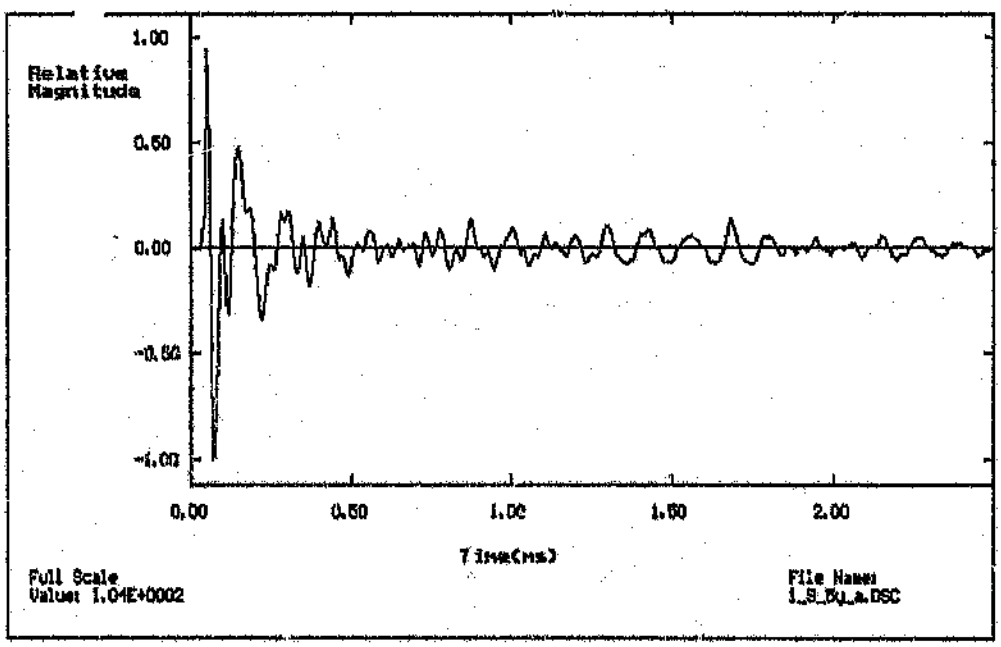

Figure A6 Pulse response of smooth bar: five concrete cylinders

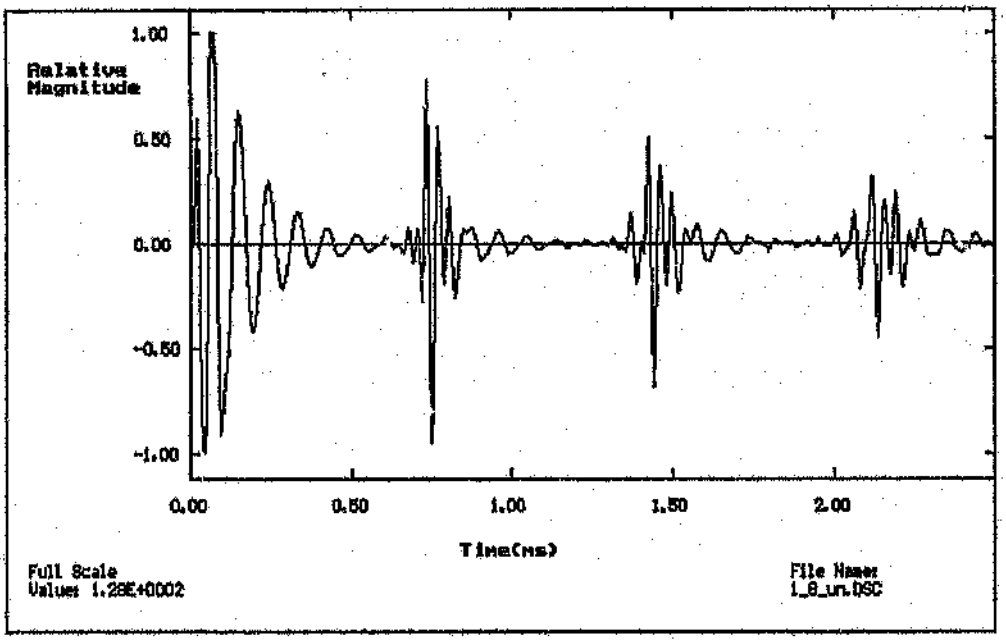

Figure A7 Pulse response of free 1,8m rebar

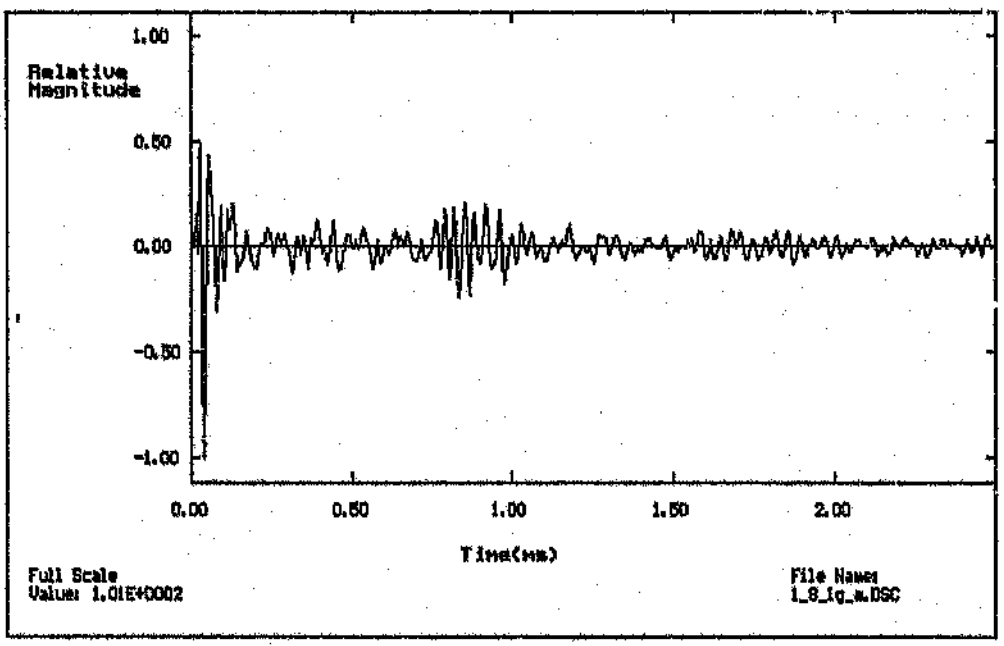

Figure A8 Pulse response of rebar: one concrete cylinder

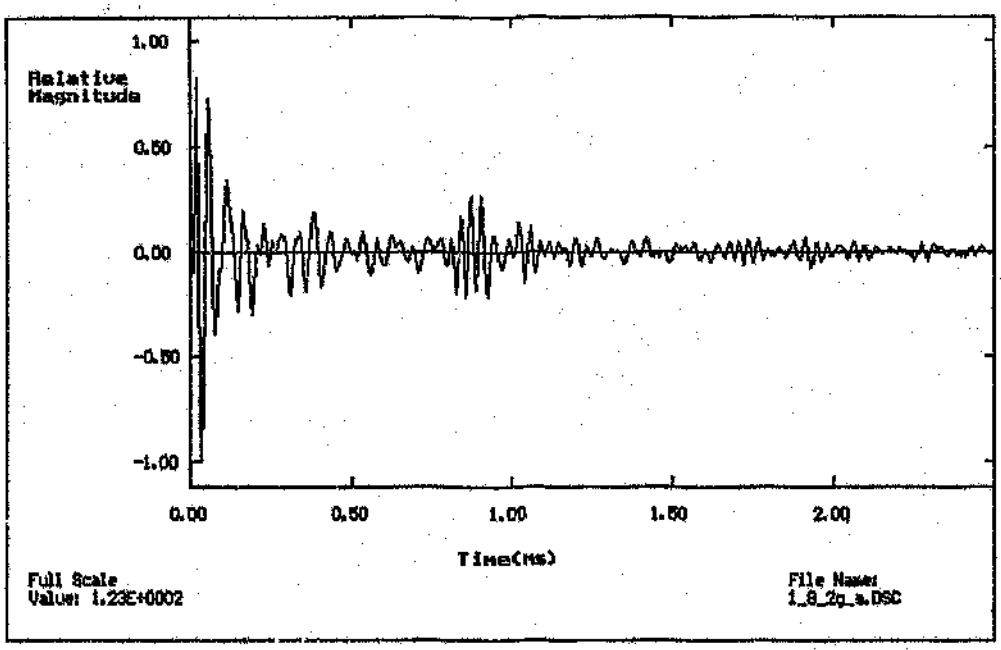

Figure A9 Pulse response of rebar: two concrete cylinders

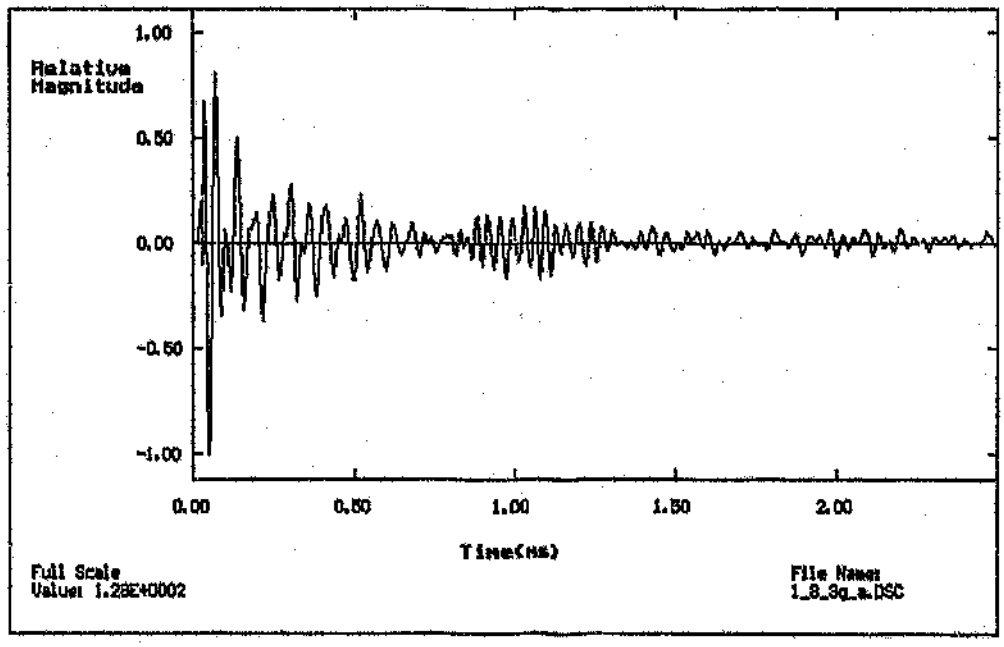

Figure A10 Pulse response of rebar: three concrete cylinders

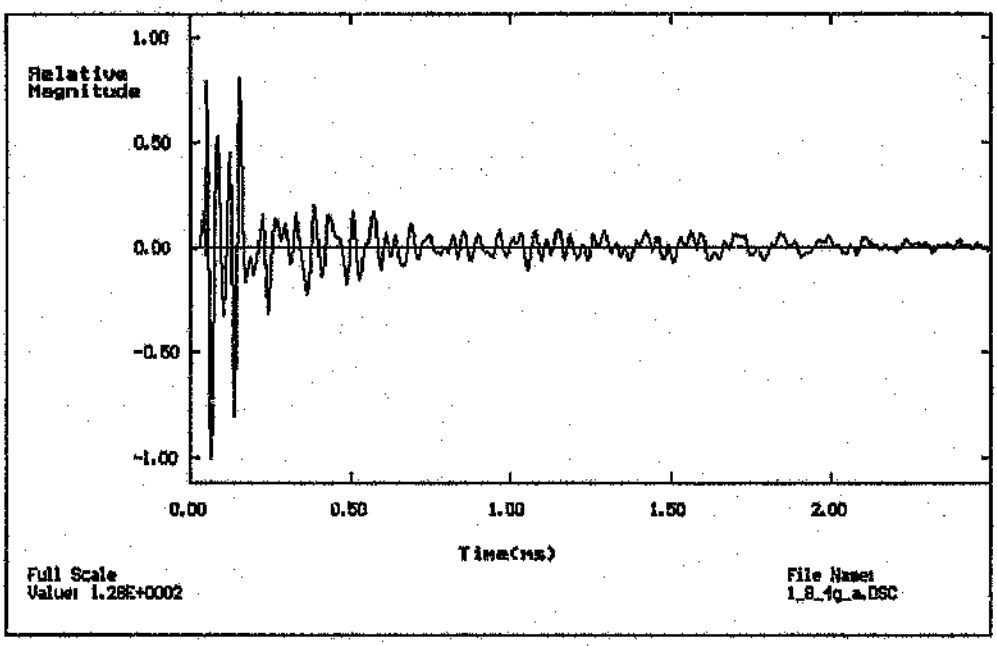

Figure A11 Pulse response of rebar: four concrete cylinders

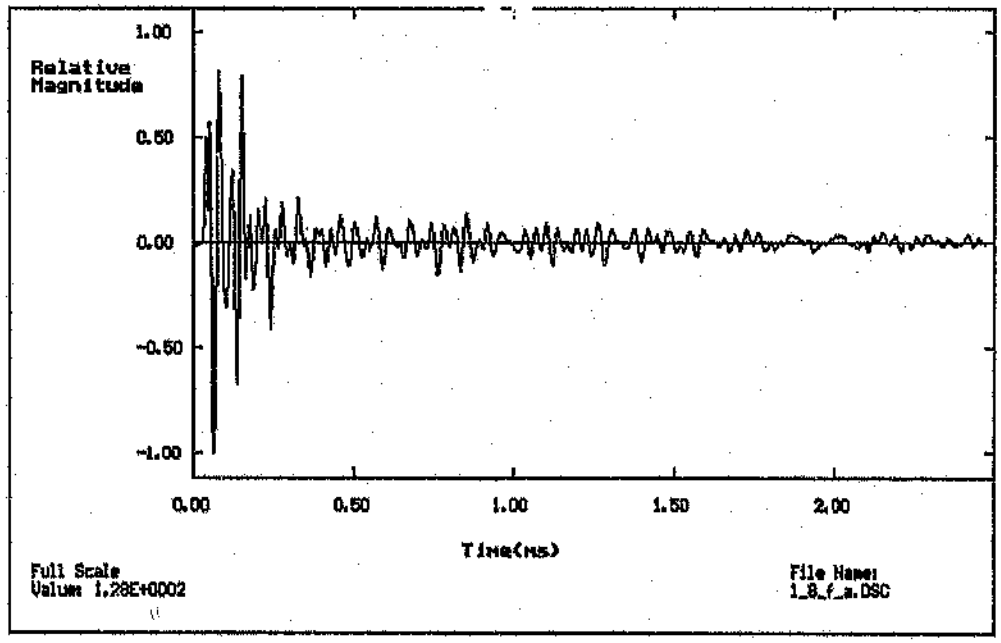

Figure A12 Pulse response of rebar: five concrete cylinders

APPENDIX B

Log magnitude spectra for the two sample rock anchors

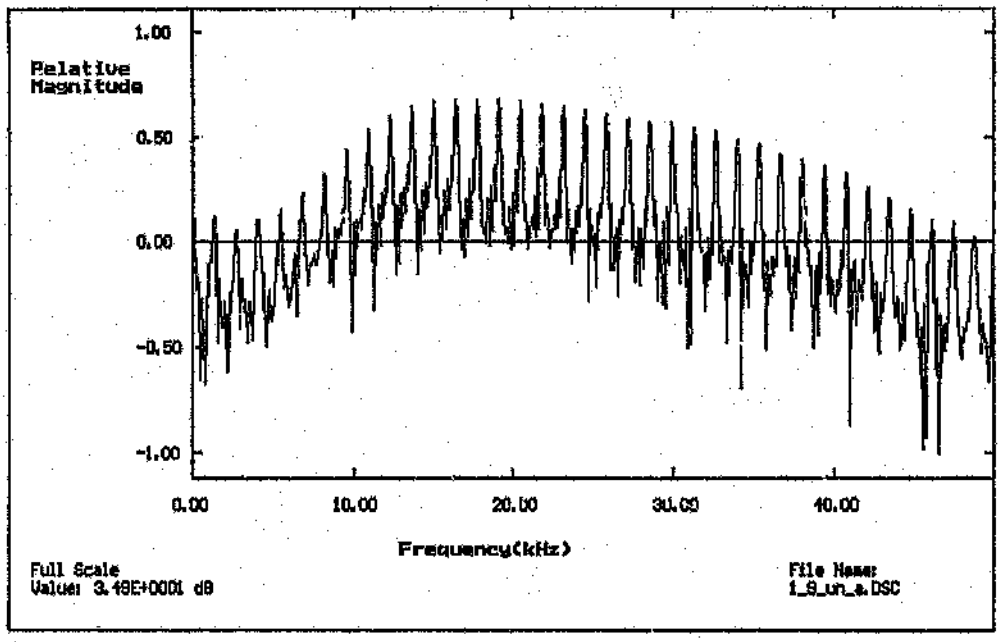

Figure B1 Log magnitude spectrum for free 1,9m smooth bar

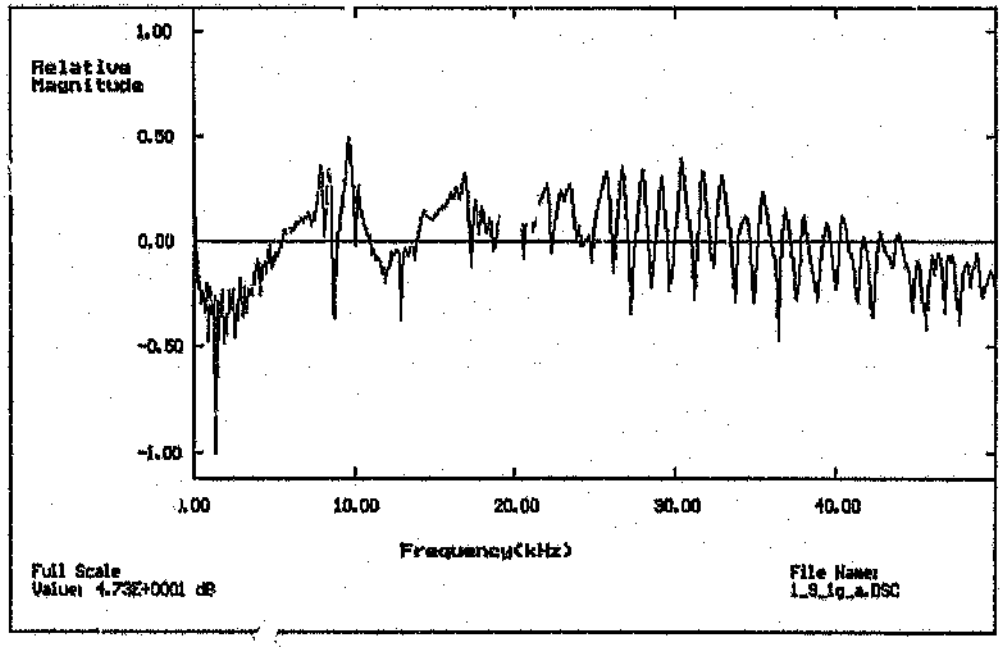

Figure B2 Log magnitude spectrum for smooth bar: one concrete cylinder

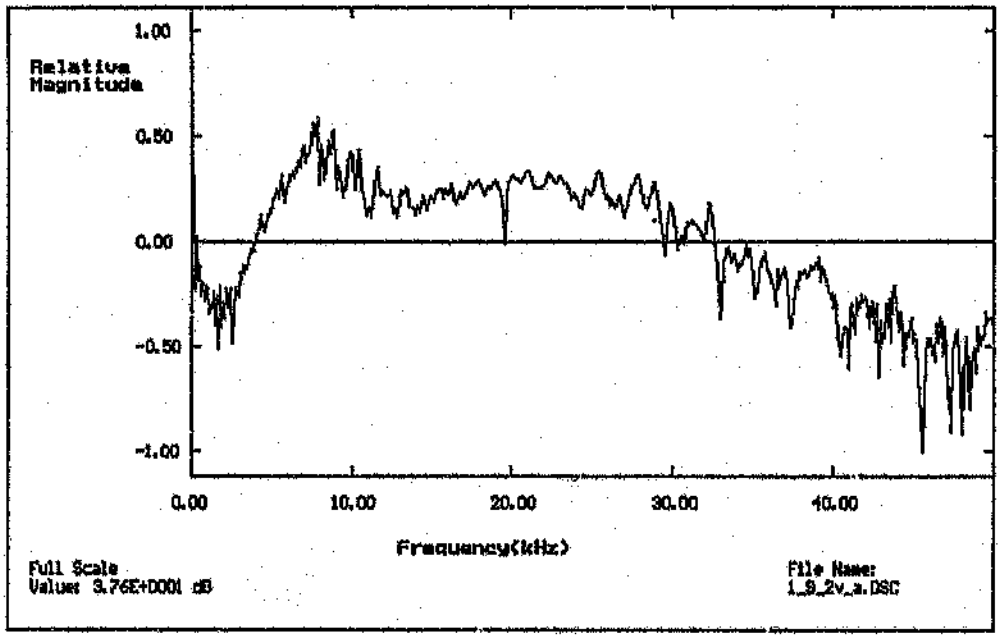

Figure B3 Log magnitude spectrum for smooth bar: two concrete cylinders

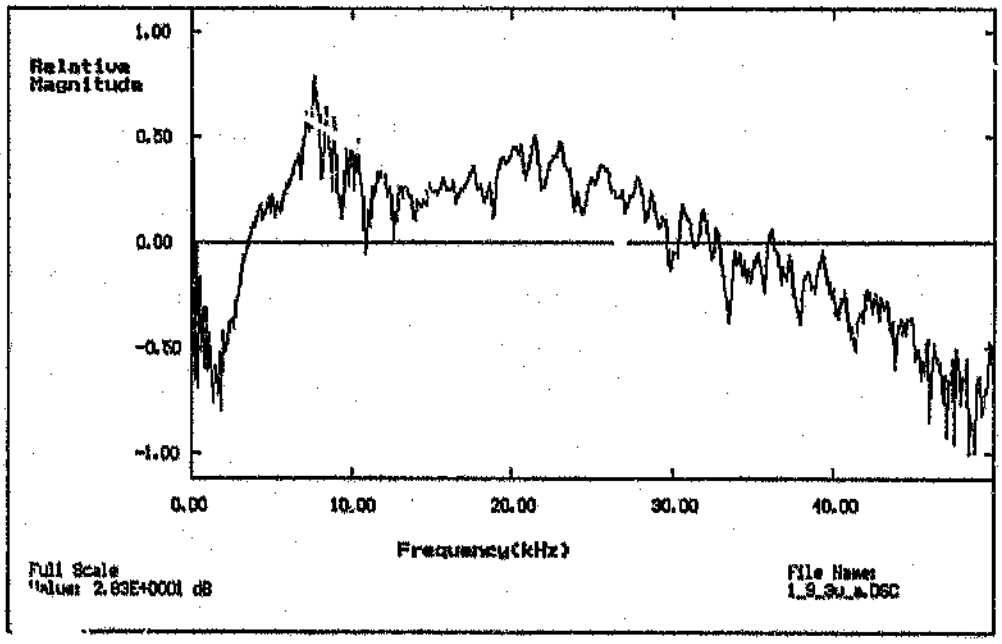

Figure B4 Log magnitude spectrum for smooth bar: three concrete cylinders

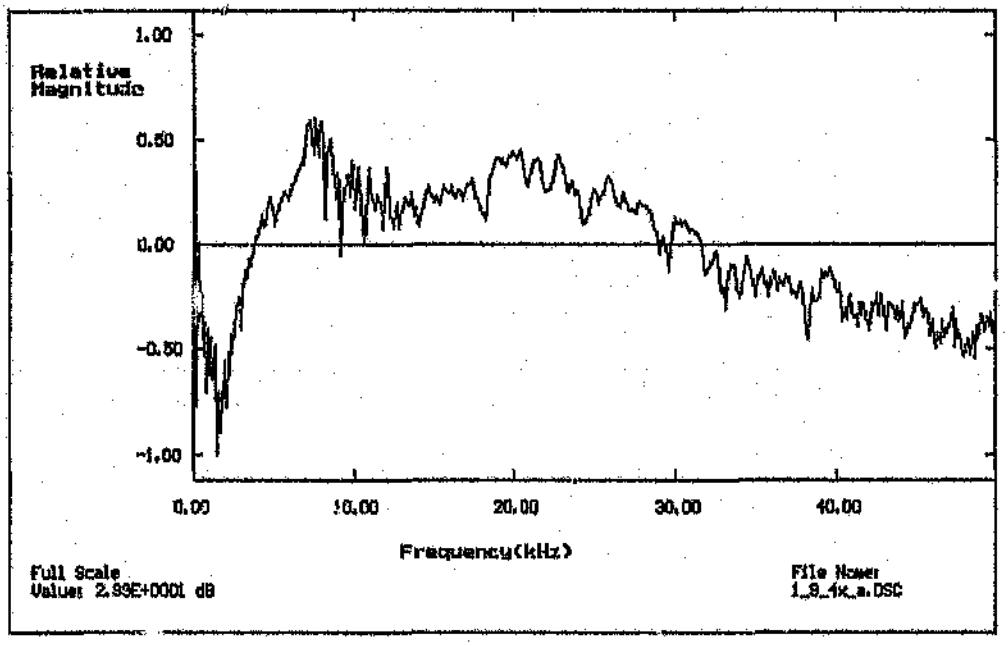

Figure B5 Log magnitude spectrum for smooth bar: four concrete cylinders

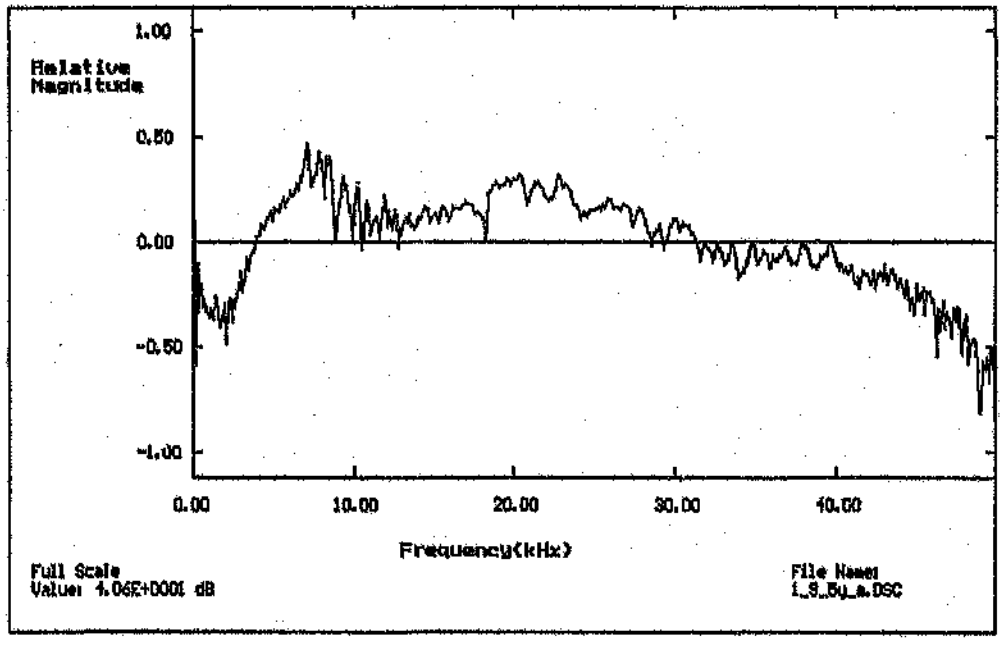

Figure B6 Log magnitude spectrum for smooth bar: five concrete cylinders

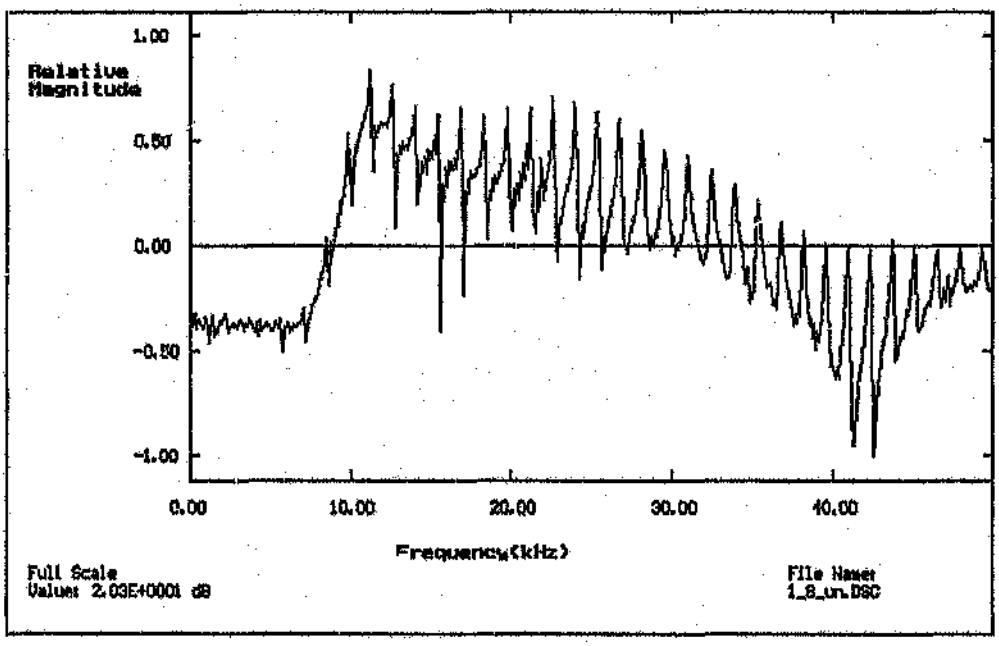

Figure B7 Log magnitude spectrum for free 1,8m rebar

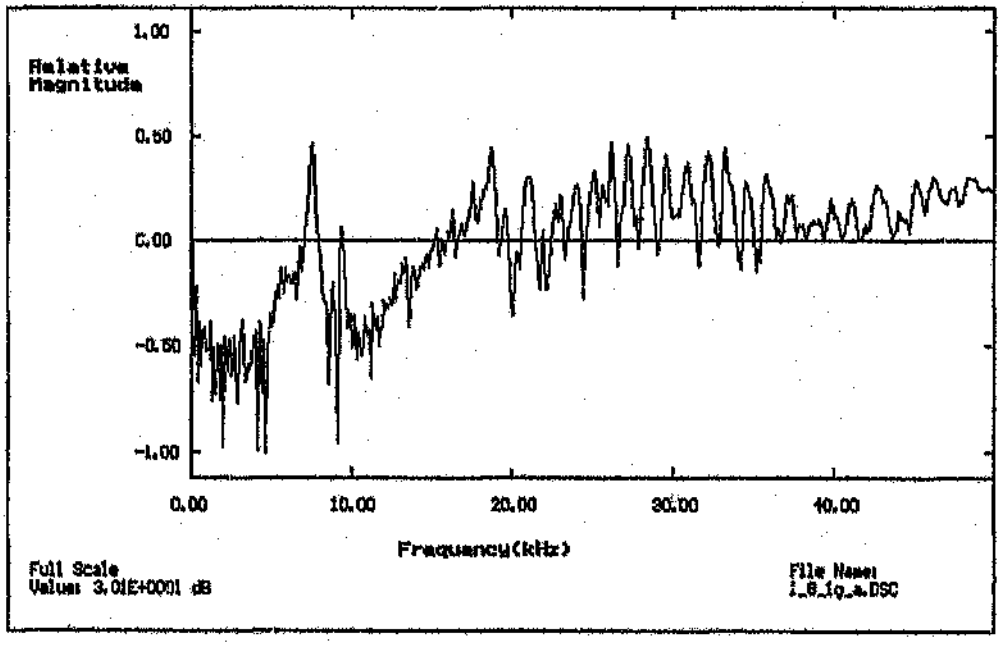

Figure B8 Log magnitude spectrum for rebar: one concrete cylinder

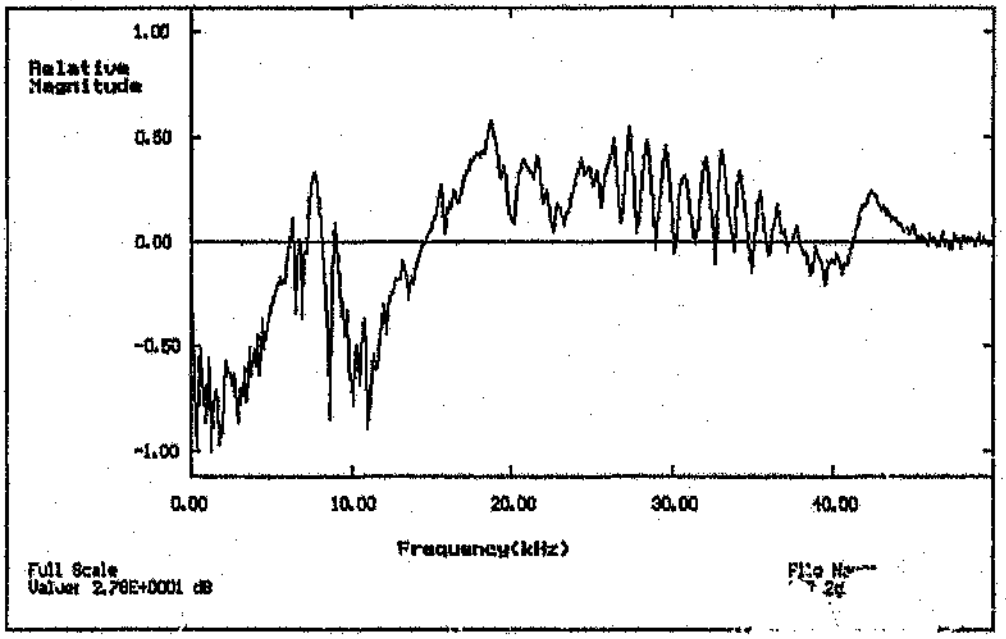

Figure B9 Log magnitude spectrum for rebar: two con. cylinders

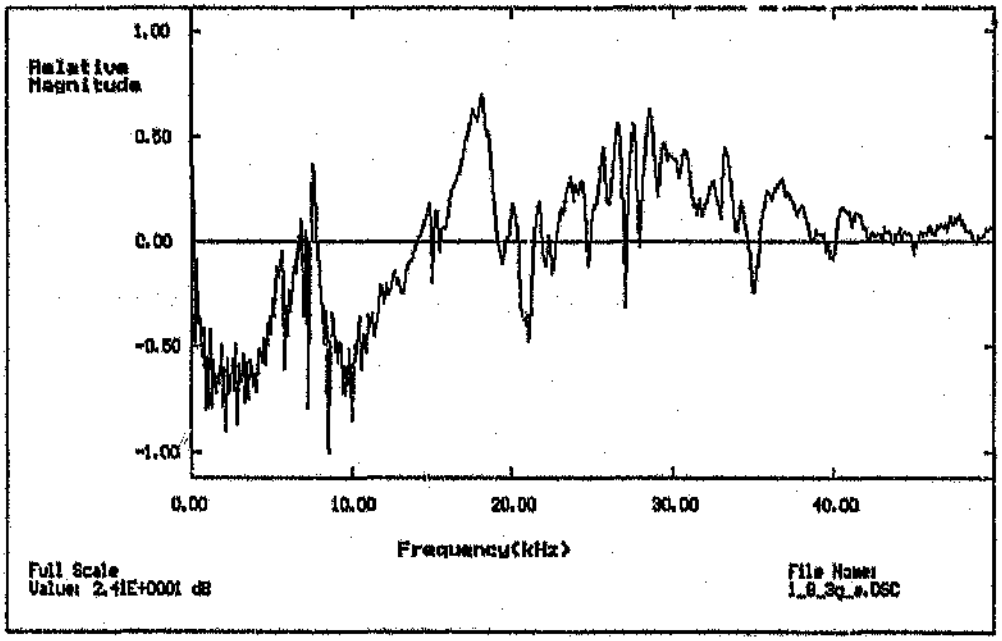

Figure B10 Log magnitude spectrum for rebar: three concrete cylinders

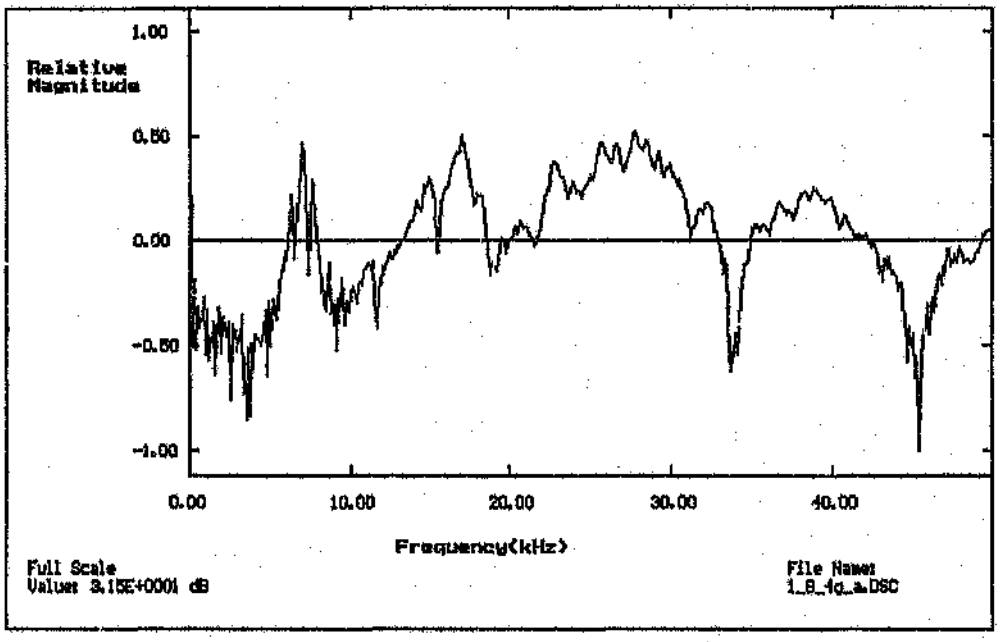

Figure B11 Log magnitude spectrum for rebar: four concrete cylinders

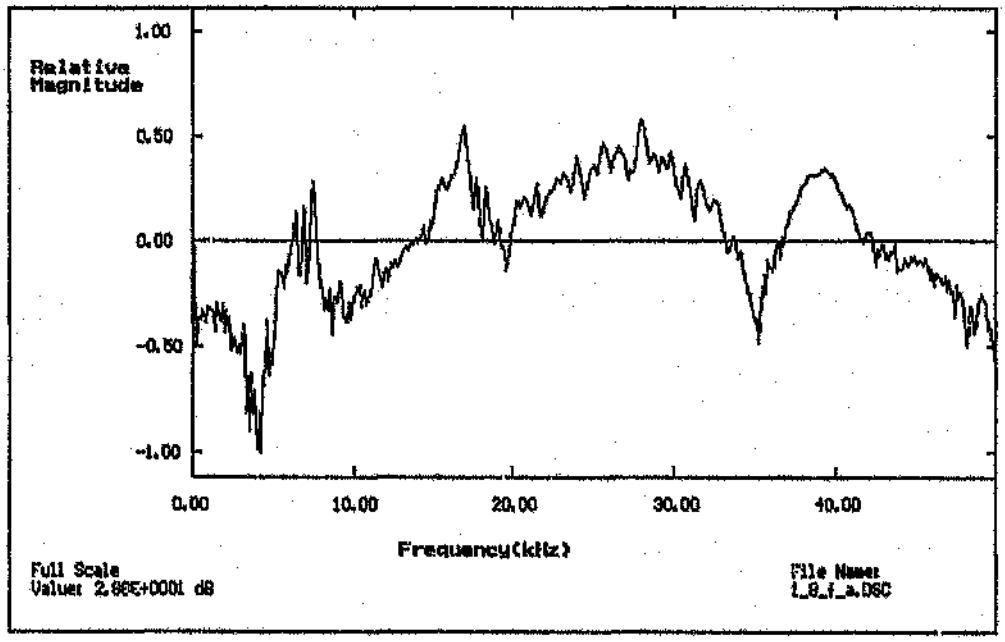

Figure B12 Log magnitude spectrum for rebar: five concrete cylinders

APPENDIX C

Band-limited envelope cepstra for the two sample rock anchors

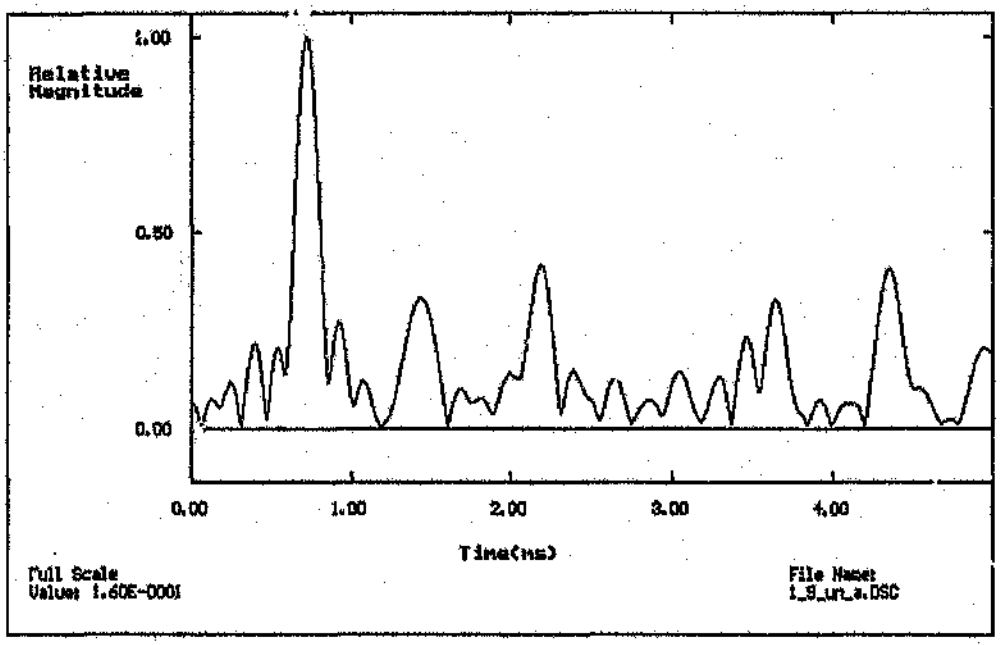

Figure C1 Band-limited envelope cepstrum for free 1,9m smooth bar

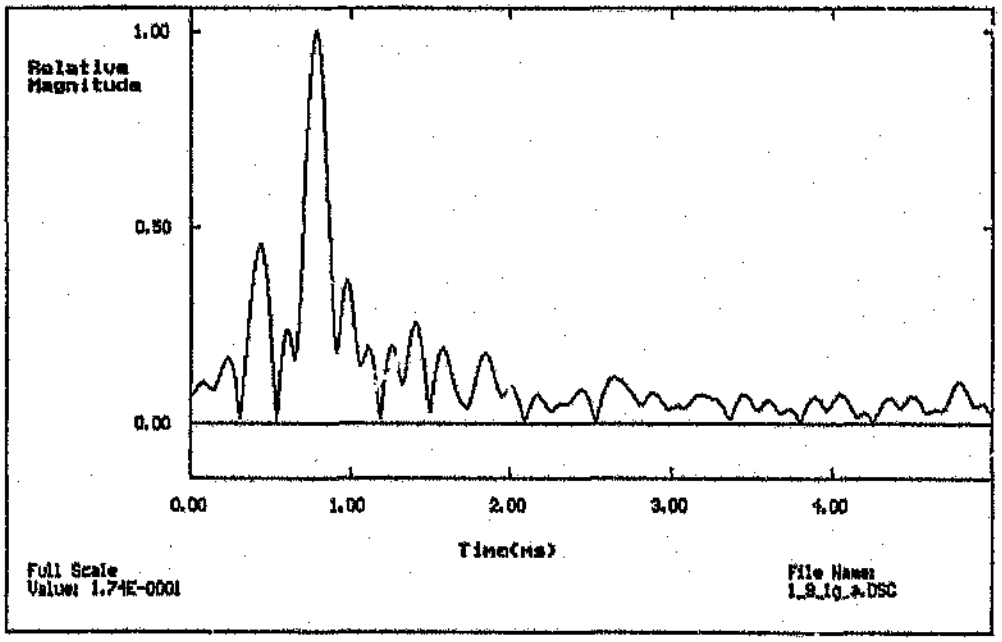

Figure C2 Band-limited envelope cepstrum for smooth bar: one concrete cylinder

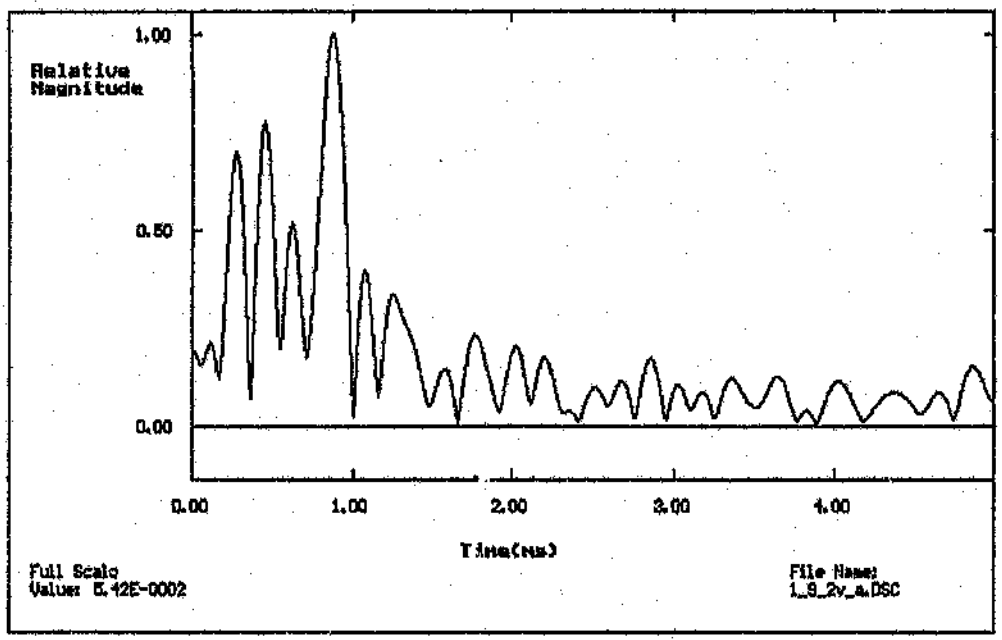

Figure C3 Band-limited envelope cepstrum for smooth bar: two concrete cylinders

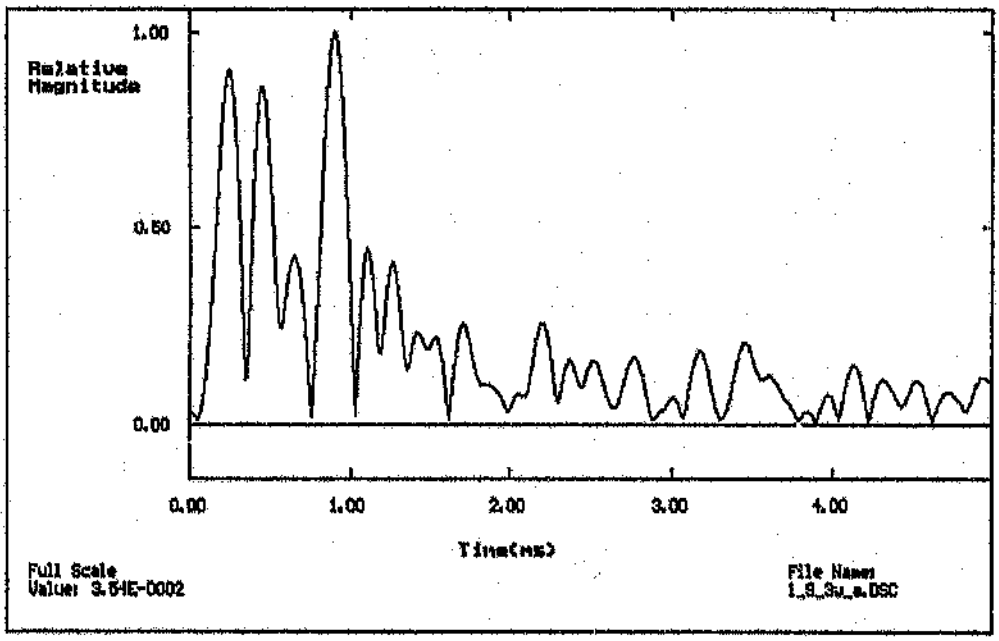

Figure C4 Band-limited envelope cepstrum for smooth bar: three concrete cylinders

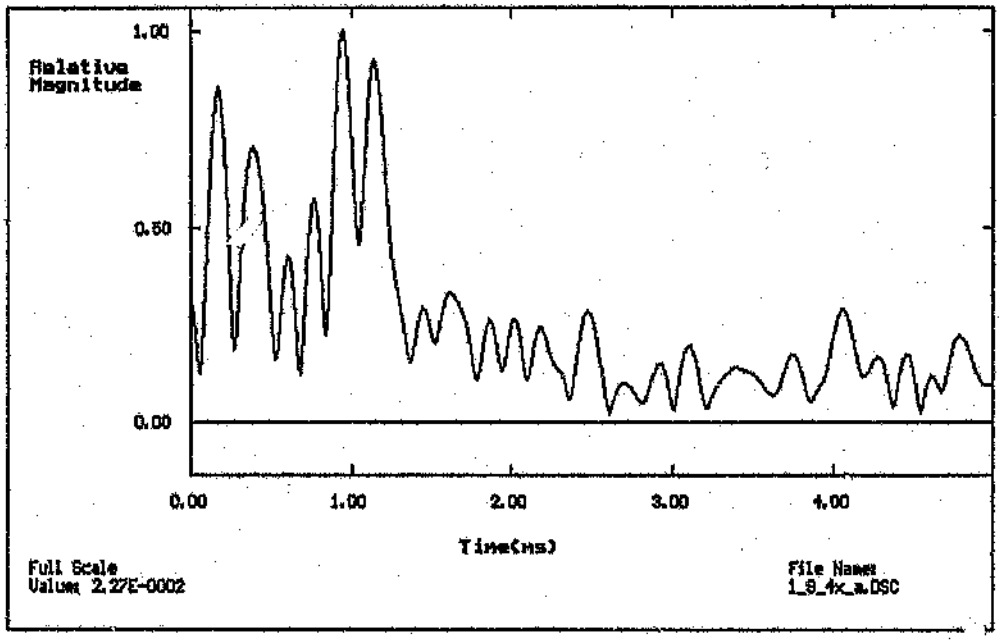

Figure C5 Band-limited envelope cepstrum for smooth bar: four concrete cylinders

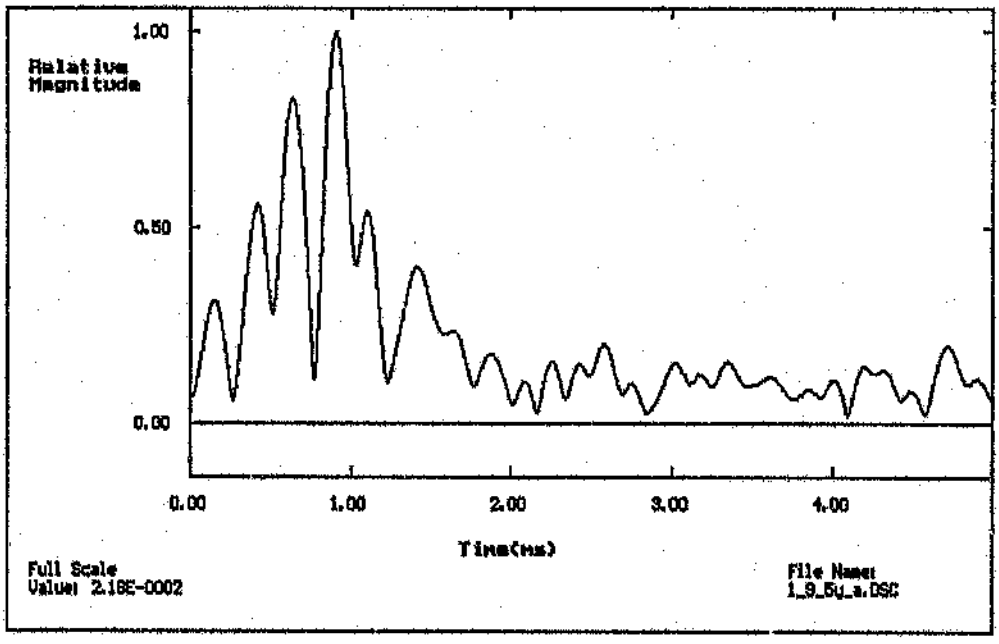

Figure C6 Band-limited envelope cepstrum for smooth bar: five concrete cylinders

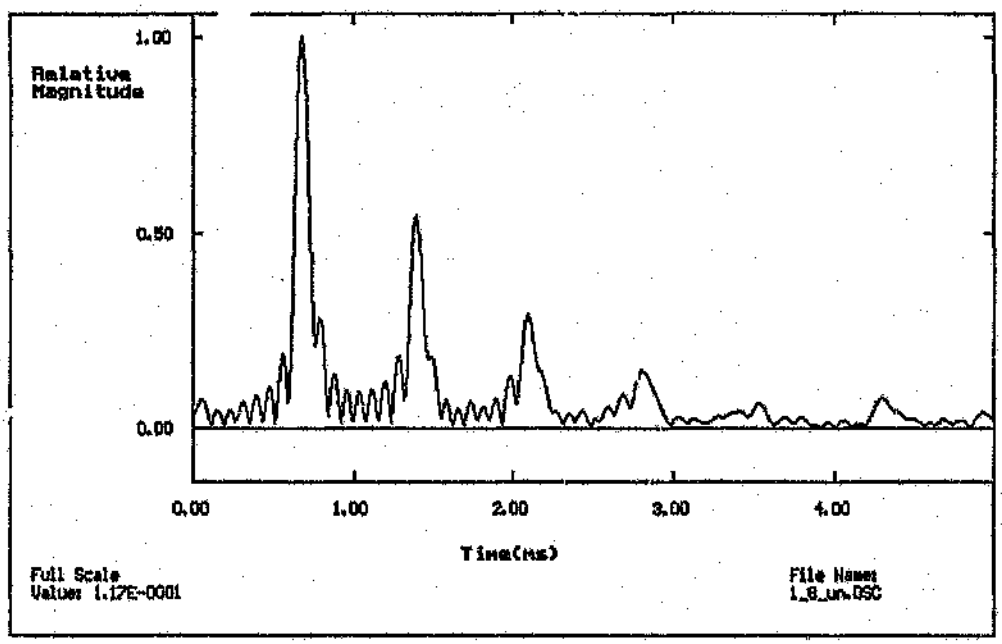

Figure C7 Band-limited envelope cepstrum for free 1,8m rebar

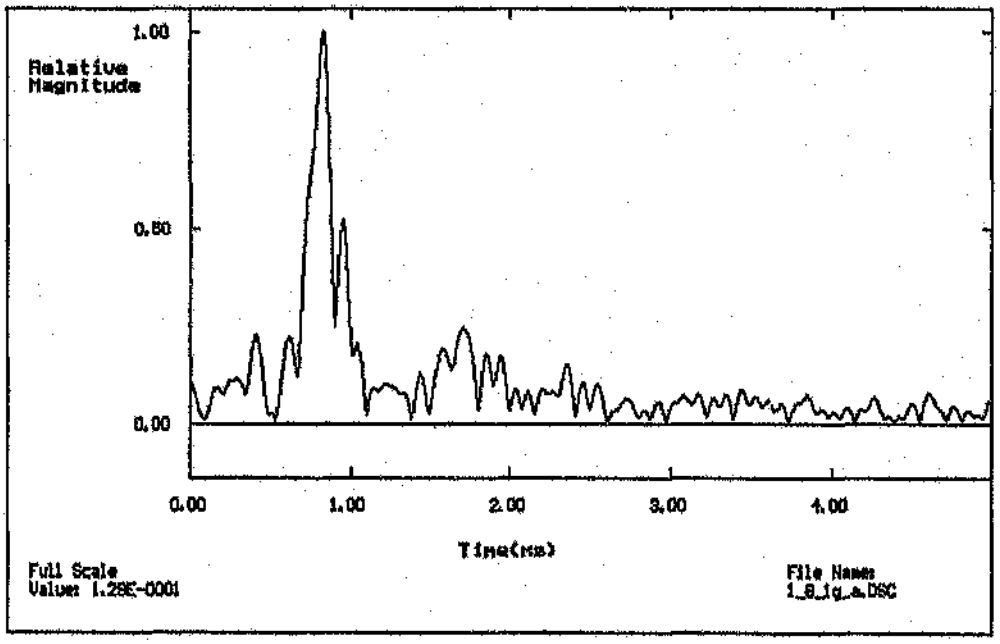

Figure C8 Band-limited envelope cepstrum for rebar: one concrete cylinder

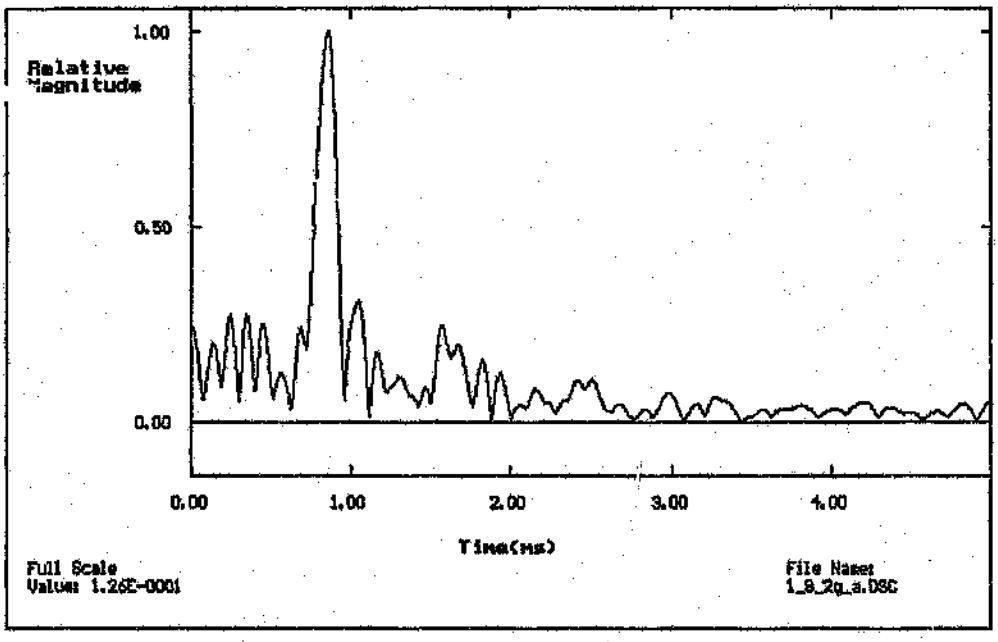

Figure C9 Band-limited envelope cepstrum for rebar: two concrete cylinders

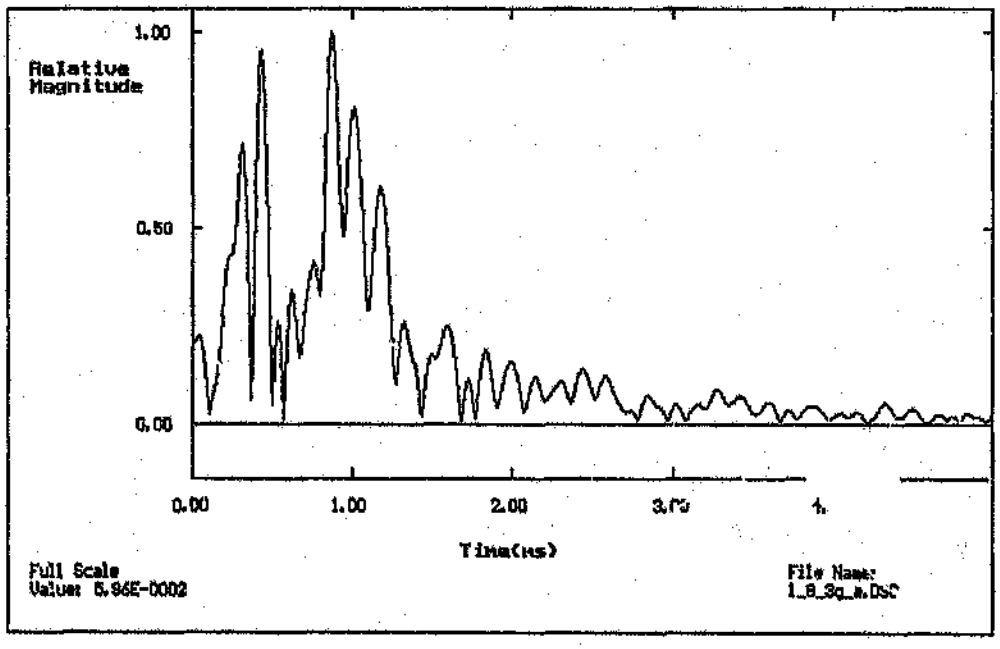

Figure C10 Band-limited envelope cepstrum for rebar: three concrete cylinders

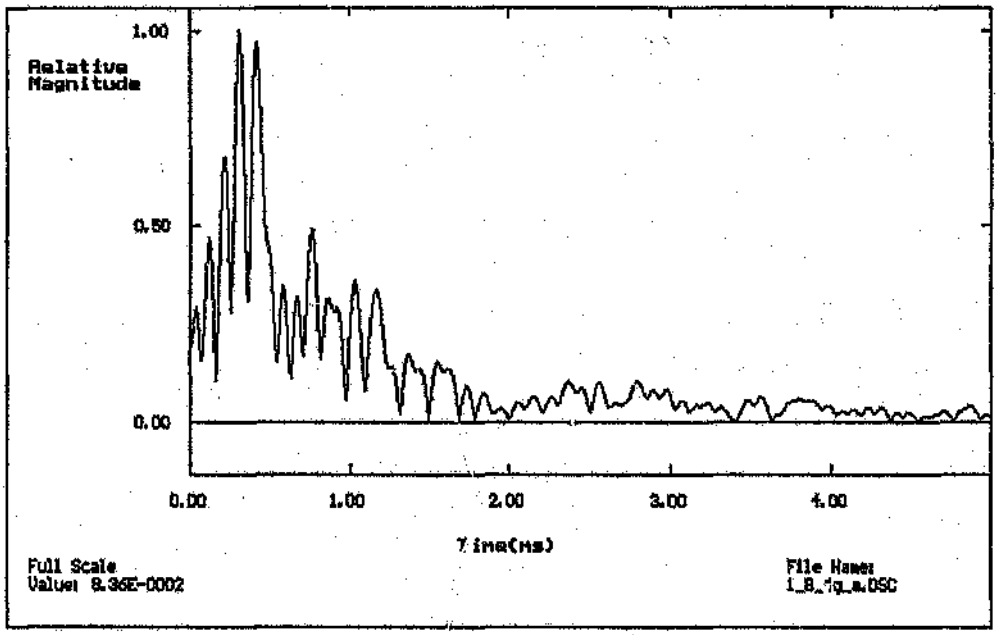

Figure C11 Band-limited envelope cepstrum for rebar: four concrete cylinders

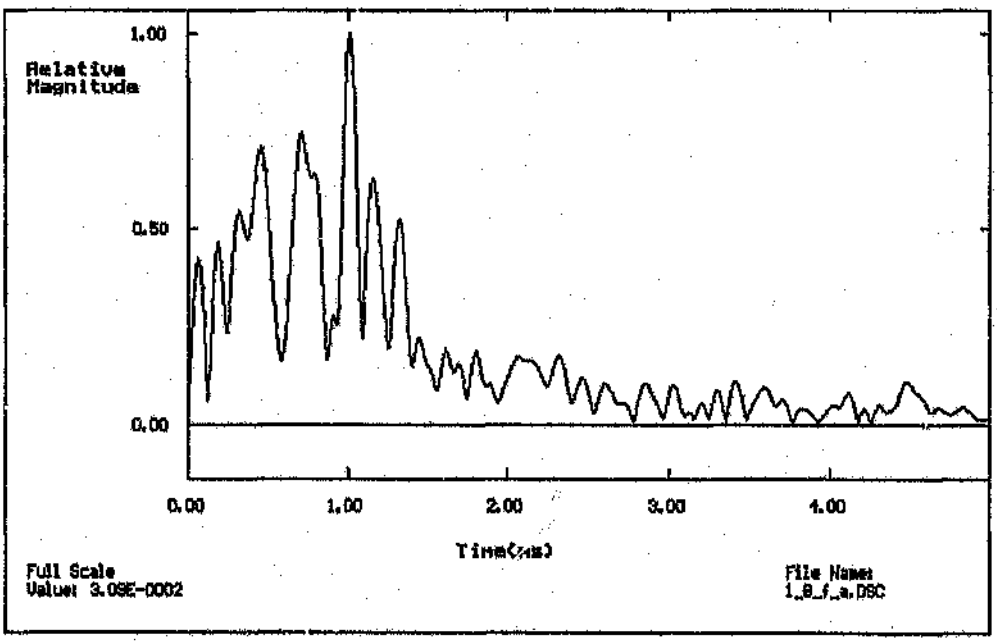

Figure C12 Band-limited envelope cepstrum for rebar: five concrete cylinders

APPENDIX D

FURTHER RESULTS - RECORDINGS OF REAL ROCK ANCHOR RESPONSES

CONTENTS

D1 INTRODUCTION

In order to investigate the acoustic response of real rock anchor installations, 13 rock anchors were recently installed at the Boart Experimental Mine. Pairs of 2m smooth, straight bar rock anchors of 18mm diameter were installed with 20%, 40%, 60%, 80% and 100% grout coverage. Each rock anchor was installed with approximately 20cm of its near end protruding from the rock face. Three further rods of length 1,07m, 1,30m and 2,00m of the same description and 100% grout coverage were installed.

Table D1 gives a summary of the set of rock anchors installed, and the exact lengths of the protruding near ends. Grout percentages are expressed over the full length of the rod, except where the rod is fully grouted - in this case, the grouted length is the full length minus the length of the exposed end. All rods were grouted continuously, from the front end backwards, for the grouted length. All rods had M20 threads cut into the near end, at which the magnetostrictive transducer was applied. Ends were filed flat for application of the piezo receiver and Prestik was used as the acoustic interface material. The grout used has a full strength curing time of 10-14 days. The rods were tested a day after they had been grouted. The rods were tested without nuts, plates, doughnuts or mesh and lacing. All data are quantised to 8 bits, and were recorded in the memory of a Thurlby DSA524.

Fig. No.	Rod, File No.	Rod Length (m)	Grout %	Exposed End (cm)
D1	1	2	0	Free Rod
D2	2	2	20	15
D3	11	2	20	22
	3 (data lost)	2	40	19
D4	10	2	40	19
D5	4	2	60	23
D6	7	2	60	27
D7	5	2	80	25
D8	6	2	80	20
D9	9	2	100	19
D10	13	2	100	18
D11	14	2	100	24
D12	8	1.30	100	20
D13	12	1.07	100	19

Table D1 Test rock anchors installed at Boart Mine

The time responses of these installations are shown in Figures D1 to D13, except for one of the 2m rods with 40% grout coverage. Unfortunately, this record was somehow lost at the test site. It can be said, however, that the e amplitude in the lost record was about 10% of the amplitude of the direct pulse. Echoes from the far end of the rock anchors are marked with arrows in the time response graphs, where they are discernible. The log magnitude spectra for time records where an echo pulse is discernible are shown in Figs. 14 to 18. The band of frequencies containing the echo information is marked in each spectrum. Spectra for time records which do not show echoes are not very useful, and so are not included here. Cepstra and attenuation curves for the recordings are not given here because too few records displayed an echo, and data were inconsistent - attenuation curves and cepstra would not be useful. This problem will be commented on in the conclusion.

D2 ASSESSMENT OF RESULTS

D2.1 Evaluation of Concrete Cylinders used to Simulate Rock

A comparison of the real rock anchor responses with the responses from the simulation using concrete cylinders shows that:

* A resonance in the protruding end of the rod is visible in each time record and its spectrum.

* The reflection in the real responses is much smaller but more coherent. That is, the reflection is less distorted.

From these observations can be drawn the following conclusions:

* The stronger, more distorted echoes of the simulation are due to multipath effects in the concrete cylinders: acoustic energy entering the cylinders is not dissipated, but returns to the near end of the rod.

* The concrete cylinders used for the simulation are therefore inadequate, and the simulation does not give responses which are similar to (or representative of) the responses of real rock anchor installations.

* The simulation was nevertheless useful in laying the groundwork for both the hardware and software for an instrument. The simulation did identify the echo band-limiting effect which is also visible in the real responses.

The longer travel time of the pulse with increasing grout coverage is not seen in the real rock anchors responses (assuming that the given length and grout coverage information is correct). The arrival time in the real installations is fairly consistent, at about 0,88ms. From this it can be concluded that the increasing pulse arrival time seen in the simulation is an artefact produced by multipath effects in the concrete cylinders, and is a further indication of the inadequacy of the concrete cylinders.

D2.2 Recommendations for Signal Processing

In the light of the new results, the following comments on the signal processing should be made:

* The cepstrum retains its usefulness: the real rock anchor responses are band-limited, and the advantage of selecting the band of frequencies containing the echo therefore remains.

* The cepstrum derived from the band-limited spectrum unambiguously identifies the echo amplitude and time of arrival for the real results, where the echo is large enough: because the A/D used to record the responses quantised the data to 8 bits, the echo in well grouted rods was irrecoverably lost.

* An A/D with a better dynamic range is required (16 bits) if echoes in rods grouted over 120cm to 160cm are to be detected.

D3 CONCLUSIONS AND FURTHER RESEARCH

A disturbing observation regarding the real rock anchor responses is the lack of agreement in the size of the echo in rod pairs which are 20, 40 and 60% grouted. This lack of agreement is clearly visible in the time signals Fig. D2 and Fig. D3 for the case of 20% grouting. Fig. D2 shows a reflection which is about ten times the size of the reflection seen in Fig. D3. In the case of 60% grouting, Fig. D5 shows a reflection which is not at all visible in Fig. D6. For identical rock anchors, grout, drillhole size, grout distribution and coverage and rock type (that is, identical installations), one would expect echoes of comparable size. This difference in echo sizes is not an artefact of the signal recording but is truly representative of the acoustic behaviour of the rods. The large difference in echo amplitudes therefore appears to be attributable to one, or a combination, of the following:

(i) The tests were performed only one day after the rock anchors had been installed. The full strength curing time of the grout used is 10 to 14 days. The discrepancy in pulse amplitudes could be due to the fact that the grout on one of the rods had been curing for longer than it had on the other.

(ii) The echo amplitude may, in each case, be truly representative of the grout bond effectiveness of the rods: the difference in grout coverage could be due to an error in the amount of grout applied to the rods, or due to a bad grout bond on the rod with larger echo (caused by grease on the rod surface, for example).

(iii) Lack of repeatability in almost identical rock anchor installations due to some unexpected acoustic property of the system. In this case, pulse attenuation cannot be unambiguously related to grout coverage with the required precision and the principle of the instrument fails. If this speculation is verified with further tests, the acoustic method should be abandoned immediately.

The discrepancy can be attributed to (i) if, after the full curing time of the grout, the echo amplitudes of rods with the same grout coverage concur.

If the discrepancy in echo amplitude still exists after the grout curing time, the validity of (ii) can be investigated by performing a pull test on the rods. If the pull test supports the observed difference in echo amplitudes, all is well, and further installations can be carefully made (ensuring correct grout coverage) for further repeatability tests on the rock anchors.

If the pull test indicates the same grout coverage in the rock anchors, the discrepancy in results must be attributed to point (iii). The veracity of (iii) can be assessed by installing a further two rock anchors which are grouted over 40cm, paying special attention to ensure that grout coverage is correct and that the two rod surfaces are clean and in the same condition. If, after the full curing time of the grout, the discrepancy in pulse amplitudes still exists, a pull test can be applied to verify grout coverage. If the pull tests indicate that the rods have the same grout coverage, the acoustic method must be abandoned. In this case, finding the reason for the discrepancy (in acoustical terms) is unlikely to lead to an improvement in the method which will make the instrument viable.

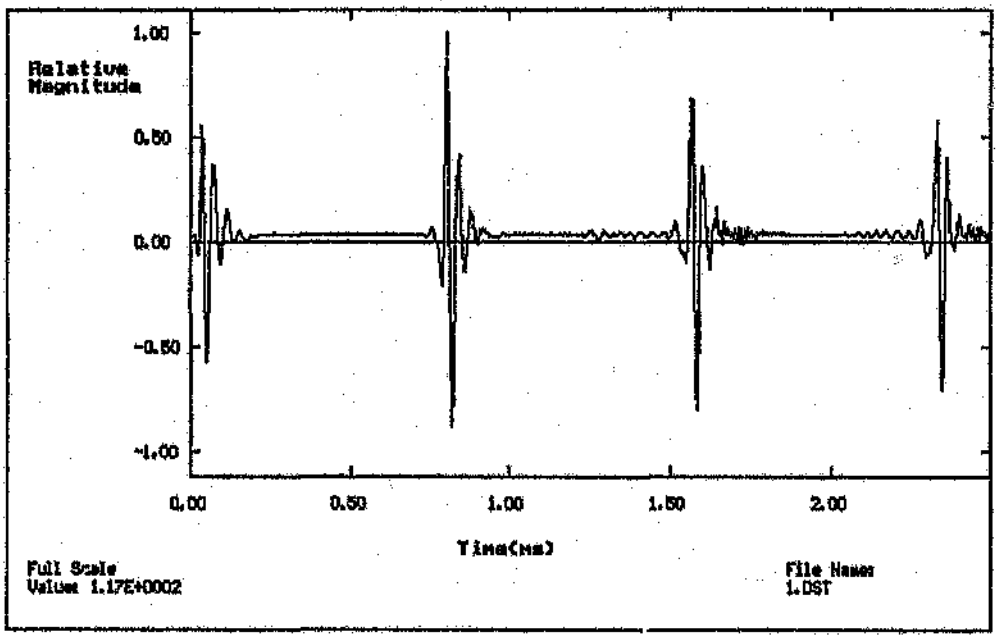

Figure D1 Time response of 2m rod, ungrouted

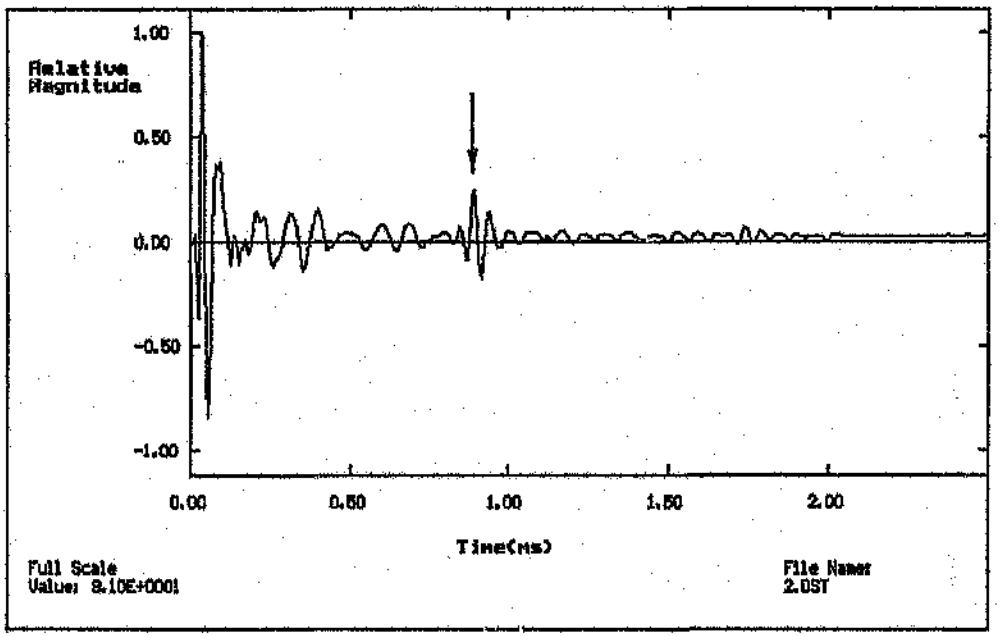

Figure D2 Time response of 2m rod, 20% grouted

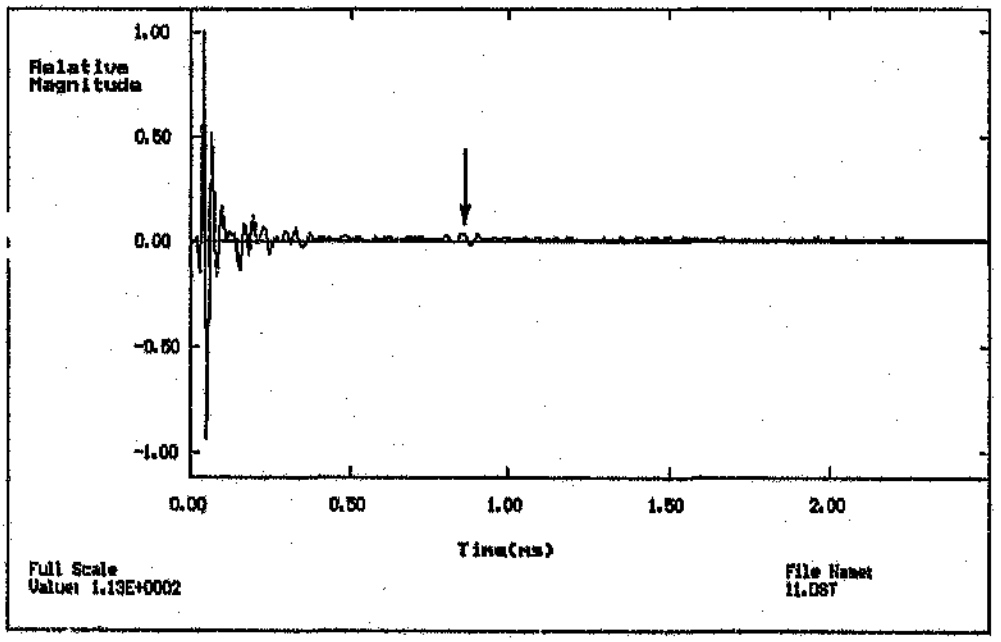

Figure D3 Time response of 2m rod, 20% grouted

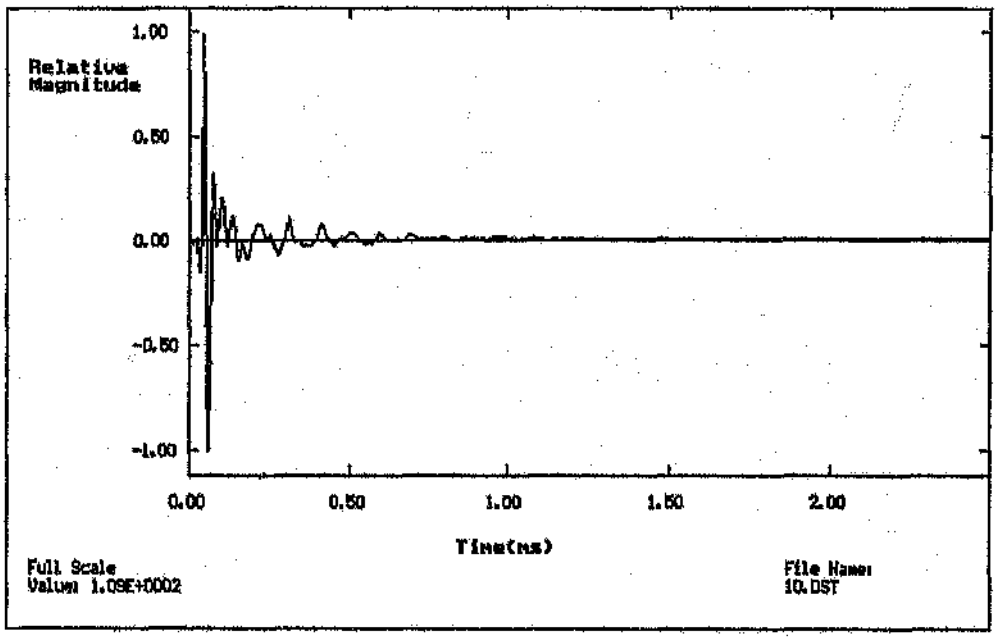

Figure D4 Time response of 2m rod, 40% grouted

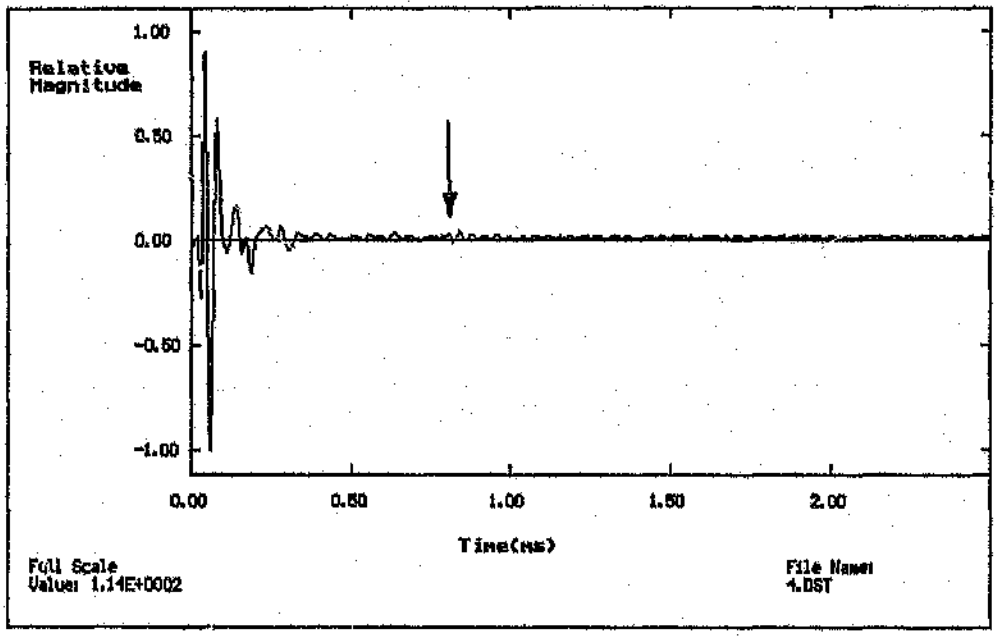

Figure D5 Time response of 2m rod, 60% grouted

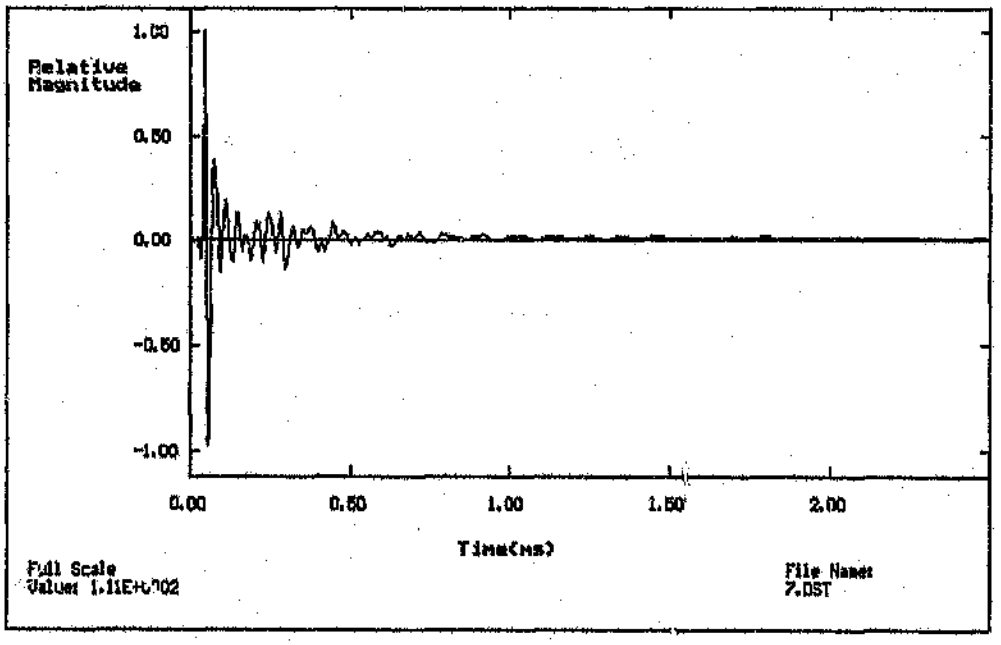

Figure D6 Time response of 2m rod, 60% grouted

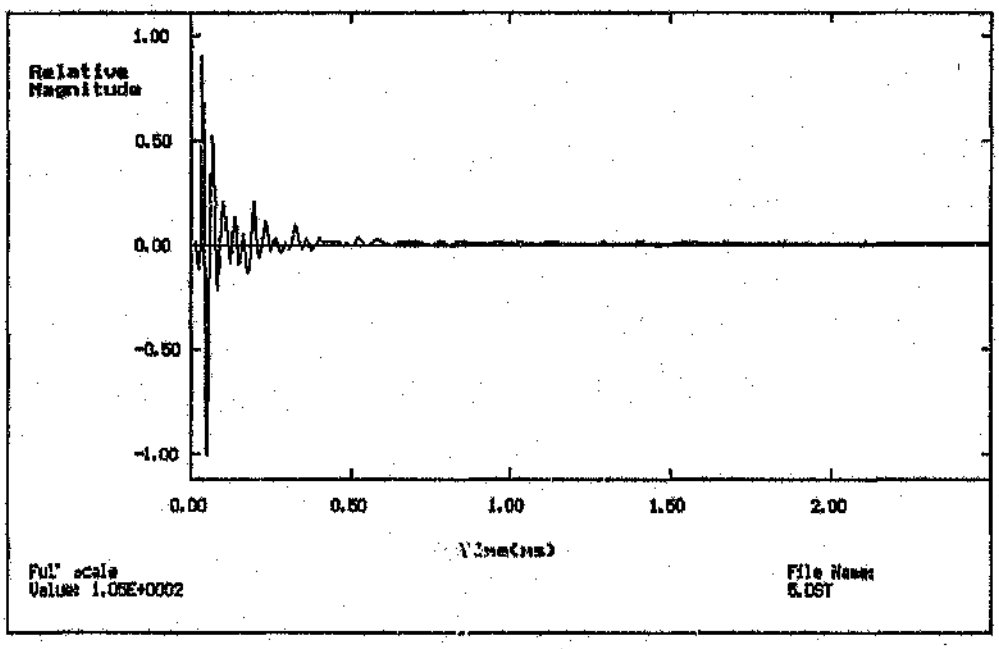

Figure D7 Time response of 2m rod, 80% grouted

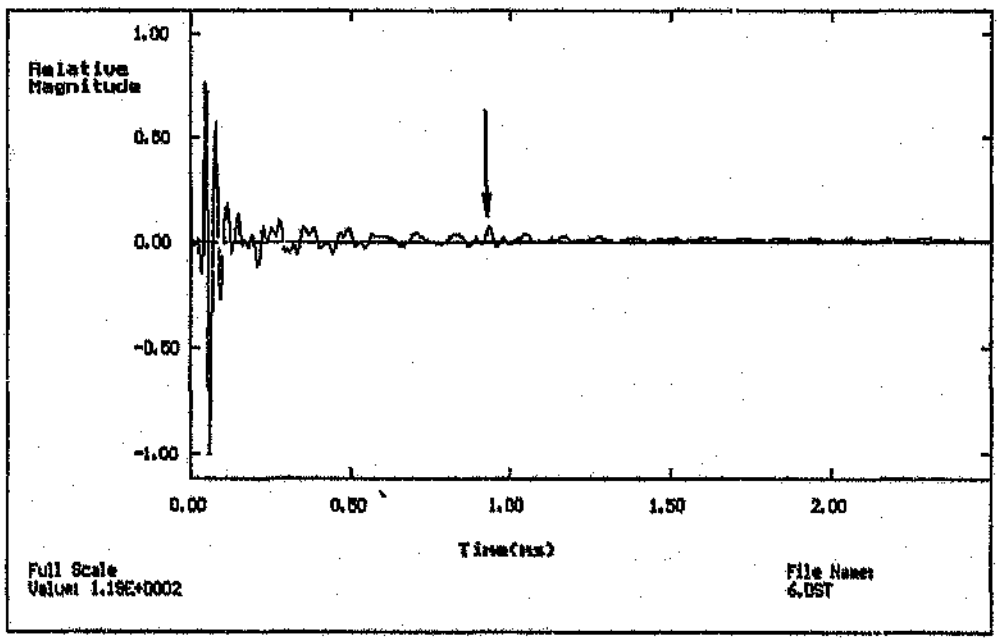

Figure D8 Time response of 2m rod, 80% grouted

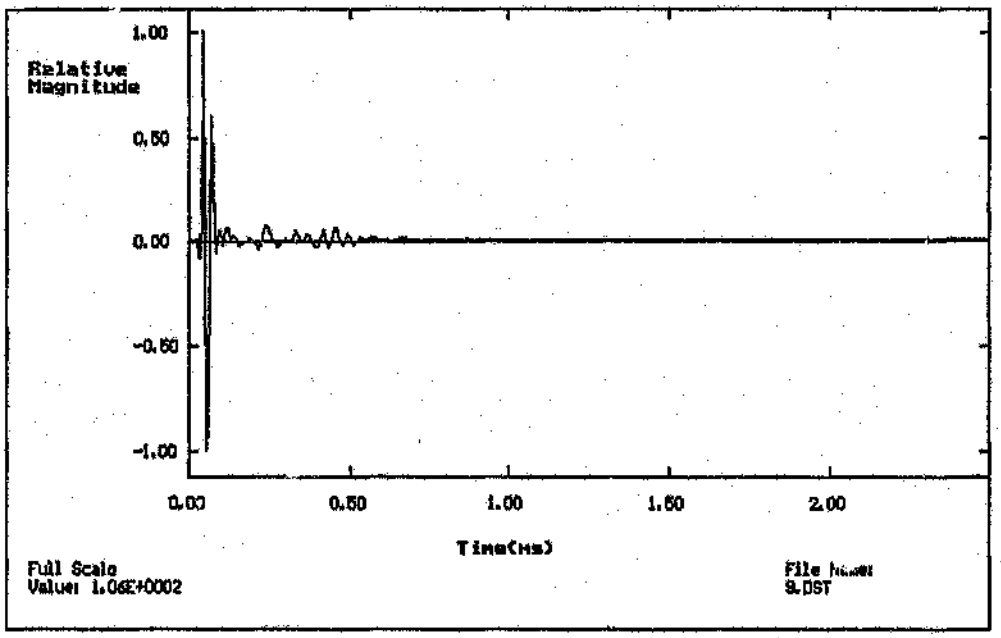

Figure D9 Time response of 2m rod, 100% grouted

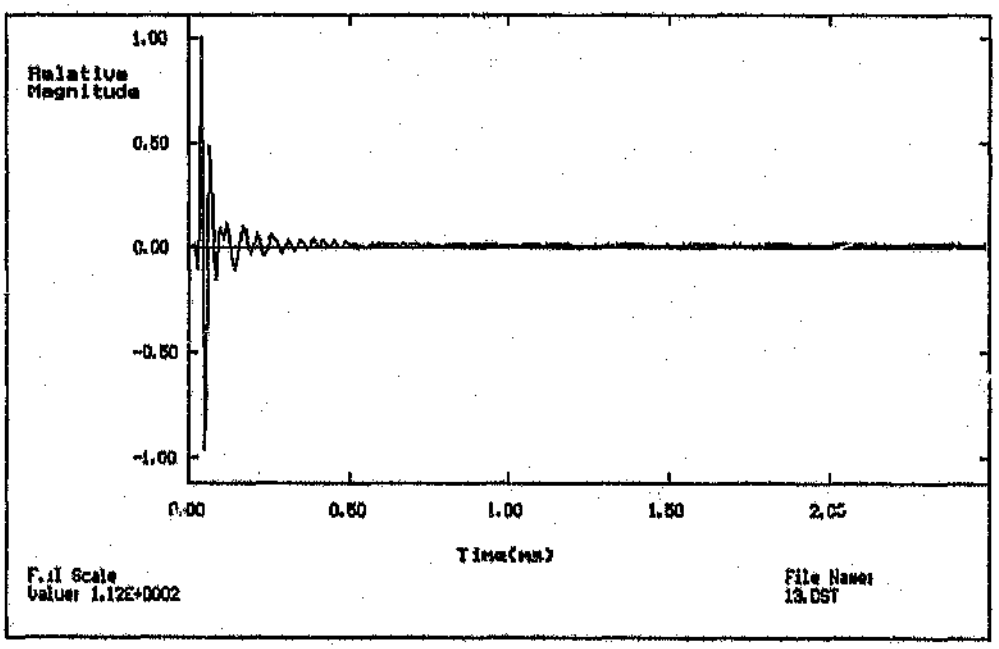

Figure D10 Time response of 2m rod, 100% grouted

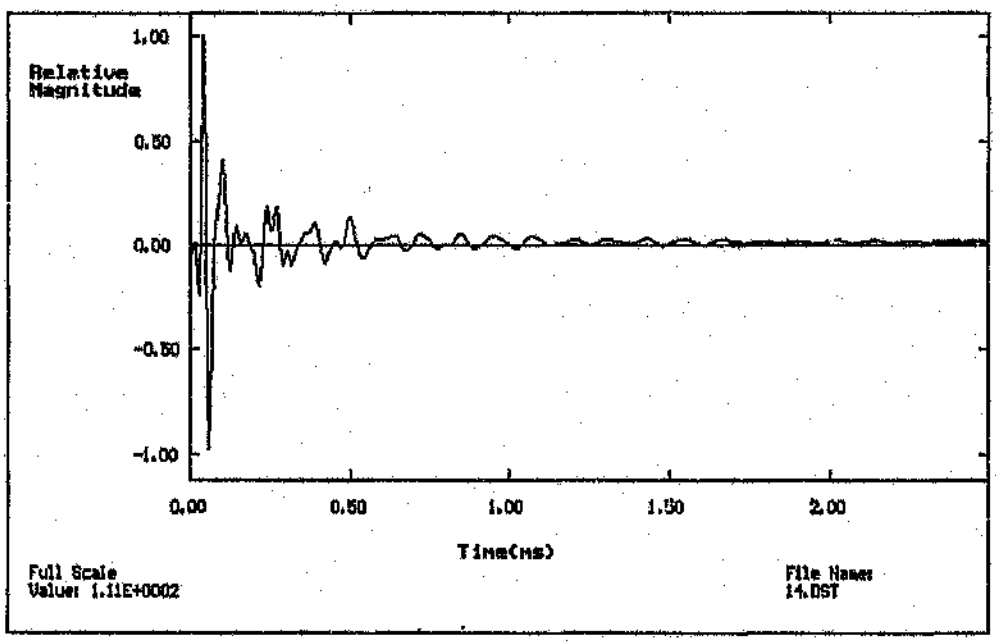

Figure D11 Time response of 2m rod, 100% grouted

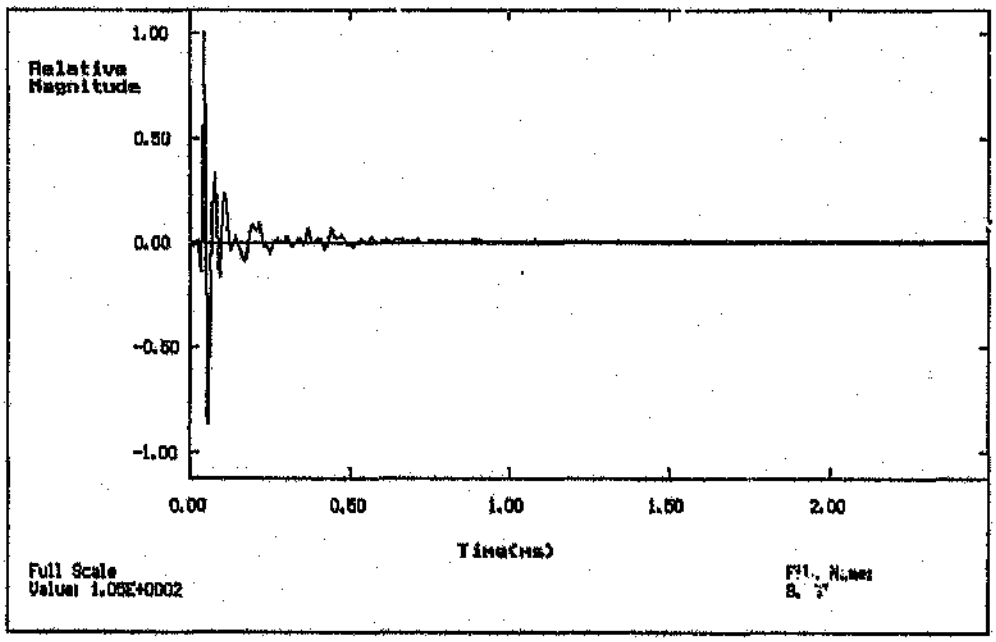

Figure D12 Time response of 1,30m rod, 100% grouted

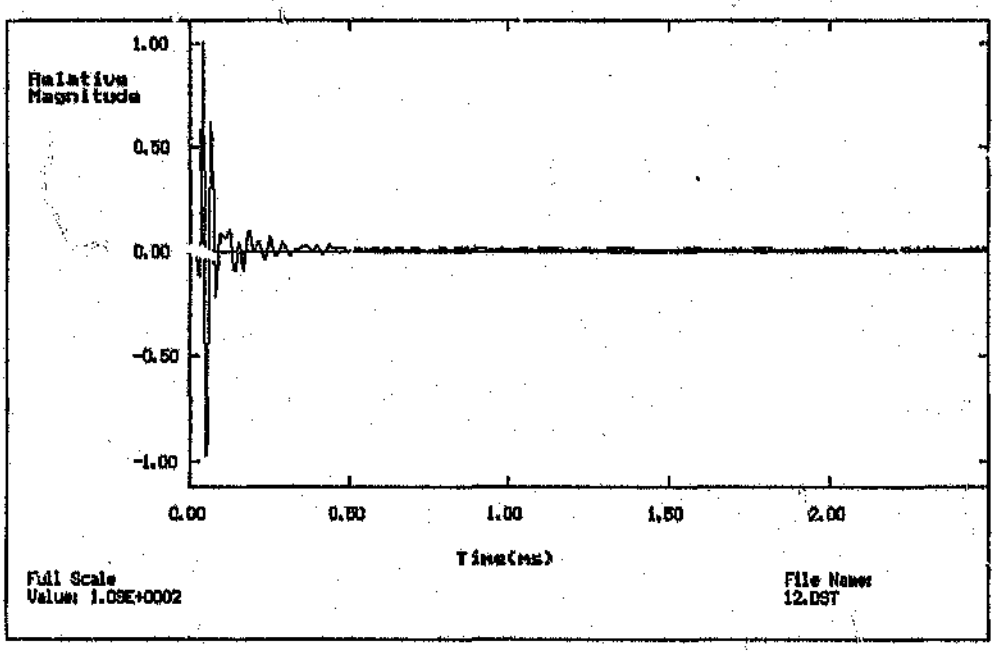

Figure D13 Time response of 1,07m rod, 100% grouted

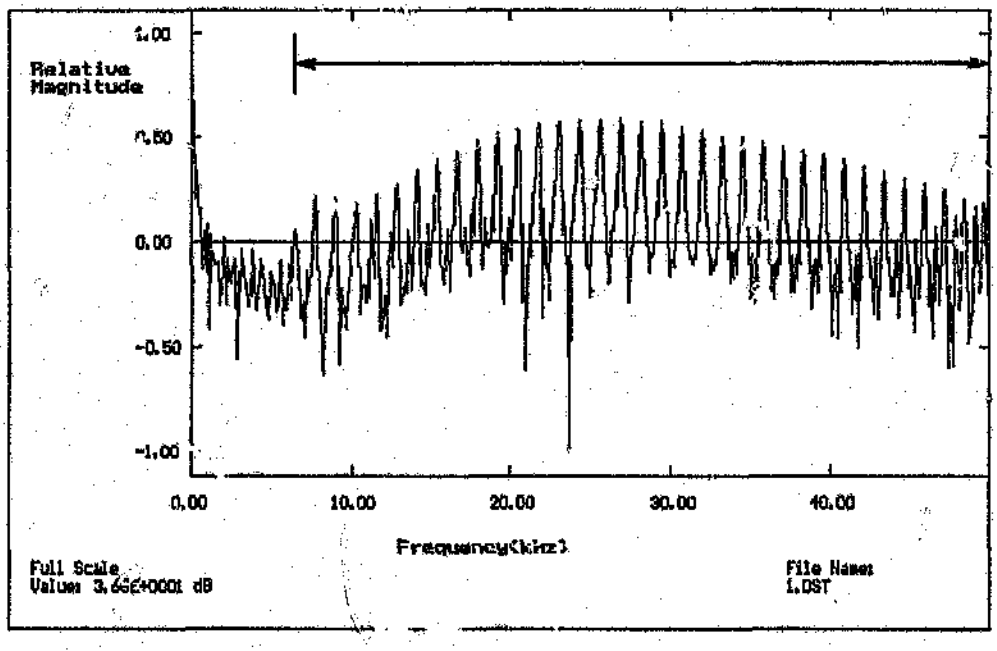

Figure D14 Log magnitude spectrum of Fig. D1

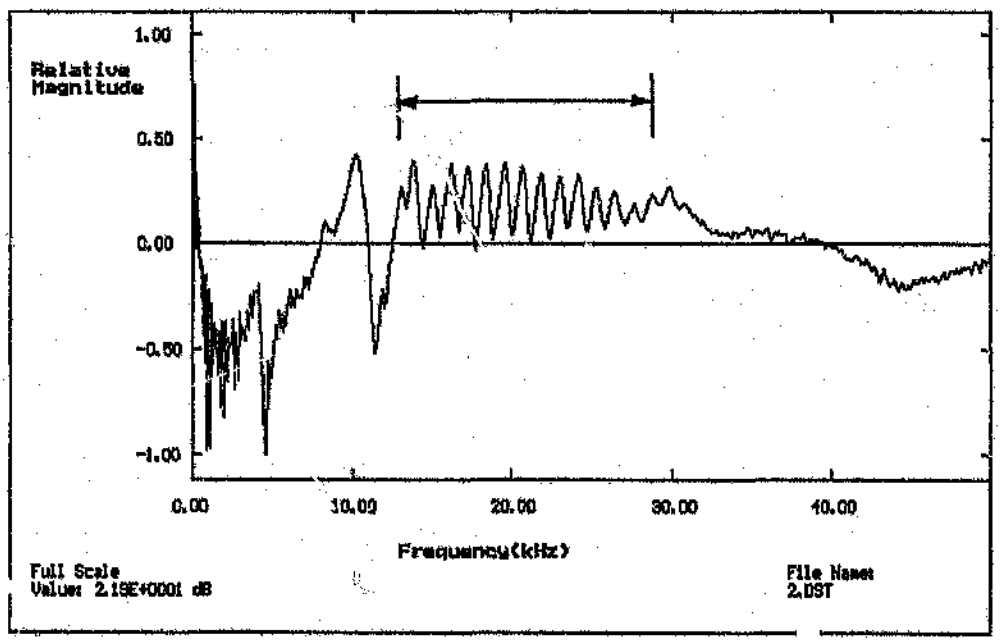

Figure D15 Log magnitude spectrum of Fig. D2

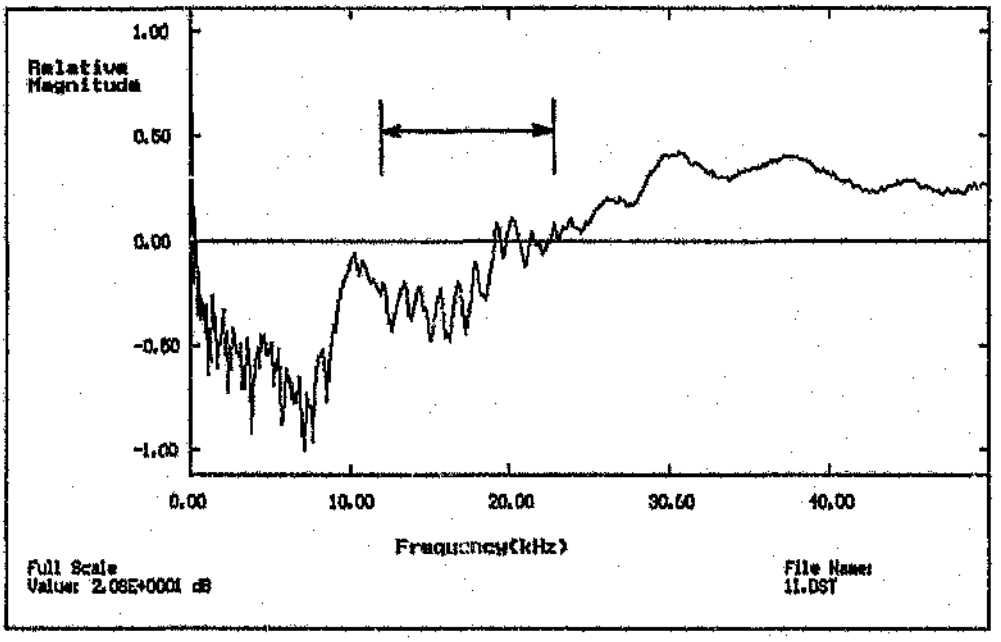

Figure D16 Log magnitude spectrum of Fig. D3

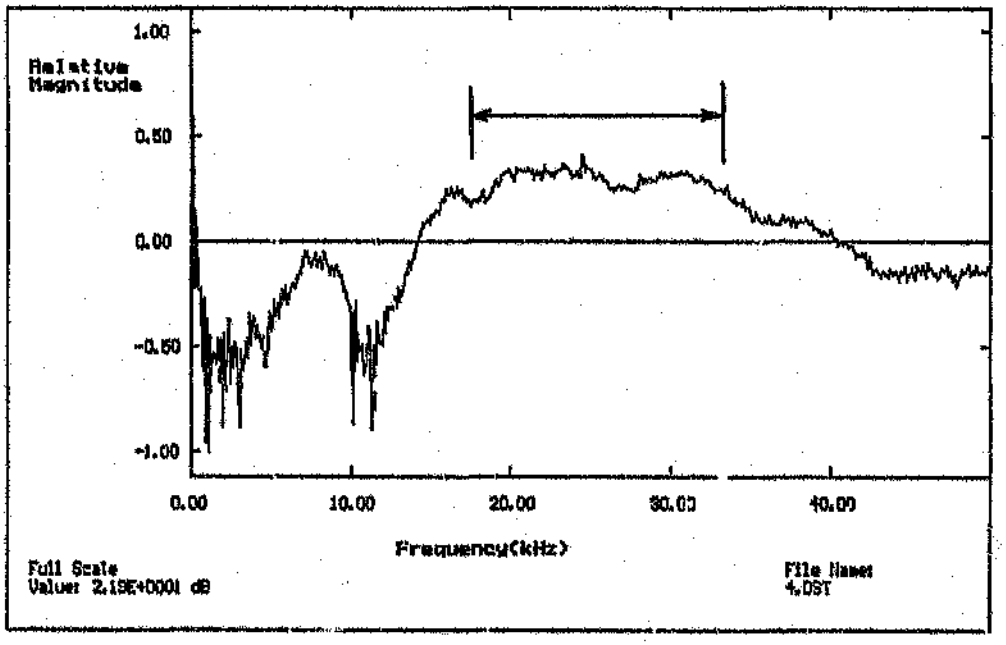

Figure D17 Log magnitude spectrum of Fig. D5

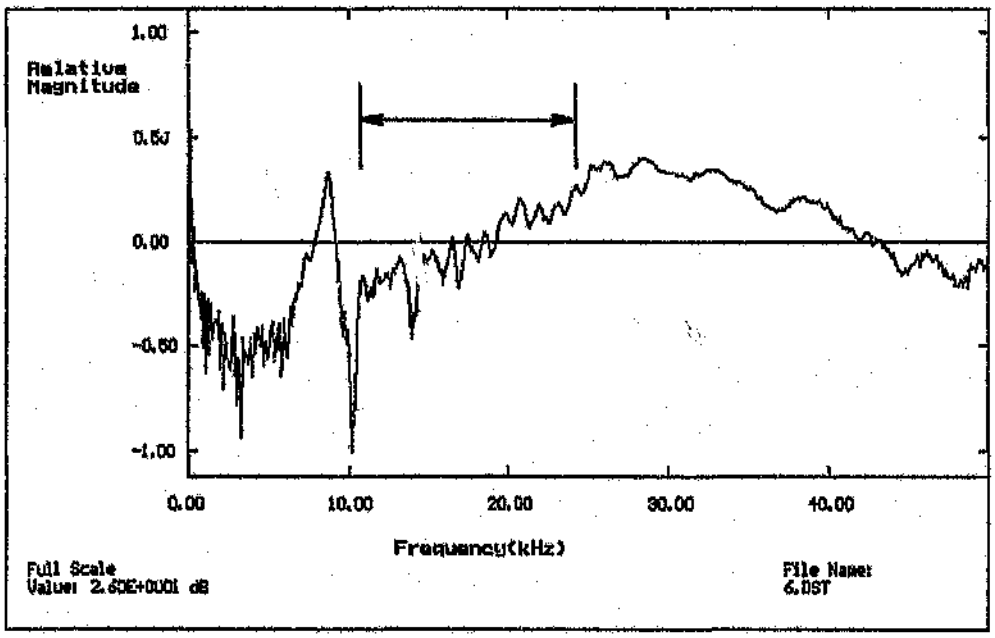

Figure D18 Log magnitude spectrum of Fig. D8

REFERENCES

[1] Moulder G R, Howard P L, Hesler J C and Tarpley W B, "Ultrasonic Stress Transfer: A Direct Test of Rock Bolt Integrity", United States Department of the Interior, Bureau of Mines : Denver, Colorado, Contract J0295037, August 1983.

[2] Stateham R M, "Roof Bolt Bond Tester; A Device for Nondestructive Testing of Grouted Bolts", United States Department of the Interior, Bureau of Mines, Denver Colorado, pp. 183-187. (No date or contract number given).

[3] Burke Harry E, "Handbook of Magnetic Phenomena", Van Nostrand Reinhold Company, 1986, pp. 253-270.

[4] Oppenheim A V and Shafer R W, "Digital Signal Processing", Prentice-Hall, 1975, pp. 480-528.

[5] Hassab J C and Boucher R, "Analysis of Signal Extraction, Echo Detection and Removal by Complex Cepstrum in Presence of Distortion and Noise", IEEE Journal of Sound and Vibration, Vol. 40, No. 3, 1975, pp. 321-335.

[6] Borgert B P, Healy M J and Tukey J W, "The Quefrency Analysis of Time Series for Echoes: Cepstrum, Pseudo-Autocovariance and Saphe-Cracking", in Proc. Symp. on Time Series Analysis by M Rosenblatt, Ed., New York: Wiley, 1963, pp. 209-243.

[7] Randall R B and Hee J, "Cepstrum Analysis", Bruel & Kjaer Technical Review, 3-1981, pp. 3-40.

[8] Tribolet J M, "Seismic Applications of Homomorphic Signal Processing", Prentice-Hall Inc., 1979.

[9] Al-Nashi H, "Phase Unwrapping of Digital Signals", IEEE Trans ASSP, Vol. 37, No. 11, November 1989, pp. 1693-1702.

[10] Childers D G, Skinner D P and Kemerait R C, "The Cepstrum: A Guide to Processing", Proceedings of the IEEE, Vol. 65, No. 10, October 1977, pp. 1428-1443.

[11] Ulrych T J, Jensen O G, Ellis R M and Somerville P G, "Homomorphic Deconvolution of some Teleseismic Events", Bulletin of the Seismological Society of America, Vol. 62, No. 5, 1972, pp. 1253-1265.

[12] Jin D J and Eisner E, "A Review of Homomorphic Deconvolution", Reviews of Geophysics and Space Physics, Vol. 22, No. 3, August 1984, pp. 255-263.

[13] Bolton J S and Gold E, "The Application of Cepstral Techniques to the Measurement of Transfer Functions and Acoustical Reflection Coefficients", IEEE Journal of Sound and Vibration, Vol. 93, No. 2, 1984, pp. 217-233.

[14] Kemerait R C and Childers D G, "Signal Detection and Extraction by Cepstrum Techniques", IEEE Transactions on Information Theory, Vol. IT-18, No. 6, November 1972, pp. 745-759.

[15] Van Veen B D and Rogers J C, "Measurement of Acoustic Reflection Coefficients Using the Power Cepstrum", IEEE Transactions on Instrumentation and Measurement, Vol IM-35, No. 1, March 1986, pp. 24-30.

[16] "CRC Handbook of Chemistry and Physics", 55th ed., CRC Press, 1974-1975, pp. E-47.

BIBLIOGRAPHY

Rock Anchors

de Kock A, "Proposal for a Project Topic for the Degree of M.Ing. (Elek): Development of an Instrument to Evaluate the Quality of Grouted Tendon Installations", RAU (Randse Afrikaanse Universiteit), Johannesburg, 1987. (de Kock's student number was 8776822).

Jurell G, "Investigation into the Failure of a Pre-stressed Rock Anchor", Water Power & Dam Construction, February 1985, pp. 45-47.

Geodynamik AB, "The Boltometer for non-destructive testing of rock bolts", Geodynamic AB, Stockholm, Sweden - Pamphlet advertising this product, exact origin unknown. Geodynamik's telex number in Sweden is 12442; Attn:GEODYN.

Freeman T J, "The Behaviour of Fully-Bonded Rock Bolts in the Kielder Experimental Tunnel", Tunnels & Tunneling, June 1978, pp. 37-40.

Turner M J, "Rock Anchors: An outline of some current design, construction and testing practices in the United Kindom", International Conference on Structural Foundations and Rock, Sydney, 7-9 May 1980, pp. 87-103.

Farmer I W, "Stress Distribution along a Resin Grouted Rock Anchor", Int. J. Rock Mech. Min. Sci. & Geomech Abstr., Vol. 12, pp. 347-351, Pergamon Press 1975.

Littlejohn G S and Bruce D A, 'Rock Anchors - Design and Quality Control", Design Methods in Rock Mechanics, Geotechnics Research Group, University of Aberdeen, Scotland, pp. 77-88.

Sawyer S G and Karabin G J, "The Development and Use of Instrumentation for the In-Situ Measurement of Axial Loads in a Fully Resin-Grouted Roof Bolt", Roof Control Group, Pittburgh Technical Support Center, Mining Enforcement and Safety Administration, Pittsburgh, Pa., pp. 90-103.

Simpson R E, Fraley J E and Cox D J, "Inorganic Cement for Mine Roof-Bolt Grouting", United States Department of the Interior Bureau of Mines, Report of Investigations 8494, 32 pp.

Acoustics

Kino G S, "Acoustic Waves: Devices, Imaging & Analog Signal Processing", Prentice-Hall Inc., Englewood Cliffs, New Jersey, 1987, pp. 8-9.

Brown B and Goodman J E, "High-Intensity Ultrasonics", Iliffe Books Ltd: London, 1965.

Gooberman G L, "Ultrasonics: Theory and Application", 1st ed., The English Universities Press LTD, 1968, pp. 1-2.

Hunter Joseph L, "Acoustics", Prentice-Hall Inc.: Englewood Cliffs N.J., 1957.

Neubert Hermann K P, "Instrument Transducers: An Introduction to their Performance and Design", 2nd ed., Clarendon Press: Oxford, 1975.

Papadakis E P, "Traveling Wave Reflection Methods for Measuring Ultrasonic Attenuation and Velocity in Thin Rods and Wires", Journal of Applied Physics, Vol. 42, No. 7, June 1971, pp. 2990-2995.

Parnes R, "Dispersion Relations of Waves in a Rod Embedded in an Elastic Medium", Journal of Sound and Vibration, Vol. 76, No. 1, 1981, pp. 65-75.

Poole D, "Acoustic Evaluation of Rock Quality", Tunnels & Tunneling, November 1984, pp. 41-42.

Hanson D R, " Rock Stability Analysis Using Acoustic Spectroscopy", United States Department of the Interior, Bureau of Mines: Report of investigations 8950.

Singh R N and Buddery P S, "An assessment of the efficiency of roofbolt anchorage based on laboratory and field experimentation", Proceedings of the International Symposium on Rock Bolting, Abisko, 28 August - 2 September 1983, pp. 445-457.

Signal Processing

Kim J Y and Behrens J, "Recovery of Reflector series by Determining the Begi... Position of Estimated Wavelets Using Short-Time Homomorphic Analysis", Annales C... ysicae, Vol. 1, No. 1, 1983, pp. 11-15

Kalkbrenner M, Kim J Y and Behrens J, "Enhancement of Resolution in Self-Adaptively Deconvolved Seismograms Using Short-Time Homomorphic Wavelet Estimation", Annales Geophysicae, Vol. 1, No. 2, 1983, pp. 103-107.

Fjell P O, "Use of the Cepstrum Method for Arrival Times Extraction of Overla ignals Due to Multipath Conditions in Shallow Water", Journal Acoust. Soc. Ame . ol. 59, No. 1, January 1976, pp. 209-211.

Skinner D P and Childers D G, "Real-Time Composite Signal Decomposition", IEEE Trans. ASSP, Vol. 24, June 1976, pp. 267-270.

Hassab J C, "Homomorphic Deconvolution in Reverberant and Distortional Channels: An Analysis", Journal of Sound and Vibration, Vol. 53, No. 2, 1978, pp. 215-231.

Kalme J S, Uldrick J P, Robinson W A and Larrabbee D, "Use of Recompressed Impulse Response to Identify Sources and Paths of Structure-Borne Noise in Wide Flange I-Beams and Pipes Conveying Fluid", Journal of Sound and Vibration, Vol. 95, No. 4, 1984, pp. 439-467.

Bredenberg H, "Application of Stress-Wave Theory on Piles", Proceedings of the International Seminar on the Application of Stress Wave Theory on Piles, Stockholm, 4-5 June 1980, A A Balkema, Rotterdam, 1981.

Gold B and Rader C M, "Digital Processing of Signals", McGraw-Hill Inc., 1969, pp. 233-264.

Schwartz Mischa and Shaw Leonard, "Signal Processing: Discrete Spectral Analysis, Detection, and Estimation", McGraw-Hill, 1975.

Stanley W D, Dougherty G R and Dougherty R, "Digital Signal Processing", Reston Inc, 2nd Ed, 1984.